



Norwegian University of
Science and Technology

Investigation of Cracking Behavior in Reinforced Concrete Panels with Bond-slip Reinforcement

Magnus Eriksen
Magnus Kolstad

Master of Science in Civil and Environmental Engineering

Submission date: June 2016

Supervisor: Max Hendriks, KT

Norwegian University of Science and Technology
Department of Structural Engineering



Department of Structural Engineering

Faculty of Engineering Science and Technology

NTNU- Norwegian University of Science and Technology

ACCESSIBILITY

Open

MASTER THESIS 2016

SUBJECT AREA: Nonlinear analysis of reinforced concrete	DATE: 10.06.2016	NO. OF PAGES: 164
---	------------------	-------------------

TITLE:

Investigation of Cracking Behavior in Reinforced Concrete Panels with Bond-slip Reinforcement

Undersøkelse av rissoppførsel i armerte betongpanel med «bond-slip» armering

BY:

Magnus Tegelsrud Kolstad

Magnus Eriksen



SUMMARY:

This thesis aims at investigating the cracking behaviour in reinforced concrete panels with bond-slip reinforcement. In order to study the crack patterns, numerical models for two reinforced concrete panels were established, and nonlinear analyses were run in DIANA10. In short terms, the bond-slip models are valid when assuming that there no longer is a perfect bond between the concrete and the reinforcement, and slip between concrete and reinforcing steel occurs.

Experiments performed by Torbjørn Dyngeland are used as the basis for the numerical work performed in this thesis.

Two bond-slip models were assessed: a bond-slip model according to fib Model Code 2010 and a Cubic bond-slip model available as a predefined curve in DIANA10. It was seen that the choice of bond-slip curve influenced the crack patterns

It was discovered that the cubic bond-slip model by Dörr resulted in an earlier crack initiation stage for both panels.

The results showed that the shear stiffness modulus for the bond-slip models had a large impact on the behaviour of the two panels.

RESPONSIBLE TEACHER: Professor Max Hendriks

SUPERVISOR(S): Professor Max Hendriks and Ph.D-candidate Reignard Tan

CARRIED OUT AT: Department of Structural Engineering

Institutt for konstruksjonsteknikk

FAKULTET FOR INGENIØRVITENSKAP OG TEKNOLOGI

NTNU – Norges teknisk-naturvitenskapelige universitet

MASTEROPPGAVE 2016

for

Magnus Tegelsrud Kolstad

Magnus Eriksen

Investigation of Cracking Behavior in Reinforced Concrete Panels with Bond-slip Reinforcement

Undersøkelse av rissoppførsel i armerte betongpanel med «bond-slip» armering

Denne oppgaven går I korte trekk ut på følgende:

- *Litteraturstudium*
Materialmodeller for betong og stål
Numeriske løsningsmetoder i ikke-lineær analyse
Bond-slip armering
Grunnlag for elementmetodeprogrammet DIANA10
- *Modellering*
Kjøring av python-skript i DIANA10
Modellering av to armerte betongpanel
Introdusere bond-slip armering i modellene
- *Evaluering:*
Diskusjon av resultater fra ikke-lineære analyser
Sammenligning av resultater fra ikke-lineære analyser med eksperimentelle resultater samt lovverk
Forslag til videre arbeid

Besvarelsen organiseres i henhold til gjeldende retningslinjer.

Veileder(e): Professor Max Hendriks og ph.d-kandidat Reignard Tan

Besvarelsen skal leveres til Institutt for konstruksjonsteknikk innen 10. juni 2016.

NTNU, 18. januar, 2016

Faglærer: Max Hendriks

Preface

All work related to this master's thesis has been carried out in the spring 2016 at the department of structural engineering, and is the final work of a two-year long master's degree program at the Norwegian University of Science and Technology (NTNU). The thesis was performed with Professor Max Hendriks as main supervisor and PhD-candidate Reignard Tan as co-supervisor. The work has been carried out over a period of 20 weeks and provides 30 credits per student.

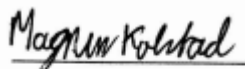
The aim of the thesis is to investigate cracking behaviour in reinforced concrete with bond-slip formulation implemented in the finite element model, with the aid of nonlinear analyses. Furthermore, the thesis aims at evaluating the influence of material properties and numerical iteration methods with respect to cracking.

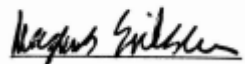
Our main motivation for taking on the work that this thesis had to offer was to establish a better understanding of how reinforced concrete behaves and how nonlinear analyses are performed for such structures. Both of us had quite good knowledge with respect to general design of concrete structures. Before we started our work with this thesis, we had no knowledge with respect to the procedure of performing nonlinear analyses. For this reason, a lot of research had to be done in order to get an overview over the different features and methods that a nonlinear analysis consists of. Neither of us were familiar with DIANA, but had heard about the program, and we saw this thesis as an opportunity to learn how to use a new FEM program.

We would like to thank our supervisor Max Hendriks and our co-supervisor Reignard Tan for good supervision and expert advice underway. We would also like to thank PhD-candidate Morten Engen for good guidance regarding scripting in Python and general modelling in DIANA10.

It is safe to say that we have learned a lot during this process.

Trondheim 10.06.2016


Magnus Kolstad


Magnus Eriksen

Abstract

This thesis aims to investigate the crack pattern of two reinforced concrete panels subjected to a tensile load. Numerical models for two reinforced concrete panels were established in the finite element program DIANA10. Results from the nonlinear analyses were compared with results from experiments performed by Dyngeland [8].

An important aspect of this thesis is the implementation of *bond-slip* reinforcement instead of regular embedded reinforcement. Bond-slip reinforcement models are valid when it is assumed that there no longer exist a perfect bond between the concrete and the reinforcement bars. This results in slip, or relative displacement, between the concrete and the reinforcement. This slip causes interface tractions along the reinforcement bars. Two bond-slip models were assessed, one from fib Model Code 2010 and one model proposed by Dörr, which is called *Cubic Bond-slip*. It was seen that the two different slip-models described the bond stress-slip relation quite differently, which evidently had an impact on the crack patterns. It was also desirable to establish a basis for which material properties and iterative procedures that gave the best results. Important aspects related to discussion and evaluation are the experimental results, crack widths and crack spacing from the nonlinear analyses and theoretical crack widths and crack spacing calculated according to Eurocode 2 and fib Model Code 2010.

It was discovered that the cubic bond-slip model by Dörr resulted in an earlier crack initiation stage for both panels. This is caused by the initial stiffness of the bond stress-slip curve, which is higher for the cubic bond-slip model than the fib Model Code 2010 bond-slip model.

The results showed that the shear stiffness modulus for the bond-slip models had a large impact on the behaviour of the two panels.

Of the tested numerical iteration methods, the Newton Raphson methods would result in divergence for both panels. It was concluded that a more sophisticated iterative procedure had to be used for the analyses of the two panels. The Broyden Quasi-Newton method gave stable results and all over load step convergence.

Sammendrag

Hovedmålet med denne oppgaven er å studere rissoppførselen i armert betongpanel påkjent av strekklast. To numeriske modeller ble etablert og analysert med ikke-lineære analyser i elementmetodeprogrammet DIANA10. Resultater fra analysene ble så sammenlignet med resultater fra eksperimenter utført av Dyngeland [8].

Et sentralt tema i denne masteroppgaven er implementeringen av «bond-slip» armering i stedet for «embedded» armering, og vurdere hvordan disse armeringsmodellene påvirker rissoppførselen i betongen. I korte trekk er «bond-slip» armering gyldig når perfekt heft mellom betong og armering ikke lenger er tilstede, noe som resulterer i at betongen kan «slippe» langs armeringen. Som følge av dette oppstår det en relativ forskyvning mellom betong og armering, noe som fører til heftespenninger langs armeringen. To formuleringer for bond-slip armering er vurdert i denne oppgaven: den ene formuleringen bygger på regelverket for fib Model Code 2010. Den andre formuleringen er kalt «cubic bond-slip» modell, og ble foreslått av Dörr. Dette er en forhåndsdefinert modell i DIANA10. De to bond-slip formuleringene er ganske forskjellige og dette gikk ut over rissmønstrene som oppstod. Det var også ønskelig å finne ut hvilke materialparametere og iterasjonsmetoder som gav best resultater. Rissvidde og rissavstand fra de eksperimentelle forsøkene og de numeriske resultatene blir diskutert og evaluert til slutt. Beregnede rissvidder og rissavstander ifølge Eurocode 2 og fib Model Code 2010 er også diskutert.

Det ble oppdaget at cubic bond slip formulering av Dörr førte til tidligere rissdannelse for begge panelene. Dette skjer fordi den initielle stivheten til bond-slip kurven er høyere i cubic formuleringen enn for fib Model Code formuleringen.

Resultatene viste at skjærstivhetsmodulen til bond slip modellne hadde stor innvirkning på oppførselen til panelene.

Forskjellige iterasjonsmetoder ble utprøvd, og Broyden Quasi-Newton gav til slutt best resultat. Newton-Raphson metodene førte bare til divergens for begge panelene.

Content

Preface.....	i
Abstract.....	iii
Sammendrag	v
Introduction.....	1
General.....	2
Problem description.....	2
Experiment description	2
Part I: Theory	3
1. Finite Element Method (FEM)	4
1.1 Nonlinear problems	4
2. Materials and Methods	5
2.1 Plasticity.....	5
2.1.1 Introducing a simple slip model.....	5
2.2 Flow Theory of Plasticity.....	10
2.2.1 Yield function	10
2.2.2 Flow rule	13
2.2.3 Hardening behaviour.....	16
2.3 Integration of the Stress-Strain Relation	18
2.3.1 Euler Forward Integration Rule	18
2.4 Tangent Stiffness.....	21
2.5 Crack models.....	22
2.5.1 Introduction.....	22
2.6 Smearred crack models.....	23
2.6.1 Fixed crack models	23
2.6.2 Rotating crack models.....	25
2.7 Material models.....	27
2.7.1 Concrete in tension	27
2.7.2 Concrete in compression.....	30
2.8 Reinforcement	31
2.8.1 Embedded reinforcement	31
2.8.2 Bond-slip reinforcement	31
2.9 Elements.....	35
2.9.1 Plane stress elements.....	35
2.9.2 Interface elements	37
2.9.3 Bond-slip interface elements.....	38

2.9.4	Truss Elements.....	39
3.	Numerical solution methods.....	40
3.1	Iterative procedures.....	40
3.1.1	Regular Newton-Raphson.....	41
3.1.2	Modified Newton-Raphson.....	41
3.1.3	Quasi-Newton.....	42
3.1.4	Broyden.....	43
3.1.5	Broyden-Fletcher-Goldfarb-Schanno(BFGS).....	43
3.1.6	Chrisfield method.....	43
3.1.7	Linear and constant stiffness iteration.....	44
3.1.8	Line Search.....	44
3.2	Convergence criteria.....	45
3.3	Load versus Displacement Control.....	46
4.	Calculation of crack width and crack spacing.....	48
4.1	Eurocode 2.....	48
4.2	fib Model code 2010.....	51
4.2.1	Reinforcement with an angle to the principal stress axis.....	54
Part II: Modeling.....		55
5.	Concrete panels TP1 and TP2.....	56
5.1	Python scripting.....	56
5.2	Geometry.....	57
5.3	Supports and tyings.....	58
5.4	Mesh and element types.....	58
5.5	Loads.....	59
5.6	Material properties.....	60
5.6.1	Reinforcement.....	60
5.6.2	Bond slip reinforcement.....	61
5.6.3	Shear stiffness and normal stiffness.....	62
5.6.4	Concrete.....	64
Part III: Analysis and results.....		66
6.	Reference model.....	67
6.1	Loading procedure.....	69
7.	Results.....	70
7.1	TP1 Reference model.....	71
7.1.1	Load-displacement curve.....	71
7.1.2	Stress-Average strain.....	71
7.1.3	Plots panel TP1 – reference analysis.....	72

7.2	Parameter study TP1	83
7.3	TP2 Reference model	89
7.3.1	Load displacement	89
7.3.2	Stress – average strain.....	89
7.3.3	Plots panel TP2 - reference	90
7.4	Parameter study TP2	101
7.5	Crack widths and crack spacing TP1 and TP2	108
Part IV: Evaluation and conclusion		110
8.	Evaluation.....	111
8.1	Bond-slip models.....	111
8.2	Material models.....	113
8.3	Mesh properties and sensitivity.....	114
8.4	Numerical iterative procedures	116
8.5	NLFEA versus Eurocode 2 and fib Model Code 2010	117
8.6	Comparison of numerical and experimental crack patterns	118
8.7	Sources to error	119
9.	Conclusion.....	120
10.	Suggestions to further work.....	122
11.	References.....	124
Part V: Appendices		125
Appendix A – Python Scripts TP1		i
	Modelling Script TP1	i
	Analysis Script TP1.....	vi
Appendix B – Python Scripts TP2		x
	Modelling Script TP2	x
	Analysis Script TP2.....	xvii
Appendix C – Calculations according to Eurocode 2 and Model Code		xxi

List of Figures

Figure 1 - Spring-sliding system with two degrees of freedom.....	5
Figure 2 - Loading, unloading and reloading: Slip model, (De Borst et.al. [7]).....	9
Figure 3 - Mohr's Circle, (de Borst et.al. [7])	10
Figure 4 - Mohr-Coulomb and Drucker-Prager yield criteria, (de Borst. et.al [7])	12
Figure 5: Isotropic Hardening.....	17
Figure 6 - Explicit integration scheme.....	19
Figure 7 - Predefined tension softening curves TSC model. (TNO DIANA [18]).....	27
Figure 8 - Predefined compression curves for Total Strain models (TNO DIANA [18])	30
Figure 9 - Cubic function by Dörr, (Tejchman and Bobinski [17]).....	33
Figure 10 - Bond stress-slip relationship, (fib Model Code 2010 [11]).....	34
Figure 11 - Characteristics of a plane stress element, (TNO DIANA [18])	35
Figure 12 - 4-Noded Quadrilateral Element, (TNO DIANA [18]).....	35
Figure 13 - CQ16M: 8-noded plane stress element. (TNO DIANA [18]).....	36
Figure 14: Two-dimensional interface element, (TNO DIANA [18]).....	37
Figure 15: Bond-slip interface implementation in a .dat-file.....	38
Figure 16 - Truss element with corresponding coordinate system, (TNO DIANA [18]).....	39
Figure 17 - Regular Newton-Raphson iteration, (TNO DIANA [18])	41
Figure 18 - Modified Newton-Raphson iteration, (TNO DIANA [18])	41
Figure 19 - Quasi-newton iteration, (TNO DIANA [18]).....	42
Figure 20 - Linear Stiffness iteration, (TNO DIANA [18]).....	44
Figure 21 – Load control and displacement Control, (TNO DIANA [18]).....	46
Figure 22 - Effective tension area. (Eurocode 2, [16])	49
Figure 23 - Crack width at concrete surface relative to distance from reinforcing bar (Eurocode 2,[16]).....	50
Figure 24 - Load-strain relation centrally reinforced member subjected to tension (fib Model Code 2010 [11]).....	51
Figure 25 - Transmission of forces in a distributed area next to a crack, (fib Model Code 2010 [11])	53
Figure 26 - Geometry TP1	57
Figure 27: Geometry TP2	57
Figure 28 - Load attachment TP1 and TP2	59
Figure 29: Stress-Strain relation KS400	60
Figure 30: Bond-slip Diagram TP1 and TP2	61
Figure 31: Cubic bond-slip curve (TNO DIANA [18]).....	62
Figure 32: Illustration DSNY.....	64
Figure 33: Loading Procedure TP1 and TP2	69
Figure 34: Load-displacement TP1 vs. S1/S2.....	71
Figure 35: Stress-average strain curve TP1 vs. S1/S2	72
Figure 36: Load-displacement TP1 reference - interesting points.....	72
Figure 37: Load-Displacement TP2 vs. S3/S4.....	89
Figure 38: Stress-Average strain TP2 vs. S3/S4.....	90
Figure 39: Load-displacement TP2 reference-interesting points.....	90
Figure 42: Panel S3/S4, experimental.....	119

List of tables

Table 1 - Values of G_{F0}	29
Table 2 - Parameters for defining mean bond stress-slip curve, (fib Model Code 2010, [11])	34
Table 3: Interface elements bond-slip reinforcement (TNO DIANA [18]).....	38
Table 4 – Values for τ_{bm} , η_r and β for deformed reinforcing bars. (fib Model Code 2010 [11])	54
Table 5: Tabulated values Stress-strain curve KS400	60
Table 6: Tabulated values Bond-slip diagram TP1 and TP2	61
Table 7 - Material Properties panel P1 and P2	64
Table 8: Average crack widths and spacing from Nonlinear Analyses	108
Table 9: Crack widths and spacing according to Eurocode 2 and fib Model Code 2010.....	109
Table 10: Experimental crack widths and spacing	109

Introduction

Finite Element Method (FEM)-computer programs are suitable tools for simulating reinforced concrete. At the institute of structural engineering at NTNU, the FEM-program DIANA is often used. In February 2016 a brand new version of DIANA, namely DIANA10 was launched, and was used in this thesis. DIANA10 has new features regarding the pre- and post-processing environment, and is compatible with *python-scripting*. Numerical simulations are vital in order to predict a satisfactory response of reinforced concrete subjected to a certain type of loading. In order to analyze the results provided in a good manner it is important to have a good understanding about linear and non-linear FEM in general. It is also of great importance to understand the theory implemented in the calculations performed by the finite element computer program that is being used. DIANA is a highly sophisticated program that provides many options regarding material models and numerical solution methods. A great deal of effort has for that reason been put into investigating the many choices the analyst is provided, and how the various material models and numerical solution methods influence the results.

The motivation behind this thesis is the ongoing research project called “Durable Advanced Concrete Structures (DACS)”. DACS was initiated as an extension of the work done in “Concrete Innovation Center (COIN)” and is planned to be finished in 2019. The purpose of DACS is to develop knowledge, methods and tools which enables sustainable and competitive concrete structures that can withstand environmental stresses in an arctic-marine environment. The project is led by Kværner Concrete Solutions. Other participants are Multiconsult, Statens Vegvesen, Norcem, Concrete Structures, Norbetong, Skanska, Unicon, AF Gruppen, Mapei, Veidekke, St. Gobain Weber, Sintef Byggforsk and NTNU. DACS is divided into 4 “work packages”, where this master thesis is related to the first package: “Early age cracking and crack calculation in design”. The topic of this thesis was decided in cooperation with main supervisor Professor Max Hendrix and PhD-candidate Reignard Tan.

The main motivation for this thesis was to establish a basis to evaluate the accuracy regarding design of reinforced concrete structures in the Serviceability Limit State with non-linear finite element analyses. These analyses were considered as virtual experiments that *could* help us predict crack behavior in the concrete. In order to assess the cracking behavior, numerical models for two reinforced concrete panels were established. One panel had horizontal reinforcement, and one panel had orthogonal reinforcement oriented in a 45-degree angle to the concrete. The structures were analyzed with different material models and numerical solution procedures in order to obtain the best possible results. An important aspect of this thesis is the implementation of bond-slip reinforcement in the models.

General

This thesis is divided into five parts: Theory, Modelling, Results, Evaluation and Appendices. In the theory part, material models, iterative procedures and bond-slip models are described. Then follows the modelling part which contains a detailed description regarding the modelling procedure of the two models. Part III contains analyses details and relevant results. In part IV, the results are evaluated and a suggestion for further work will be stated. Part V consists of appendices where python scripts and calculations according to Eurocode 2 and fib Model Code 2010 are attached.

Problem description

The aim of this thesis is to investigate the cracking behavior in reinforced concrete panels subjected to tensile loading when bond-slip reinforcement is implemented in the finite element model. Bond-slip reinforcement models are valid when there no longer is a perfect bond between the reinforcement and the concrete, resulting in a relative displacement between concrete and reinforcement nodes. Two different types of panels with bond-slip reinforcement will be modelled and analyzed using DIANA10. Furthermore, it is desirable to establish a basis regarding how the different bond-slip formulations influence the cracking behavior of the concrete, and which material parameters that are best suited to predict crack patterns when comparing numerical results with experimental results.

Experiment description

Experiments performed by Torbjørn Dyngeland are used as the basis for the numerical work of this thesis. Dyngeland [8] developed an analytical model for prediction of crack patterns. He also did experimental testing on several concrete panels with different loading and reinforcement layout. Some of these panels where loaded in pure tension until failure. When a stable crack pattern had developed, the cracks where measured and documented. The experimental test results and results from the analytical model where then compared.

Part I: Theory

1. Finite Element Method (FEM)

In general FEM is a method for numerical solution of field problems (Cook et al. [6]). When dealing with a field problem, we must determine the spatial distribution of one or more dependent variables, e.g. distribution of displacements and stresses in a slab. The main principle for solving a FEM-problem is the relationship between displacement, stiffness and load. This relationship can be expressed by the following equation:

$$[K] \times \{D\} = \{R\} \quad (1.1)$$

where $[K]$ denotes the system stiffness matrix, $\{D\}$ the translation or rotation and $\{R\}$ the external loading. Eq. (1) is solvable in a linear manner given constant stiffness, i.e. we have linear material behavior, and the outer and inner forces are in equilibrium.

1.1 Nonlinear problems

According to Cook et al. [6], in structural mechanics, types of nonlinearity include the following:

Material nonlinearity

- Material properties are functions of the state of stress or strain. Examples include nonlinear elasticity, plasticity and creep.

Contact nonlinearity

- A gap between adjacent parts may open or close.
- The contact area between parts changes as the contact force changes.
- Frictional forces caused by sliding contact.

Geometric nonlinearity

- Deformations are so large that the equilibrium equations must be written with respect to the deformed structural geometry.
- Loads may change direction as they increase.

Problems in these categories above are nonlinear because the stiffness, and sometimes the loading, become functions of the displacement or deformation of the structure. Eq. (1.1) can be rewritten to the following:

$$[K(D)] \times \{D\} = \{R(D)\} \quad (1.2)$$

It cannot immediately be solved for $\{D\}$ since the information required to establish $[K]$ and $\{R\}$ are not known in advance. This requires an iterative process in order to obtain $\{D\}$ and its associated $[K]$ and $\{R\}$, such that the left hand side of the equation ($[K]\{D\}$) is in equilibrium with the right hand side in the equation ($\{R\}$). Iterative procedures will be discussed in section 3.1.

2. Materials and Methods

A literature study regarding numerical material models has been performed. Furthermore, it is chosen to present general aspects and mathematical statements with respect to concrete and steel with the intention of establishing a basis for how the different material models are implemented in DIANA10. In order to study plasticity models, crack models and bond-slip reinforcement models, literature such as De Borst et.al. [7], Tejchman and Bobinski [17] and TNO DIANA [18] have been used.

2.1 Plasticity

The theory of plasticity is one of the most well-developed theories in order to describe material non-linearity (De Borst et.al. [7]). In the following sections, the essence of the theory of plasticity will be presented, *the Flow Theory of Plasticity*. The main ingredients of this theory is *the Yield Function*, *the Flow Rule* and *the Hardening Behavior*.

2.1.1 Introducing a simple slip model

In order to understand the non-linear behavior in a material, one should start with a simple model, e.g. a spring-sliding system.

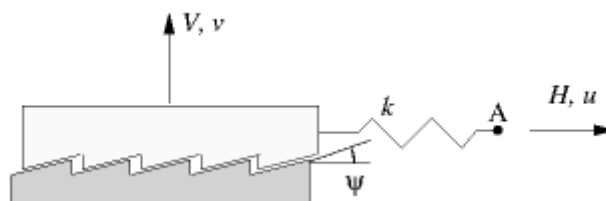


Figure 1 - Spring-sliding system with two degrees of freedom

Figure 1 represents a simple spring-sliding system, and in this formulation the entire horizontal displacement of point A is initially caused by the spring deformation. This is due to the fact that for low force levels, the adhesion and the friction between the floor and the block prevent any sliding of the block. The block will only start sliding when the shear force exceeds what can be absorbed by bond and friction. From that moment on, the horizontal displacement of point A is composed of a contribution from the spring and a contribution from the sliding between the block and the floor. The total horizontal displacement of point A is now represented by u . The total displacement u can further be divided into two parts which represent the deformation of the spring and the sliding of the block, respectively. We can now write the total displacement u as:

$$u = u^e + u^p \quad (2.1)$$

The first term in eq. (2.1) represents the deformation of the spring, and is called elastic because when removing the force, the deformation in the spring also disappears. The second term in eq. (2.1) represents the sliding of the block. This displacement does not disappear during unloading and because of this permanent behaviour, it is denoted plastic. If it is assumed that the surface between

the sliding block and the floor is not perfectly smooth, which will result in horizontal and vertical displacement of the block, we can denote the plastic displacement by two displacement components:

$$\mathbf{u}^p = \begin{pmatrix} u^p \\ v^p \end{pmatrix} \quad (2.2)$$

The elastic displacements may also be assembled in a vector:

$$\mathbf{u}^e = \begin{pmatrix} u^e \\ v^e \end{pmatrix} \quad (2.3)$$

From eq. (2.3) it is seen that the term v^e got no physical meaning and is equal to zero. An extension of eq. (2.2) to incorporate the vertical displacements may be written as follows:

$$\mathbf{u} = \mathbf{u}^e + \mathbf{u}^p \quad (2.4)$$

Between the elastic displacement u^e and the horizontal force H there is a unique relation. This relation can be written as follows:

$$ku^e = H \quad (2.5)$$

Between the deformations attributable to those that take place in the spring and those that take place in the sliding system, lies an important distinction regarding the uniqueness between strains and stresses or between displacement and force, as the current system describes. In eq. (2.5), k is the spring constant. The “elastic” displacement will be reduced to zero as the force H vanishes after reaching a non-zero value. For the plastic displacement u^p however, such a relation is not physically possible. During a plastic deformation the inelastic deformation can be determined. It is now assumed that the ratio between plastic velocity in the horizontal direction and the plastic velocity in the vertical direction, respectively, may be obtained by:

$$\tan(\psi) = \frac{\dot{v}^p}{\dot{u}^p} \quad (2.6)$$

The direction of the plastic flow may be written as:

$$\dot{\mathbf{u}}^p = \dot{\lambda} \mathbf{m} \quad (2.7)$$

Where

$$\mathbf{m} = \begin{pmatrix} 1 \\ \tan(\psi) \end{pmatrix} \quad (2.8)$$

This \mathbf{m} determines the direction of the plastic flow. λ is denoted the plastic multiplier. This constant may be determined by requiring the stresses to remain bounded during plastic flow. The transition between elastic and plastic states can be defined quite straightforward also for multi-dimensional stress states. The flow theory of plasticity will be described in the next section. For the deformation theory of plasticity, this convenient property does not apply, since the deformation theory of plasticity is built on the assumption that the plastic strain, and not the plastic strain rate, is determined by the values of the stresses. The force vector \mathbf{f} is defined in a similar manner as the displacement vector stated in eq. (2.2) and eq. (2.3):

$$\mathbf{f} = \begin{pmatrix} H \\ V \end{pmatrix} \quad (2.9)$$

The elastic displacement vector can be related to the force vector by the following relation:

$$\mathbf{f} = \mathbf{D}^e \mathbf{u}^e \quad (2.10)$$

Where \mathbf{D}^e denotes the elastic stiffness matrix. In this case, the elastic stiffness matrix is defined as:

$$\mathbf{D}^e = \begin{pmatrix} k & 0 \\ 0 & 0 \end{pmatrix} \quad (2.11)$$

By differentiating the fundamental decomposition, we obtain:

$$\dot{\mathbf{u}} = \dot{\mathbf{u}}^e + \dot{\mathbf{u}}^p \quad (2.12)$$

$$\dot{\mathbf{f}} = \mathbf{D}^e \dot{\mathbf{u}}^e \quad (2.13)$$

Combining these results with the relation from eq. (2.11), the relation that states the direction of the plastic velocity, yields the following relation:

$$\dot{\mathbf{f}} = \mathbf{D}^e (\dot{\mathbf{u}} - \lambda \dot{\mathbf{m}}) \quad (2.14)$$

There must be established a criterion that sets a border between the elastic displacements and when the plastic displacements occur, i.e. when the block starts sliding for the system being dealt with. The

assumption that the “block-sliding” starts when the Coulomb friction with adhesion is fully mobilized, results in:

$$H + V \tan(\varphi) - c = 0 \quad (2.15)$$

Where:

φ Friction coefficient

c Adhesion

V Shear force

In order for friction to be mobilized between the surface and the block, the force V must act in a downward direction, i.e. V must be less than zero.

At the state when the expression in eq. (2.15) is less than zero, only elastic deformation takes place. The state where the expression in eq. (2.15) is greater than zero is physically impossible due to the fact that the horizontal force H is bounded by eq. (2.15). By assuming that c and φ are constants and then differentiate eq. (2.15) we obtain:

$$\dot{H} + \dot{V} \tan(\varphi) = 0 \quad (2.16)$$

Eq. (2.16) written with symbols gives:

$$\mathbf{n}^T \dot{\mathbf{f}} = 0 \quad (2.17)$$

Where \mathbf{n} denotes the introduced vector:

$$\mathbf{n} = \begin{pmatrix} 1 \\ \tan(\varphi) \end{pmatrix} \quad (2.18)$$

$$\dot{\lambda} = \frac{\mathbf{n}^T \mathbf{D}^e \dot{\mathbf{u}}}{\mathbf{n}^T \mathbf{D}^e \mathbf{m}} \quad (2.19)$$

Eq. (2.19) is obtained by pre-multiplying eq. (16) by \mathbf{n}^T and the use of the fact that eq. (2.17) holds during plastic flow.

The expression for the plastic multiplier $\dot{\lambda}$ inserted in eq. (2.14) yields:

$$\dot{\mathbf{f}} = \left(\mathbf{D}^e - \frac{\mathbf{D}^e \mathbf{m} \mathbf{n}^T \mathbf{D}^e}{\mathbf{n}^T \mathbf{D}^e \mathbf{m}} \right) \dot{\mathbf{u}} \quad (2.20)$$

Eq. (2.20) sets an explicit relation between the rate of the force vector $\dot{\mathbf{f}}$ and the velocity vector $\dot{\mathbf{u}}$.

The expression from eq. (2.20) are denoted *rate equations*, and are non-symmetric in general due to the fact that $\varphi \neq \psi$.

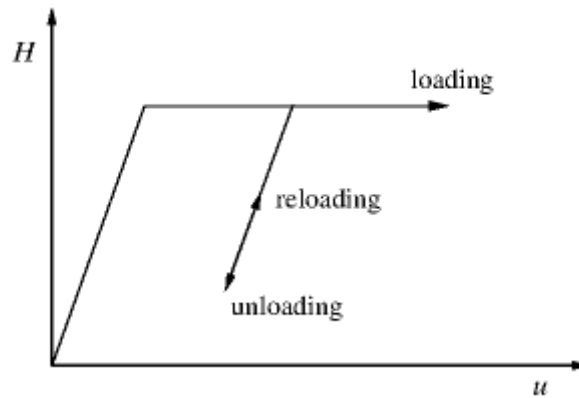


Figure 2 - Loading, unloading and reloading: Slip model, (De Borst et.al. [7])

The flow theory of plasticity only provides a relation between the *rate* of force/stress and the velocity/strain rate, and not the direct relation between force/stress and displacement/strain. It is of great importance that the incremental equations are integrated in an exact manner. To carry out this task, implicit integration schemes are best suited.

A prominent feature for the theory of plasticity, and also for the slip model described, is that when the condition for continued sliding, represented by eq. (2.15), is no longer satisfied, purely elastic behaviour applies. This means that the process of unloading is purely elastic. The same applies for reloading. If eq. (2.15) again is satisfied, permanent contributions to the incremental displacement again occurs, as presented in Figure 2.

2.2 Flow Theory of Plasticity

2.2.1 Yield function

Mohr-Coulomb

In the previous section a slip model for frictional sliding along a fixed plane was presented. This was done in order to establish a good base for the continuation, in which stresses rather than forces are being dealt with. The extension of Coulomb's assumption, i.e. the sliding along a plane occurs when the shear force on a plane exceeds the normal force multiplied by a friction factor in addition to some adhesion, will lead to the search for the plane on which the combination of normal stress σ and shear stress τ is critical, expressed by the condition:

$$\tau + \sigma \tan(\varphi) - c = 0 \quad (2.21)$$

The condition expressed in eq. (2.21) must be satisfied in order for the extension of Coulomb's assumption to be valid. In the expression above, c denotes the respective material's cohesion. It is based on one-axial testing of the compression strength f_c :

$$c = \frac{1 - \sin(\varphi)}{2 \cos(\varphi)} f_c \quad (2.22)$$

We now consider a two-dimensional stress state. It is now possible to relate σ and τ to the principal stresses by utilizing Mohr's Circle, which is shown in Figure 3 below:

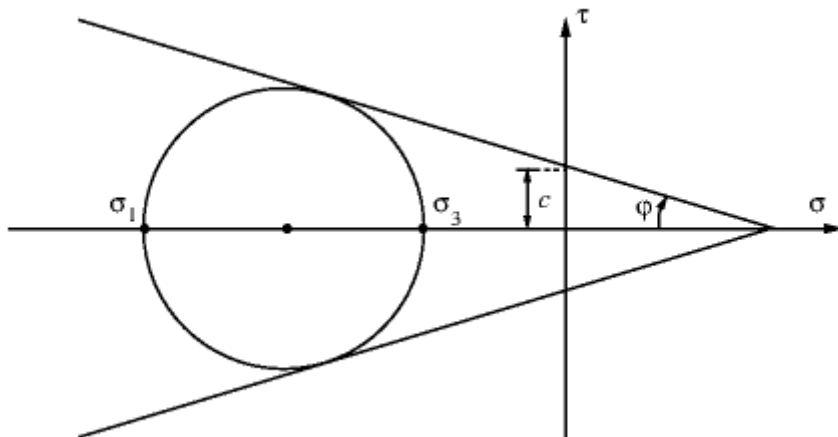


Figure 3 - Mohr's Circle, (de Borst et.al. [7])

$$\sigma = \left(\frac{\sigma_3 + \sigma_1}{2} \right) + \left(\frac{\sigma_3 - \sigma_1}{2} \right) \sin(\varphi) \quad (2.23)$$

And:

$$\tau = \left(\frac{\sigma_3 - \sigma_1}{2} \right) \cos(\varphi) \quad (2.24)$$

By substituting the expressions for σ and τ into eq. (2.21) and multiplying with $\cos(\varphi)$ results in:

$$\left(\frac{\sigma_3 - \sigma_1}{2} \right) + \left(\frac{\sigma_3 + \sigma_1}{2} \right) \cos(\varphi) - c \cos(\varphi) = 0 \quad (2.25)$$

Eq. (2.25) represents the two-dimensional state of the Mohr-Coulomb yield criterion. The Mohr-Coulomb criterion may be extended to fully three-dimensional stress states. Eq. (2.24) is valid as long as $\sigma_1 \leq \sigma_2 \leq \sigma_3$. For instance, if $\sigma_2 \leq \sigma_3 \leq \sigma_1$, the shear stress on the plane on which combination of stresses becomes critical yields $\tau = 0.5(\sigma_1 - \sigma_2) \cos(\varphi)$ and the normal stress $\sigma = 0.5(\sigma_1 + \sigma_2) + 0.5(\sigma_1 - \sigma_2) \sin(\varphi)$. The yield condition may now be formulated in terms of σ_1 and σ_2 :

$$\left(\frac{\sigma_1 - \sigma_2}{2} \right) + \left(\frac{\sigma_1 + \sigma_2}{2} \right) \sin(\varphi) - c \cos(\varphi) = 0 \quad (2.26)$$

Three-dimensional principal stress space Mohr-Coulomb yield criterion

This condition is complemented by the following four conditions:

$$\frac{1}{2}(\sigma_2 - \sigma_3) + \frac{1}{2}(\sigma_2 + \sigma_3) \sin(\varphi) - c \cos(\varphi) = 0 \quad (2.27a)$$

$$\frac{1}{2}(\sigma_1 - \sigma_3) + \frac{1}{2}(\sigma_1 + \sigma_3) \sin(\varphi) - c \cos(\varphi) = 0 \quad (2.27b)$$

$$\frac{1}{2}(\sigma_2 - \sigma_1) + \frac{1}{2}(\sigma_2 + \sigma_1) \sin(\varphi) - c \cos(\varphi) = 0 \quad (2.27c)$$

$$\frac{1}{2}(\sigma_3 - \sigma_2) + \frac{1}{2}(\sigma_3 + \sigma_2) \sin(\varphi) - c \cos(\varphi) = 0 \quad (2.27d)$$

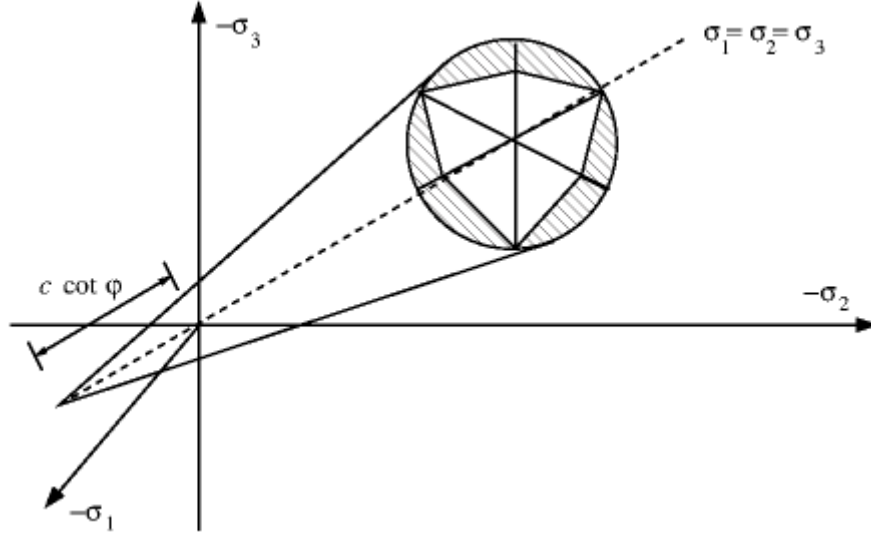


Figure 4 - Mohr-Coulomb and Drucker-Prager yield criteria, (de Borst. et.al [7])

Figure 4 shows the yield criteria for Mohr-Coulomb and Drucker-Prager in three-dimensional principal stress space. The figure shows the permutations of the 4 conditions stated above represented graphically in the three-dimensional principal stress space. Together, they form a cone which meet in the apex of the yield surface were $\sigma_1 = \sigma_2 = \sigma_3 = c \cot(\varphi)$. This represents the yield surface of for Mohr-Coulomb. Stresses inside this contour causes elastic deformations, while stress states on the yield surface may cause elasto-plastic deformations. Stress states on the “outside” of the yield surface is by definition not possible.

A loading function bounding all stress states may now be introduced:

$$f(\sigma) \leq 0 \tag{2.28}$$

Eq. (2.28) holds for the stress states within the yield surface ($f(\sigma) < 0$) and for stress states at the yield surface ($f(\sigma) = 0$).

$$f(\sigma) = \frac{1}{2}(\sigma_3 - \sigma_1) + \frac{1}{2}(\sigma_3 + \sigma_1) \sin(\varphi) - c \cos(\varphi) \tag{2.29}$$

Eq. (2.29) is obtained by consideration of the Mohr-Coulomb yield function.

Other well-known yield criteria may be considered as approximations of the Mohr-Coulomb yield criterion.

Von Mises

The Von Mises yield function forms a circular cylinder in the principal stress space, and a circle in the π -plane. The von Mises yield function can be written, in terms of principal stresses, as:

$$f(\sigma) = \sqrt{\frac{1}{2} [(\sigma_1 - \sigma_2)^2 + (\sigma_2 - \sigma_3)^2 + (\sigma_3 - \sigma_1)^2]} - \bar{\sigma} \quad (2.30)$$

In terms of normal and shear stresses the von Mises yield functions becomes:

$$f(\sigma) = \sqrt{\frac{1}{2} [(\sigma_{xx} - \sigma_{yy})^2 + (\sigma_{yy} - \sigma_{zz})^2 + (\sigma_{zz} - \sigma_{xx})^2] + 3\sigma_{xy}^2 + 3\sigma_{yz}^2 + 3\sigma_{zx}^2} - \bar{\sigma} \quad (2.31)$$

The von Mises yield function, written in a different manner, reads:

$$f(\sigma) = q - \bar{\sigma} \quad (2.32)$$

Where:

$$q = \sqrt{3J_2} \quad (2.33)$$

Eq. (2.35) states the second invariant of the deviatoric stresses, and is proportional to the expression beneath the square root in eq. (2.33).

2.2.2 Flow rule

In order for plastic deformations to occur, the stress point must remain on the yield contour for a “short period of time”. When the stress point merely touches the yield surface and then jumps back inward again, no plastic flow will take place. Plastic straining will only take place if the following criteria is fulfilled:

$$f = 0 \quad (2.34)$$

The Prager consistency condition may be expressed as:

$$\dot{f} = 0 \quad (2.35)$$

The Prager consistency condition states that the yield function f , must remain zero for a small time increment in order for plastic flow to occur. Within the elastic domain the relation $\boldsymbol{\sigma} = \mathbf{D}^e : \boldsymbol{\varepsilon}$ sets the stress and strain dependence. Such a relationship can only be set between the stress and the elastic strain:

$$\boldsymbol{\sigma} = \mathbf{D}^e : \boldsymbol{\varepsilon}^e \quad (2.36)$$

The total strain reads:

$$\boldsymbol{\varepsilon} = \boldsymbol{\varepsilon}^e + \boldsymbol{\varepsilon}^p \quad (2.37)$$

From eq. (2.37) we can now write:

$$\boldsymbol{\sigma} = \mathbf{D}^e : (\boldsymbol{\varepsilon} - \boldsymbol{\varepsilon}^p) \quad (2.38)$$

In three-dimensional stress space we have six equations with a total of twelve unknown components; six unknown stress components and six unknown plastic strain components. The plastic strain rate can be written as:

$$\dot{\boldsymbol{\varepsilon}}^p = \dot{\lambda} \mathbf{m} \quad (2.39)$$

$\dot{\lambda}$ A variable that sets magnitude of plastic flow.

\mathbf{m} Sets the relative magnitude of the plastic flow components.

The function f has been assumed to be a function of the stress tensor, the consistency condition stated in eq. (2.35) can be written as:

$$\mathbf{n} : \dot{\boldsymbol{\sigma}} = 0 \quad (2.40)$$

$$\mathbf{n} = \frac{\partial f}{\partial \boldsymbol{\sigma}} \quad (2.41)$$

which is the gradient of the yield function, perpendicular to the yield surface at the respective stress point.

The magnitude of plastic flow may be written as:

$$\dot{\lambda} = \frac{\mathbf{n} : \mathbf{D}^e : \dot{\boldsymbol{\varepsilon}}}{\mathbf{n} : \mathbf{D}^e : \mathbf{m}} \quad (2.42)$$

As for the introduced simple slip model, a linear relation between the stress rate and the strain rate may be established:

$$\dot{\boldsymbol{\sigma}} = \left(\mathbf{D}^e - \frac{(\mathbf{D}^e : \mathbf{m}) \otimes (\mathbf{D}^e : \mathbf{n})}{\mathbf{n} : \mathbf{D}^e : \mathbf{m}} \right) : \dot{\boldsymbol{\varepsilon}} \quad (2.43)$$

Mohr – Coulomb

By utilizing eq. (2.29) and invoking the concept of an associated flow rule it can be derived that the plastic volumetric strain rate:

$$\dot{\varepsilon}_{vol}^p = \dot{\varepsilon}_1^p + \dot{\varepsilon}_2^p + \dot{\varepsilon}_3^p \quad (2.44)$$

The plastic shear deformation rate becomes:

$$\dot{\gamma}^p = \dot{\varepsilon}_3^p - \dot{\varepsilon}_1^p \quad (2.45)$$

The volumetric strain rate and the plastic shear deformation is related in the following way:

$$\dot{\varepsilon}_{vol}^p = \dot{\gamma}^p \sin \varphi \quad (2.46)$$

By introducing the Mohr-Coulomb plastic potential function, the plastic dilatancy can be avoided to some extent, and the prediction of the plastic volume change will be much better. The plastic potential function reads:

$$g = \frac{1}{2}(\sigma_3 - \sigma_1) + \frac{1}{2}(\sigma_3 + \sigma_1) \sin \psi + constant \quad (2.47)$$

Where:

ψ Is the dilatancy angle.

ψ is an independent parameter. A relation between plastic volume change and plastic shear intensity can be stated as:

$$\dot{\epsilon}_{vol}^p = \dot{\gamma}^p \sin \psi \quad (2.48)$$

that opens for the possibility to match experimental data.

2.2.3 Hardening behaviour

According to Beson et.al. [2], mechanical energy transmitted to a material in any transformation, is only partly returned. The part which is not returned is dissipated under one of the following forms:

- Temperature increase
- Phase transformation
- Heat production absorbed by the surrounding environment
- Internal structural modification of the material, e.g. creation of new cracks, slip at grain boundaries etc.

The rearrangement of the microstructure of the material during the transformation results in a new stage where mechanical properties can evolve. For perfect plasticity, and no hardening, the strain will leave the yield surface unchanged. If the strain leaves the yield surface smaller, negative hardening and softening occurs. On the other hand, if the yield surface is left bigger, positive hardening and stiffening occurs.

Materials that are exposed to plastic strains often develops a change in material properties which will have an influence on the yield strength of the material. An example of such an effect is the occurrence of yielding in the reinforcement. When stresses exceed the yield strength of the reinforcement a change in the mechanical properties occurs.

The yield function described earlier in this chapter was assumed only to be dependent on the stress tensor. By making the yield function dependent on a scalar measure of the plastic strain tensor as well, the yield function can be stated as:

$$f = f(\boldsymbol{\sigma}, \kappa) \quad (2.49)$$

In eq. (2.49) κ denotes the scalared value hardening parameter. This parameter will depend on the strain history through invariants of the plastic strain tensor $\boldsymbol{\epsilon}^p$. The hardening parameter may be defined by use of the work-hardening hypothesis:

$$\dot{\kappa} = \boldsymbol{\sigma} : \dot{\boldsymbol{\epsilon}}^p \quad (2.50)$$

The strain-hardening parameter can also be stated as:

$$\dot{\kappa} = \sqrt{\frac{2}{3} \dot{\boldsymbol{\varepsilon}}^p : \dot{\boldsymbol{\varepsilon}}^p} \quad (2.51)$$

The yield function is only dependent on the strain-history through a scalar-valued hardening parameter. The yield surface can shrink or expand, but not rotate or translate in stress space. This type of hardening behaviour is called isotropic hardening, as seen in figure 5.

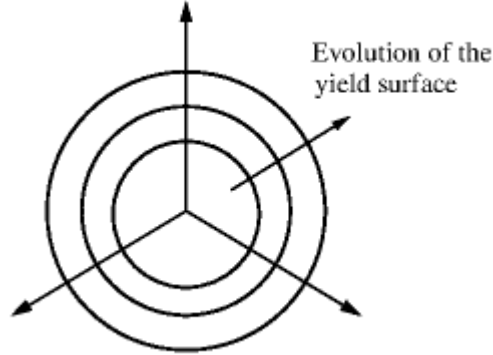


Figure 5: Isotropic Hardening

The general format for a yield function that includes isotropic and kinematic hardening may be written as:

$$f(\boldsymbol{\sigma}, \boldsymbol{\kappa}) = 0 \quad (2.52)$$

By introducing a hardening parameter in the yield function, the relation between the stress rate and the strain rate will change. The consistency condition, stated in eq. (2.35), may now be taken as follows:

$$\mathbf{n}^T \dot{\boldsymbol{\sigma}} + \left(\frac{\partial f}{\partial \boldsymbol{\kappa}} \right)^T \dot{\boldsymbol{\kappa}} = 0 \quad (2.53)$$

By introducing the hardening modulus, the consistency condition can be replaced with:

$$\mathbf{n}^T \dot{\boldsymbol{\sigma}} - h \dot{\lambda} = 0 \quad (2.54)$$

Where:

h Hardening modulus. $h = -\left(\frac{\partial f}{\partial \boldsymbol{\kappa}} \right)^T \mathbf{p}(\boldsymbol{\sigma}, \boldsymbol{\kappa})$

The hardening modulus, h regulates the plastic strain velocity in a similar manner as Young's Modulus of Elasticity, E , determines the elastic strain velocity. With *Sherman-Morrison formula*, the relation between the stress- and strain velocity can be expanded to:

$$\dot{\sigma} = \left(\mathbf{D}^e - \frac{\mathbf{D}^e \mathbf{m} \mathbf{n}^T \mathbf{D}^e}{h + \mathbf{n}^T \mathbf{D}^e \mathbf{m}} \right) \dot{\boldsymbol{\varepsilon}} \quad (2.55)$$

2.3 Integration of the Stress-Strain Relation

2.3.1 Euler Forward Integration Rule

In order to obtain stresses and strains in a structure that is combined with loading steps, eq. (2.55), must be integrated along the path of loading. A common way of doing this is to use a *one-point Euler forward* integration rule. This integration scheme is fully explicit, which means that the stresses and the value of the hardening modulus, h , are known at the beginning of the strain increment. This is very convenient because the tangential stiffness matrix may be directly evaluated. When the initial stress point, σ_0 , is located on the yield contour, the stress increment may be calculated as:

$$\Delta\sigma = \left(\mathbf{D}^e - \frac{\mathbf{D}^e \mathbf{m}_0 \mathbf{n}_0^T \mathbf{D}^e}{h_0 + \mathbf{n}_0^T \mathbf{D}^e \mathbf{m}_0} \right) \Delta\boldsymbol{\varepsilon} \quad (2.56)$$

The subscript "0" means that the quantities are evaluated at the beginning of the load step. The stress estimate in iteration $i + 1$ at the end of the loading step σ_{i+1} is given from:

$$\sigma_{i+1} = \sigma_0 + \Delta\sigma \quad (2.57)$$

If the stress point initially lies inside the yield contour, the total strain increment must then be divided into a purely elastic part and a part that involves elasto-plastic straining. The stress increment may now be calculated by the following expression:

$$\Delta\sigma = \mathbf{D}^e \Delta\boldsymbol{\varepsilon}_A + \left(\mathbf{D}^e - \frac{\mathbf{D}^e \mathbf{m}_c \mathbf{n}_c^T \mathbf{D}^e}{h_c + \mathbf{n}_c^T \mathbf{D}^e \mathbf{m}_c} \right) \Delta\boldsymbol{\varepsilon}_B \quad (2.58)$$

The subscript c means that the quantities are evaluated at $\sigma = \sigma_c$.

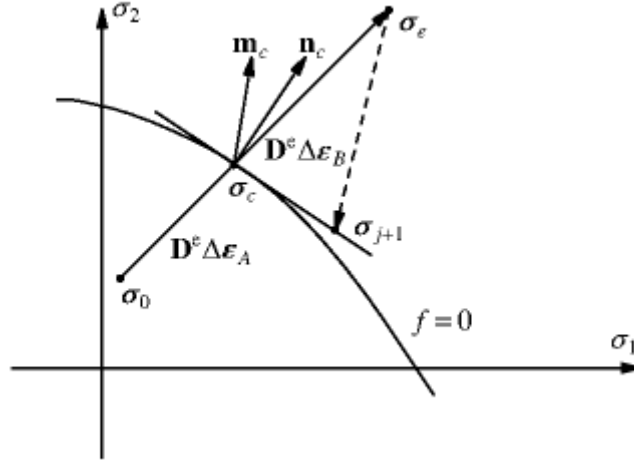


Figure 6 - Explicit integration scheme

Figure 6 is a presentation of an explicit integration scheme where the total strain increment is divided into two parts; an elastic part and a plastic part. The latter is integrated by an *Euler Forward Rule*. The *Euler Forward* method has a disadvantage, namely that the contact stresses must be calculated explicitly.

First, the elastic strain increment is calculated:

$$\Delta\sigma_e = \mathbf{D}^e \Delta\boldsymbol{\varepsilon} \quad (2.59)$$

During this increment the location of the initial stress with respect to the yield contour is irrelevant. This stress increment can be viewed upon as a trial stress increment, and within this trial stress increment the assumption of purely elastic behaviour holds, i.e. eventual plastic straining is not considered.

$$\sigma_e = \sigma_0 + \mathbf{D}^e \Delta\boldsymbol{\varepsilon} \quad (2.60)$$

Eq. (2.60) states the expression for the total trial stress increment, which is given as the sum of the stress at the beginning of the load step and the elastic strain increment. It must be evaluated whether the trial stress violates the yield condition or not, given by $f(\sigma_e, \kappa_0) > 0$. If the trial stress indeed violates the yield condition, a correction is applied. The direction and magnitude of the correction is governed by:

$$\sigma_{j+1} - \sigma_e = -\frac{\mathbf{n}_c^T \mathbf{D}^e \Delta\boldsymbol{\varepsilon}_B}{h_c + \mathbf{n}_c^T \mathbf{D}^e \mathbf{m}_c} \mathbf{D}^e \mathbf{m}_c \quad (2.61)$$

In the explicit Euler method, if the initial stress state is within the yield contour, the flow direction \mathbf{m} , the hardening modulus h and the gradient to the yield surface \mathbf{n} are computed either at the initial stress state or at the stresses at the intersection point at the elastic stress path with the yield contour σ_c . The correction process, called *predictor-plastic corrector processor*, obtain the following form:

$$\sigma_{j+1} = \sigma_e - \Delta\lambda \mathbf{D}^e \mathbf{m}_c \quad (2.62)$$

Where:

$\Delta\lambda$ Amount of plastic flow within each step, and is given by:

$$\Delta\lambda = \frac{\mathbf{n}_c^T \mathbf{D}^e \Delta\boldsymbol{\varepsilon}_B}{h_c + \mathbf{n}_c^T \mathbf{D}^e \mathbf{m}_c} \quad (2.63)$$

This type of integration method is often referred to as a *return-mapping algorithm*. This is because, initially, a trial stress state is computed under the assumption of elastic behaviour. Next, the computed trial stress is “mapped” back, i.e. projected in the yield surface direction. A problem that arises for the *Forward Euler Method* is that there is no guarantee that the trial stresses are “mapped” back to the yield surface. An error with a magnitude dependent on the curvature of the yield surface is committed. Large errors arise with a steep curved yield surface. The accumulated errors become especially large during large loading steps. This results in a decrease of the accuracy and may lead to instability in the algorithm. *Euler Forward* algorithm stability is only ensured for small loading steps, and the *Euler Forward Method* is for this reason referred to as *conditionally stable*.

2.4 Tangent Stiffness

The non-linear equations result in a tangential stiffness matrix that has an influence on the performance of the iteration method.

The dependence of the stress increment on the prescribed strain increment, within the loading step, can be conceived as a total stress-strain relationship. When a *return-mapping* algorithm as the *implicit Euler method* is used, we have a deformation theory of plasticity within a finite loading step. The tangential stiffness relation between stress- and strain rate required for a Newton-Raphson method used at a structural level, has similarities with respect to the tangential operators from a deformation theory of plasticity.

The total stress-strain relation can be formulated by the following expression:

$$\dot{\sigma} = D^e \dot{\varepsilon} - \dot{\lambda} D^e m - \Delta \lambda D^e \frac{\partial m}{\partial \sigma} \dot{\sigma} - \Delta \lambda D^e \frac{\partial m}{\partial \lambda} \dot{\lambda} \quad (2.64)$$

A pseudo-elastic stiffness matrix H given by:

$$H = A^{-1} D^e \quad (2.65)$$

And:

$$A = I + \Delta \lambda D^e \frac{\partial m}{\partial \sigma} \quad (2.66)$$

The algorithmic tangential stiffness relation between stress and strain rate can be written as:

$$\dot{\sigma} = \left(H - \frac{H \bar{m} n^T H}{h + n^T H \bar{m}} \right) \dot{\varepsilon} \quad (2.67)$$

Eq. (2.67) is called *the consistent tangential stiffness matrix*. The use of this *consistent tangential stiffness matrix* is meaningful when a full *Newton-Raphson* procedure is used to solve the set of non-linear equation on a structural level. This is due to the fact that within each load step, the magnitude of the plastic strain enters the tangential stiffness matrix.

2.5 Crack models

2.5.1 Introduction

There exist two main approaches for modeling of the cracking behavior in concrete. These two approaches are called *discrete cracking* and *smearred cracking*. In the discrete cracking approach, fracture is assumed to occur when the nodal force normal to the element boundaries is larger than the tensile capacity. New degrees of freedom are created, and a geometrical discontinuity is assumed to develop between the old node and the new node from the newly developed degrees of freedom.

For the smeared cracking approach, a cracked solid is imagined to be a continuum where the notations of stress and strain still are valid. The behavior of cracked concrete may then be described in terms of stress-strain relations, and after cracking, the isotropic stress-strain relations can be replaced by orthotropic stress-strain relations. As a result of this, the original finite element mesh is maintained after cracking. This is very efficient with respect to the computational time. The smeared cracking approach is the most used method when modeling crack behavior in concrete. For that reason, this section will describe the smeared cracking approach.

The *smearred crack* models can be divided into two subgroups, namely *fixed crack-* and *rotating crack* models. For fixed crack models, the direction of the normal of a crack remains constant after crack initiation, while for the rotating crack models, the normal of the crack may rotate during crack propagation.

2.6 Smearred crack models

2.6.1 Fixed crack models

Fixed crack models may be evaluated by total strains or by a decomposition of strains. The concept of decomposition of strains are utilized by *Multi-directional fixed crack* models. The fundamental idea of these models is the decomposition of the total strain into an elastic strain and a crack strain. The decomposition of the strain opens up for the possibility of combining the crack model with other non-linear phenomena, e.g. creep and thermal effects. In this thesis such effects shall not be studied, and for that reason multi-directional fixed crack models will not be investigated in detail.

Before cracking, it is in most cases sufficient to model concrete as an isotropic, linear elastic material, where the stresses depend on the strains in a linear manner. In a smeared crack approach, the nucleation of one or several cracks in a volume attributed to an integration point is interpreted as having a negative influence on the current stiffness and strength of that particular point. In general, a crack perpendicular to the principal stress direction will arise if the combination of stresses reaches a specific value, e.g. the principal stress reaches the tensile strength of the concrete. For a fixed crack model, the direction of the crack with respect to the principal stress direction will remain constant during cracking. After cracking, the isotropic stress-strain relation will be replaced by an orthotropic elastic-type relation with the axes of orthotropy, n and s . The n -axis is located normal to the crack direction. The s -axis is located in the tangential direction of the crack. The translation from a global x, y -coordinate system to a crack based n, s - coordinate system leads to an orthotropic stress-strain relation, with a plane stress situation which can be expressed by the following relation

$$\sigma_{ns} = \begin{bmatrix} \sigma_{nn} \\ \sigma_{ss} \\ \sigma_{ns} \end{bmatrix} = \mathbf{D}_{ns}^s \boldsymbol{\varepsilon}_{ns} = \begin{bmatrix} 0 & 0 & 0 \\ 0 & E & 0 \\ 0 & 0 & 0 \end{bmatrix} \begin{bmatrix} \varepsilon_{nn} \\ \varepsilon_{ss} \\ \varepsilon_{ns} \end{bmatrix} \quad (2.68)$$

\mathbf{D}_{ns}^s is the secant stiffness matrix.

In order to determine the stresses with respect to the global coordinate system x, y , the features of a transformation matrix \mathbf{T} must be used. The total stress-strain relation can be written as:

$$\boldsymbol{\sigma}_{xy} = \mathbf{T}^T(\phi_0) \mathbf{D}_{ns}^s \mathbf{T}(\phi_0) \boldsymbol{\varepsilon}_{xy} \quad (2.69)$$

\mathbf{T} is the transformation matrix, and can be taken as:

$$\mathbf{T} = \begin{bmatrix} \cos^2(\phi_0) & \sin^2(\phi_0) & 2\sin(\phi_0)\cos(\phi_0) \\ \sin^2(\phi_0) & \cos^2(\phi_0) & -2\sin(\phi_0)\cos(\phi_0) \\ -\sin(\phi_0)\cos(\phi_0) & \sin(\phi_0)\cos(\phi_0) & \cos^2(\phi_0) - \sin^2(\phi_0) \end{bmatrix} \quad (2.70)$$

ϕ_0 is the angle between the x -axis and the s -axis. “0” indicates a *fixed crack* model where the angle is constant.

The tangential stiffness relation is obtained by differentiating eq. (2.76), and the result is given by the following relation:

$$\dot{\sigma}_{xy} = \mathbf{T}^T(\phi_0) \mathbf{D}_{ns}^T \mathbf{T}(\phi_0) \dot{\epsilon}_{xy} \quad (2.71)$$

Eq. (2.68) describes the secant stiffness matrix without normal stiffness or shear stiffness. Because of ill-conditioning, the use of eq. (2.68) may result in convergence difficulties. We may also obtain distorted crack patterns by the use of this secant stiffness matrix. By introducing a shear modulus β into the secant stiffness matrix, one can not only reduce the difficulties related to the numerical solution procedures, but one may also aid the fixed smeared crack model to simulate the cracking process in a more realistic manner. The secant stiffness matrix with the shear modulus β can be taken as:

$$\mathbf{D}_{ns}^s = \begin{bmatrix} 0 & 0 & 0 \\ 0 & E & 0 \\ 0 & 0 & \beta G \end{bmatrix} \quad (2.72)$$

β is the shear retention factor. When choosing a β - value that equals 1,0, it is assumed that tensile strength is kept along the cracks, and no reduction when the tensile stresses reach the tensile strength is assumed. The use of the shear retention factor may help to represent the cracking pattern of the concrete more realistically because of the fact that when utilizing the shear retention factor, the locking effect and the friction in the crack can be represented in an indirect manner.

Setting the stiffness normal to the crack in eq. (2.72) equal to zero will result in a sudden drop in stress from the tensile strength f_t , to zero at crack initiation. This, as well as the lack of the shear modulus, may cause difficulties with respect to the numerical solution procedure. By a gradual decrease of the tensile capacity, more appealing results as well as more stable computations are obtained. This gradual decrease in tensile carrying capacity can be stated as:

$$\mathbf{D}_{ns}^s = \begin{bmatrix} \mu E & 0 & 0 \\ 0 & E & 0 \\ 0 & 0 & \beta G \end{bmatrix} \quad (2.73)$$

The motivation for introducing the reduced normal stiffness is that plain concrete is not a perfectly brittle material, but has some residual load-carrying capacity after reaching the tensile strength. This effect is called *tension softening*, and will be explained later on in this thesis.

Smeared crack models can be seen as *anisotropic damage* models, where both normal stiffness and the shear stiffness are reduced. This leads to the following definition, which incorporates the decrease of the Poisson effect upon cracking:

$$\mathbf{D}_{ns}^s = \begin{bmatrix} \frac{(1 - \omega_1)E}{1 - (1 - \omega_1)\nu^2} & \frac{(1 - \omega_1)\nu E}{1 - (1 - \omega_1)\nu^2} & 0 \\ \frac{(1 - \omega_1)\nu E}{1 - (1 - \omega_1)\nu^2} & \frac{E}{1 - (1 - \omega_1)\nu^2} & 0 \\ 0 & 0 & \frac{(1 - \omega_2)E}{2(1 + \nu)} \end{bmatrix} \quad (2.74)$$

, where:

$1 - \omega_1$: Represents the degradation of the normal stiffness, which can be related to the normal reduction factor μ .

$1 - \omega_2$: Represents the degradation of the shear stiffness, and is related to the factor β .

ν Poisson's ratio of the material.

2.6.2 Rotating crack models

In the previous section, the fixed crack model was described. The assumption for the fixed crack model is that the direction of the crack plane is fixed upon violation of the fracture criterion. During subsequent loading, shear strains along the crack plane can arise, which will result in an increase of shear stresses over the crack plane. The stress normal to the crack plane will be gradually reduced. However, the residual normal stress and the shear stress over the crack can cause principal values of the stress tensor that is higher than the tensile strength in a direction that differs from the normal to the crack plane. By introducing *rotating crack* models, this problem can be overcome.

Rotating crack model is also a total stress-strain relation, like the *fixed crack* model. The difference for the rotating crack model is that the direction of the principal stress and the normal to the crack, always are aligned. The angle between the x -axis and the s -axis, ϕ , will vary and is no longer constant. For *rotating crack* models there is no need to determine a secant shear stiffness because the shear stress σ_{ns} is always zero. For this model, there is only one damage variable left, which is the factor ω_1 . The secant stiffness matrix may now be written as:

$$\mathbf{D}_{ns}^s = \begin{bmatrix} \frac{(1 - \omega_1)E}{1 - (1 - \omega_1)\nu^2} & \frac{(1 - \omega_1)\nu E}{1 - (1 - \omega_1)\nu^2} & 0 \\ \frac{(1 - \omega_1)\nu E}{1 - (1 - \omega_1)\nu^2} & \frac{E}{1 - (1 - \omega_1)\nu^2} & 0 \\ 0 & 0 & 0 \end{bmatrix} \quad (2.75)$$

The total stress-strain relation obtains the following form:

$$\boldsymbol{\sigma}_{xy} = \mathbf{T}^T(\phi) \mathbf{D}_{ns}^T \mathbf{T}(\phi) \boldsymbol{\varepsilon}_{xy} \quad (2.76)$$

An important feature of the *rotating crack* model is that the local n,s coordinate system coincides with the coordinate system of the principal stresses. As a result of this, the shear stress σ_{ns} is zero, as stated above. The property where the principal directions of the stress- and strain tensors coincide throughout the cracking process is called *coaxiality* between the stress and strain tensors. This assumption of coaxiality is a useful feature in the sense that one can determine a stress-strain relation with principal values in the same coordinate system.

The tangential stiffness relation reads:

$$\dot{\boldsymbol{\sigma}}_{xy} = \left[\mathbf{T}^T(\phi) \mathbf{D}_{ns} \mathbf{T}(\phi) + \frac{\partial \mathbf{T}^T(\phi)}{\partial \phi} \boldsymbol{\sigma}_{ns} \frac{\partial \phi^T}{\partial \boldsymbol{\varepsilon}_{xy}} \right] \dot{\boldsymbol{\varepsilon}}_{xy} \quad (2.77)$$

The tangential stiffness matrix for the rotating crack model is more complicated due to spin of the principal axes. The expression for the tangential stiffness matrix may be stated as follows:

$$\mathbf{D}_{xy} = \left[\mathbf{T}^T(\phi) \frac{\partial \boldsymbol{\sigma}_{ns}}{\partial \boldsymbol{\varepsilon}_{ns}} \mathbf{T}(\phi) + \frac{\partial \mathbf{T}^T(\phi)}{\partial \phi} \boldsymbol{\sigma}_{ns} \frac{\partial \phi^T}{\partial \boldsymbol{\varepsilon}_{xy}} \right] \quad (2.78)$$

The first term of eq. (2.85) is equal to the tangential stiffness that follows from the *fixed* approach, and may be considered as a material tangent stiffness. The second term follows from the principal axes spin, and can be considered as a function of the stresses and the angle ϕ between the crack coordinate system and the global coordinate system. (Feenstra and de. Borst [9]).

The stress-strain relation in the n,s - coordinate system can be derived by:

$$\begin{bmatrix} \sigma_{nn} \\ \sigma_{ss} \\ \sigma_{ns} \end{bmatrix} = \begin{bmatrix} \mu E & 0 & 0 \\ 0 & E & 0 \\ 0 & 0 & \frac{\sigma_{nn} - \sigma_{ss}}{2(\varepsilon_{nn} - \varepsilon_{ss})} \end{bmatrix} \begin{bmatrix} \varepsilon_{nn} \\ \varepsilon_{ss} \\ \varepsilon_{nt} \end{bmatrix} \quad (2.79)$$

The tangential shear stiffness $\frac{\sigma_{nn} - \sigma_{ss}}{2(\varepsilon_{nn} - \varepsilon_{ss})}$ follows from the requirement of coaxiality between the stress and the strain tensors.

The decision whether to choose a *fixed crack* model or a *rotating crack* model depends highly on the problem at hand. The *rotating crack* model is the preferred model in cases with localized cracking because it provides less stress-locking than the *fixed crack* model. For smeared cracking in reinforced concrete structures, shear across fixed cracks may be of relevance. If this is the case, then the *fixed crack* model provides more possibilities of modelling that. (Hendriks and Rots [12]).

2.7 Material models

With today's development of finite-element computer programs, the difficulty related to modelling the behavior of reinforced concrete remains one of the most challenging tasks in the field of structural concrete engineering. (Chen [4]). The stress-strain relationship of concrete is modeled in a separate manner for tension and compression. Hendriks et al. [11] suggests using a parabolic curve to describe the hardening and softening of concrete in compression. For the tensile behavior, an exponential softening diagram is preferred. The parameters for this material model are the tensile strength f_{ct} , the fracture energy G_f and the equivalent length h_{eq} . In absence of an exponential softening curve, a multi-linear approximation of the exponential uniaxial stress-strain diagram may be used. For the compressive behavior it is recommended a parabolic stress-strain diagram with a softening branch in order to limit the maximum compressive stress. The softening branch is recommended to be based on the compressive fracture energy G_c in order to reduce mesh sensitivity.

2.7.1 Concrete in tension

The assumption of zero stiffness normal to the crack leads to a rapid decrease in tensile stresses from the tensile strength of the concrete, f_{ct} to zero at crack initiation. This rapid decrease in tensile stresses is somewhat unrealistic, and may just as well lead to numerical instability, as stated in section 2.6.1. Tests have shown that in plane concrete, the stress-strain graph will gradually decrease after cracking of the concrete. This phenomenon is called *tension-softening*, and is taken into account when modeling the tensile behavior of plane concrete.

In DIANA10, the tensile behavior of reinforced concrete may be modeled by using different approaches. For the *Total Strain crack* model, six softening functions that are based on fracture energy is implemented. Some of these are shown in the figure below.

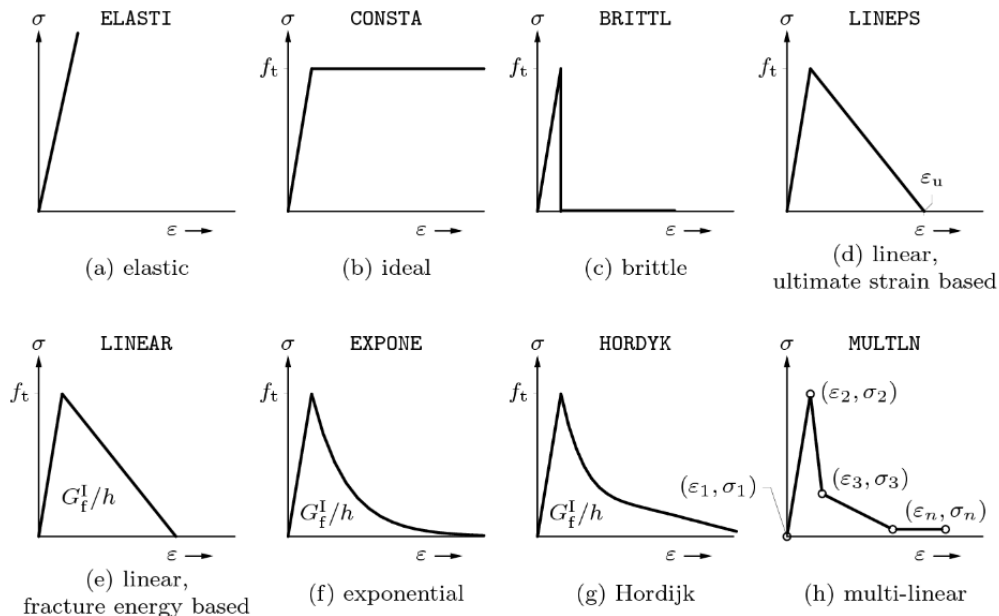


Figure 7 - Predefined tension softening curves TSC model. (TNO DIANA [18])

A similar way of modelling the gradual decrease of the stress-strain diagram after concrete cracking is called *tension stiffening*. This phenomenon is related to the effect of concrete acting in tension between cracks on the stress of steel reinforcement. (Allam et.al. [1]). At the location of a crack, all

the internal tensile force is carried by the reinforcement. Between the cracks, some tensile force is transferred by bond to the concrete surrounding the bar. This results in an increase in reinforcement strains, and causes the reinforcement strains at the uncracked location to be less than the reinforcement strains at the cracked location.

Both the *tension softening* and the *tension stiffening* models represent the gradual decrease of the stress-strain diagram of the concrete. However, the two models differ regarding the explanation of the phenomenon of decreasing tensile stress. The *tension-softening* model assumes a gradual decrease of tensile stresses caused by damage of concrete sections, while the *tension stiffening* model assume that the concrete between the cracks contribute to the stiffness, and is only valid for reinforced concrete structures.

As mentioned previously, an exponential softening curve was recommended. This curve is provided in DIANA10 as the “EXPONE” curve in Figure 7. When choosing this curve for tension in DIANA10, the analyst is asked to provide the fracture energy G_f , the tensile strength f_{ct} and alternatively the crack bandwidth. Since the area under the curve should correspond to $\frac{G_f}{h}$, where h denotes the crack bandwidth, it is sufficient to input the tensile strength and the fracture energy. The crack bandwidth is calculated automatically by DIANA10 since “EXPONE” is a so called predefined curve. According to (fib Model Code 2010 [11]), the fracture energy of concrete is defined as the required energy to propagate a tensile crack of unit area. It should be determined by tests, but in the absence of experimental data, the fracture energy G_f can be calculated by the following expression:

$$G_F = 73 f_{cm}^{0,18} \text{ [N/m]} \quad (2.80)$$

Where f_{cm} is the mean compressive strength:

$$f_{cm} = f_{ck} + \Delta f \quad (2.81)$$

And $\Delta f = 8 \text{ MPa}$.

As an alternative, Hendriks et.al. [11] also proposes a calculation procedure for the fracture energy. The fracture energy can be calculated by the following formula:

$$G_F = G_{F0} \left(\frac{f_{cm}}{f_{cm0}} \right)^{0.7} \quad (2.82)$$

, where the parameter G_{F0} depends on the maximum aggregate size D_{max} . Values for G_{F0} are listed in Table. 1.

Table 1 - Values of G_{F0}

D_{\max} [mm]	G_{F0} [Nmm/mm]
8	0,025
16	0,030
32	0,058

DIANA calculates the crack bandwidth automatically, but the analyst is provided the opportunity to input the value for the crack bandwidth manually as well. The equivalent length, i.e. the crack bandwidth, should be based on the element dimensions and the directions of the cracks. For linear two-dimensional elements, the crack bandwidth can be taken as:

$$h = \sqrt{2A} \quad (2.83)$$

And for higher order two-dimensional elements:

$$h = \sqrt{A} \quad (2.84)$$

In eq. (2.83) and (2.84), A denotes the total area of the element.

2.7.2 Concrete in compression

In a *Total Strain crack* model, the behavior of the concrete is in general nonlinear between the stress and the strain in a given direction. DIANA10 offers predefined compression curves, or the compressive behavior may be customized by the use of multi-linear curve.

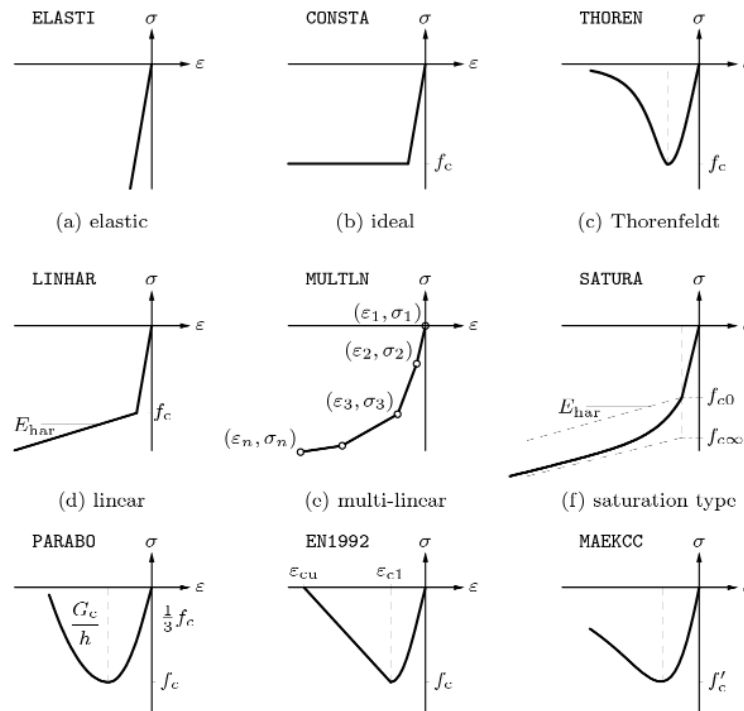


Figure 8 - Predefined compression curves for Total Strain models (TNO DIANA [18])

Figure 8 represents some of the predefined compressive curves. Hendriks et. al. [11] recommends a parabolic function in compression. The parabolic curve is based on the fracture energy by the definition of the crack bandwidth of the element, where DIANA10 assumes a value h with respect to the square root of the element area. The area under the parabolic curve should correspond to $\frac{G_c}{h}$, where G_c denotes the compressive fracture energy, which can be calculated with respect to the fracture energy G_F :

$$G_c = 250G_F \quad (2.85)$$

Different factors in which have an influence on the compressive behavior may also be specified, i.e. a *confinement model*. Concrete subjected to compressive stresses exhibits a behavior that is dependent on the pressure, meaning that the strength and ductility increase with increasing isotropic stress. This effect is called *lateral confinement*. Furthermore, the compressive behavior may be influenced by *lateral cracking*. In order to simplify the compression curve, the *confinement model* can be neglected by selecting “no increase” for the *confinement model*.

2.8 Reinforcement

The reinforcement used in the models is ordinary reinforcement. The nonlinear effect of strain hardening will be taken into account. The reinforcement is modeled individually as bar elements in each model. An important aspect of this thesis is to investigate the problem regarding *bond-slip* reinforcement, i.e. when we no longer have perfect bonding conditions between the reinforcing bar and the surrounding concrete. The basic theory regarding *bond-slip* reinforcement will be presented later on in the chapter, while the modelling procedure will be presented in part II of this thesis.

2.8.1 Embedded reinforcement

As default, DIANA10 assumes the reinforcement to be *embedded*, which means that the bond between the reinforcing bar and the surrounding concrete is “perfect”. The basic idea of embedded reinforcement is that the internal virtual work consists of two different contributions, where the stresses in the reinforcement and the concrete can be split into two separate parts. This results in a separate stress-strain relation for the reinforcement and the concrete. The reinforcement can be modelled with elasto-plastic models which includes hardening behavior, and the concrete can be modelled with any material model and include nonlinear effects such as cracking. The main assumptions regarding embedded reinforcement reads:

- Embedded in structural elements
- No degrees of freedom
- Strains are computed from the displacement field of the structural element in which the reinforcement is embedded. With other words the reinforcing bar is exposed to the same strain situation as a concrete element aligned with the bar.

These assumptions seem sufficient during the un-cracked stage, but may not be sufficient any longer when we enter the cracked stage.

2.8.2 Bond-slip reinforcement

General

In order to describe the interaction and transfer of force between concrete and reinforcement, the term bond is used (fib Model Code 2010 [11]). The bond has a major influence on the performance of reinforced concrete structures. In the serviceability limit state, bond influences the width and spacing of transverse cracks, curvature and tension stiffening.

When damage around bars take place in reinforced concrete structures the structural behaviour is changed and the bond between the concrete and the reinforcing bars are no longer perfect (Brisotto et.al. [3]). At the concrete-steel interface, two evident damage processes can be highlighted. The first occurs when the concrete close to the reinforcing bars is not sufficiently confined by pressure or transverse reinforcement, causing a so called *splitting failure*. This process is the result of the development of cracks emerging from the bar, along the length of the bar. Eventually these cracks will propagate outwards, which reduces the mechanical interlock due to rib bearing. Another source to splitting is the reduction of the bar diameter due to yielding in the steel. The second type of damage occurs when a good level of confinement is provided and is caused by concrete crushing between the ribs. The damage process is completed when the concrete in between the ribs is sheared off, and it is called *pull-out failure*. For this kind of failure, the bond stresses are much higher, and the failure occurs at a much higher level of slip than for the splitting failure. The failure by pull-out is for that reason considered to be less brittle than failure by splitting.

Different laws of bond-slip

In the modelling procedure of reinforced concrete elements, different bond-slip laws may be assumed. There does not however, exist any fundamental law for modelling the bond-slip for reinforced concrete elements since it depends on the entire system's boundary condition. (Tejchman and Bobinski [17]). In order to consider the bond-slip behaviour, it is assumed an interface with zero thickness along a surface, where a relationship between the slip and the shear traction is introduced. Several types of bond-slip laws may be applied. In this thesis, two types of bond-slip laws were investigated.

One of the bond-slip laws that were investigated was proposed by Dörr. In DIANA10, this law is referred to as *Cubic Function by Dörr*. The following relation between the slip and the shear friction applies for this type of bond-slip law:

$$\tau = f_t \left[5 \left(\frac{u}{u_1} \right) - 4.5 \left(\frac{u}{u_1} \right)^2 + 1.4 \left(\frac{u}{u_1} \right)^3 \right] \quad \text{when } 0 < u \leq u_0 \quad (2.86)$$

And:

$$\tau = \tau_{max} = 1.9 f_t \quad \text{when } u > u_1 \quad (2.87)$$

Where:

τ : Denotes the bond stress.

τ_{max} Is the bond resistance.

f_t Tensile strength of the concrete.

u_1 Displacement at which perfect slip occurs. Tejchman and Bobinski [17] recommends the value for $u_1 = 0.06 \text{ mm}$.

Equation (2.86) and (2.87) describes the slip curve shown in Figure 9.

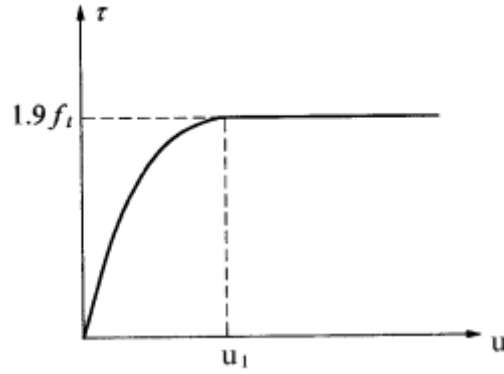


Figure 9 - Cubic function by Dörr, (Tejchman and Bobinski [17])

The second approach for the modelling of bond-slip corresponds to the *local bond-slip relationship* derived from fib Model Code 2010. In DIANA10, this approach is denoted *user defined friction stress-slip diagram*. According to fib Model Code 2010 [11], for monotonic loading, the bond stresses between the concrete and the reinforcing bar can be taken as a function of the relative displacement s , and may be derived by the use of the following formulas:

For $0 \leq s \leq s_1$:

$$\tau_0 = \tau_{max} \left(\frac{s}{s_1} \right)^\alpha \quad (2.88)$$

For $s_1 \leq s \leq s_2$:

$$\tau_0 = \tau_{max} \quad (2.89)$$

For $s_2 \leq s \leq s_3$:

$$\tau_0 = \tau_{max} - (\tau_{max} - \tau) \frac{s - s_2}{s_3 - s_2} \quad (2.90)$$

For $s_3 < s$:

$$\tau_0 = \tau_f \quad (2.91)$$

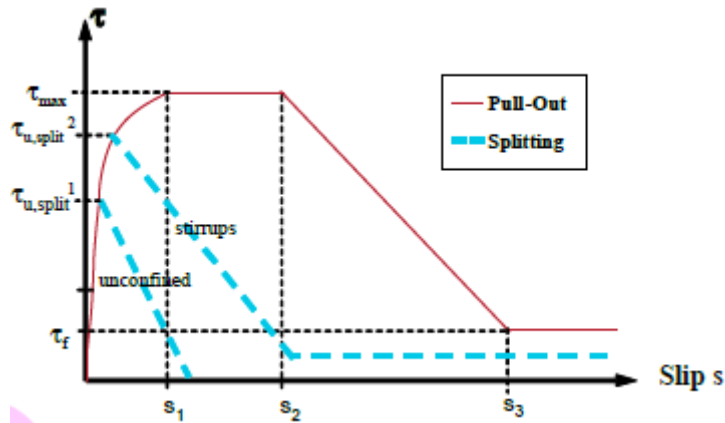


Figure 10 - Bond stress-slip relationship, (fib Model Code 2010 [11])

In parts of the structure where the reinforcement is subjected to compression, and in un-cracked concrete parts subjected to tension, the concrete and the reinforcement strain are equal. In cracked parts of the structure, the tension forces in the crack are transferred by the reinforcing bar. The absolute displacements of the steel and the concrete between two cracks are in general different. Due to the relative displacements, bond stresses develop between reinforcement and concrete. The development of these stresses depend on the surface of the reinforcing steel, the slip s , the compressive concrete strength f_{cm} and the localization of the reinforcing steel during casting. Furthermore, it is considered that a part of the tension force acting in the reinforcement between cracks, are transferred to the concrete by bond. This effect is called *tension stiffening*, and is described in section 2.7.1.

In order to determine the stress-slip curve, a table consisting of various parameters was used. This table takes into account the failure mode that is being investigated, i.e. *pull-out* or *splitting* failure, and different parameters apply for these two failure modes.

Table 2 - Parameters for defining mean bond stress-slip curve, (fib Model Code 2010, [11])

Pull-out failure		
	Good bonding conditions	All other bonding conditions
τ_{max}	$2.5\sqrt{f_{ck}}$	$1.25\sqrt{f_{ck}}$
s_1	1.0 mm	1.8 mm
s_2	2.0 mm	3.6 mm
s_3	c_{clear}	c_{clear}
α	0.4	0.4
τ_f	$0.4\tau_{max}$	$0.4\tau_{max}$

c_{clear} : Clear distance between reinforcement bar ribs

2.9 Elements

2.9.1 Plane stress elements

Flat plane stress elements, also known as *membrane elements* are common to use for modelling of structures where the loading takes place in plane. The coordinates of the element nodes must be located in the x, y -plane of the element.

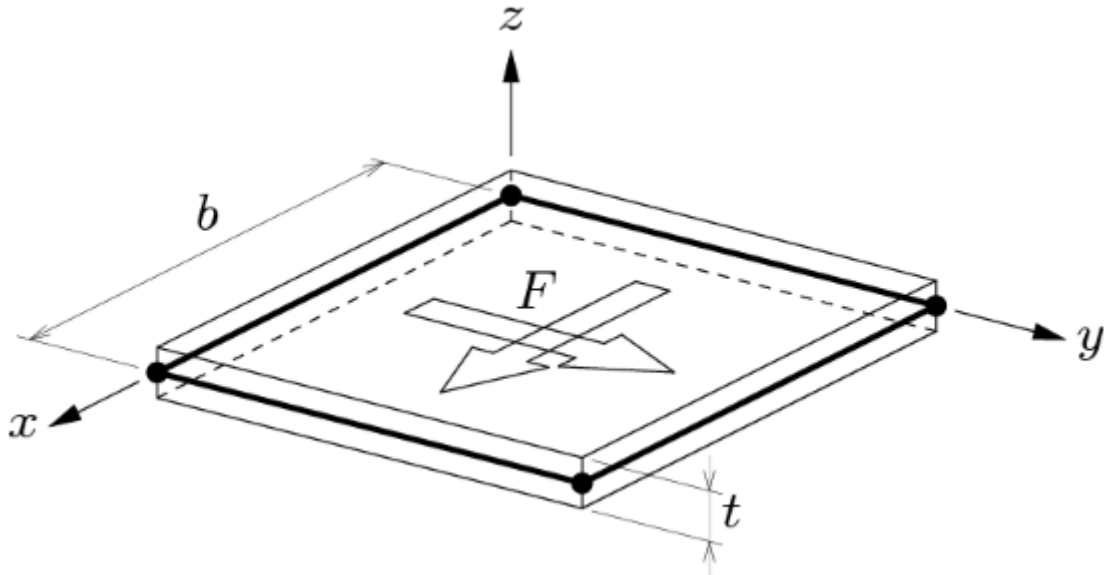


Figure 11 - Characteristics of a plane stress element, (TNO DIANA [18])

In plane stress elements, the stresses perpendicular to xy -plane, σ_{zz} , are equal to zero. These type of elements are only applicable for structures where no out-of-plane bending takes place.

4-noded quadrilateral

The *Q8MEM* as it is called in DIANA10, is a 4-noded quadrilateral plane stress element.

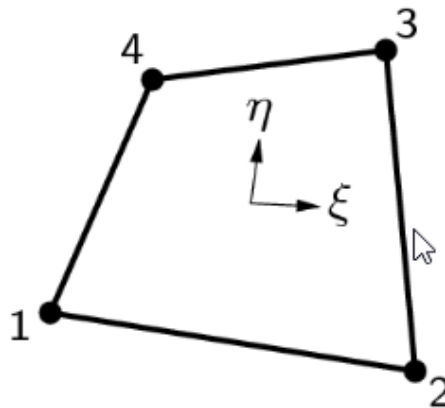


Figure 12 - 4-Noded Quadrilateral Element, (TNO DIANA [18])

The element has two translational degrees of freedom per node, and is based on Gauss integration and linear interpolation. The shape functions can be expressed as:

$$u_i(\xi, \eta) = a_0 + a_1\xi + a_2\eta + a_3\xi\eta \quad (2.92)$$

A full gauss quadrature rule for this element would correspond to 2 x 2 integration points, and a reduced gauss quadrature rule would correspond to 1 x 1 integration points. As a default, DIANA10 applies 2 x 2 integration points, which correspond to the “Regular” integration scheme.

8-noded quadrilateral

In DIANA10, the 8-noded quadrilateral is denoted CQ16M. The element is an isoparametric plane stress element and has in total 8 nodes with two translational degrees of freedom per node.

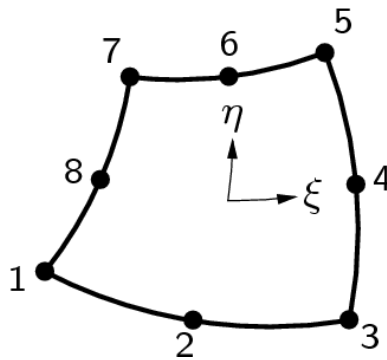


Figure 13 - CQ16M: 8-noded plane stress element. (TNO DIANA [18])

The element is based on quadratic interpolation and Gauss integration. The shape functions of the CQ16M element can be expressed as:

$$u_i(\xi, \eta) = a_0 + a_1\xi + a_2\eta + a_3\xi\eta + a_4\xi^2 + a_5\eta^2 + a_6\xi^2\eta + a_7\xi\eta^2 \quad (2.93)$$

The polynomial expressed in eq. (2.93) yields a strain ϵ_{xx} which varies linearly in x-direction and quadratically in y-direction. The strain ϵ_{yy} varies quadratically in y-direction and linearly in x-direction. The shear strain γ_{xx} varies quadratically in both x- and y-direction. The optimal sampling points for stresses corresponds to a 2 x 2 gauss quadrature rule, which is applied as a default by DIANA10.

2.9.2 Interface elements

In DIANA10, modelling of geometric discontinuities like the bond-slip layers in reinforced concrete, is commonly carried out with the use of *structural interface elements*. The idea of these type of elements is that the forces acting on the interface are related to the relative displacements on each side of the interface, as shown in figure 14.

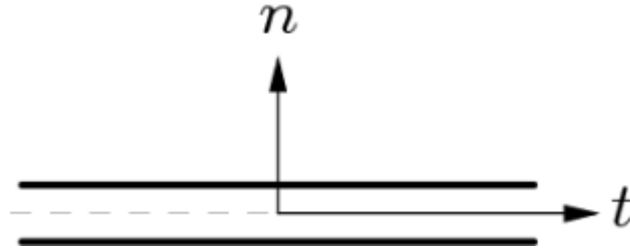


Figure 14: Two-dimensional interface element, (TNO DIANA [18])

For the two-dimensional situation, the traction vector \mathbf{t} is defined as:

$$\mathbf{t} = \begin{Bmatrix} t_n \\ t_t \end{Bmatrix} \quad (2.94)$$

The relative displacements, $\Delta \mathbf{u}$, can further be taken as:

$$\Delta \mathbf{u} = \begin{Bmatrix} \Delta u_n \\ dt \end{Bmatrix} \quad (2.95)$$

The linear relation between the traction and the displacement vector is governed by the following equation:

$$\begin{Bmatrix} t_n \\ t_t \end{Bmatrix} = \begin{bmatrix} k_n & 0 \\ 0 & k_t \end{bmatrix} \begin{Bmatrix} \Delta u_n \\ dt \end{Bmatrix} \quad (2.96)$$

The general constitutive relation, which is assumed linear between increments, can now be written as:

$$\dot{\mathbf{t}} = \mathbf{D} \Delta \dot{\mathbf{u}} \quad (2.97)$$

\mathbf{D} is the tangential stiffness matrix, $\dot{\mathbf{t}}$ is the traction vector and $\Delta \dot{\mathbf{u}}$ contains the relative displacements.

2.9.3 Bond-slip interface elements

In the previous section, structural interfaces were presented. This was done in order to describe the idea behind interface elements and how the interface forces are related to the relative displacement. However, for bond-slip reinforcements in 2D, these structural interface elements are not utilized.

According to DIANA [18], one of the differences between bond-slip reinforcement and embedded reinforcement is that bond-slip reinforcement must be defined as either beam or truss elements. This is accomplished by assigning *Element Data*. The implementation of the bond-slip interface from the .dat-file is seen in Figure 15.

```
'DATA'
 1 INTEGR REGULA
  | BUBBLE
 2 INTERF TRUSS
  | BEGINN 3722
  | ENDNOD 3745
 3 INTERF TRUSS
  | BEGINN 3746
  | ENDNOD 3793
```

Figure 15: Bond-slip interface implementation in a .dat-file

“DATA” represents the element data for the model. Element data 1 is assigned to the concrete elements, and applies “BUBBLE”, which is an integration scheme described in 5.4. Element data 2 and 3 are assigned to the reinforcing bars. “BEGINN” denotes the start node of the reinforcement, and “ENDNOD” denotes the end node of the reinforcement. “INTERF” specifies the element type used to model bond-slip reinforcements, which in this case is truss. These truss elements are connected to the mother element, i.e. the concrete element. No integration schemes can be assigned to bond-slip reinforcements. The applied truss element for the bond-slip reinforcements uses the default integration scheme of a truss element.

The type of element that is used for the bond-slip reinforcement is automatically determined by DIANA10:

Table 3: Interface elements bond-slip reinforcement (TNO DIANA [18])

Mother Element	INTERF TRUSS	INTERF BEAM
Q8MEM	L4TRU	L7BEN
Q16MEM	CL6TR	CL9BE

The mother element denotes the element type used for the concrete mesh. Q8MEM and Q16MEM are quadrilateral elements, described in 2.9.1.

2.9.4 Truss Elements

Truss elements, or bars as they also may be named, must fulfil the condition that the dimension d perpendicular to the axis, are small compared to the length of the bar.

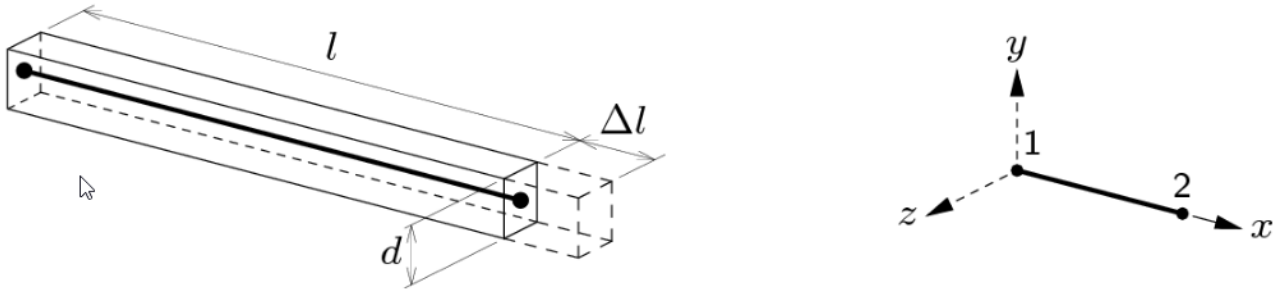
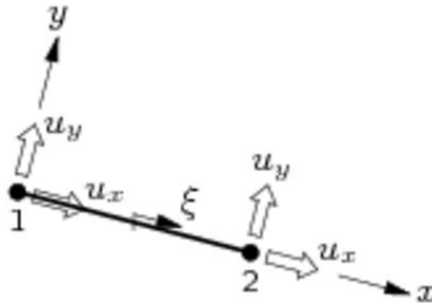


Figure 16 - Truss element with corresponding coordinate system, (TNO DIANA [18])

The truss element may only be subjected to an axial deformation, and no shear nor bending deformation takes place. Truss elements are well suited for modelling discrete reinforcement bars.

Four noded truss element

The L4TRU is an enhanced truss element in the DIANA10 element library. In addition to the two degrees of freedom in x-direction, this element has two degrees of freedom in the y-direction. This makes the element useful in two-dimensional analysis.



The shape functions of the L4TRU element can be expressed as:

$$u_i(\xi) = a_0 + a_1\xi \quad (2.98)$$

3. Numerical solution methods

3.1 Iterative procedures

In this section the general steps in an iterative procedure will be briefly discussed. " In all iterative procedures, the total displacement increment Δu is adapted iteratively by iterative increments d_u until equilibrium is reached, up to a certain prescribed tolerance." (TNO DIANA, [18]). The incremental displacements at iteration $i + 1$ is calculated as follows:

$$\Delta u_{i+1} = \Delta u_i + \delta u_{i+1} \quad (3.1)$$

There are several iteration procedures at hand. The difference between them is how δu_{i+1} is solved for. The iterative increments are calculated by using a "stiffness matrix" K , which represents a linear relation between the force vector and the displacement vector. The stiffness matrix can change every iteration, and the stiffness matrix being used in iteration i is denoted K_i .

$$\delta u_i = K_i^{-1} g_i \quad (3.2)$$

Equation (3.2) describes a direct approach to determine the iterative increments. g_i denotes the out-of-balance force vector at the end of increment i .

In the next section the different iteration methods that is available in DIANA10 will be described. The first three methods that are presented are the *Newton-Raphson* method, the *Quasi-Newton* method and the *Constant Stiffness* method. Furthermore, two variations, *Continuation* and *Line Search* will be described. These two variations can be used in combination with the three methods mentioned above.

Within the class of Newton-Raphson methods, it is usually distinguished between two sub methods: *Regular Newton-Raphson* and *Modified Newton Raphson*. Both methods can be used to solve for the iterative increment displacement vector. In general for a Newton-Raphson method, the stiffness K_i represent the tangential stiffness of the structure, and can be written as:

$$K_i = \frac{\partial g}{\partial \Delta u} \quad (3.3)$$

3.1.1 Regular Newton-Raphson

In a regular Newton-Raphson method, the stiffness relation from eq. (3.3) is evaluated after every iteration.

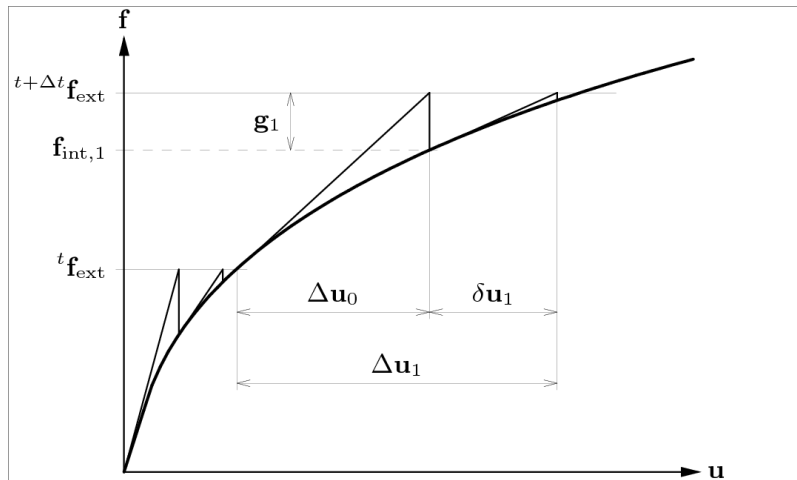


Figure 17 - Regular Newton-Raphson iteration, (TNO DIANA [18])

The regular Newton-Raphson method provides quadratic convergence, which means that the method needs few iterations in order to converge towards a “correct” solution. A regular Newton-Raphson method requires relatively few iterations, but the iterations are on the other hand time consuming.

3.1.2 Modified Newton-Raphson

In a modified Newton-Raphson method, the stiffness relation from eq. (3.3) is only evaluated at the start of the increment.

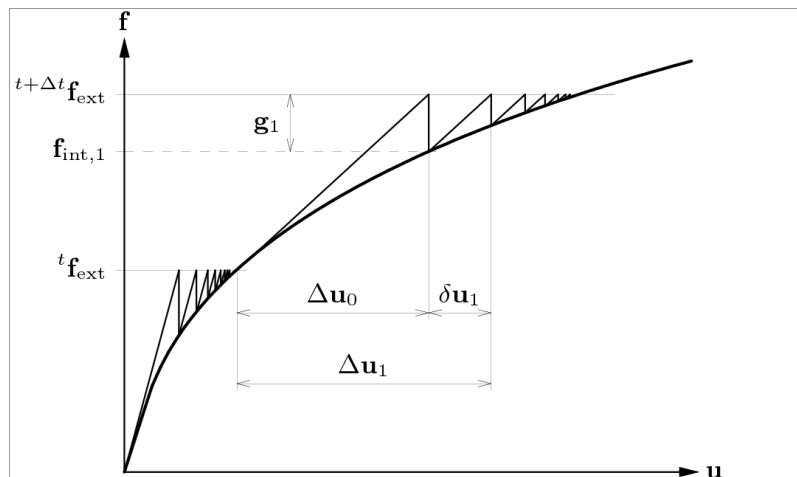


Figure 18 - Modified Newton-Raphson iteration, (TNO DIANA [18])

The modified Newton-Raphson Method usually converges slower towards the «correct» solution than the Regular Newton-Raphson method. However, for the Modified Newton-Raphson method, it is not necessary to set up a new stiffness matrix after every iteration. This means that there will be more iterations, but the iterations are less time consuming.

3.1.3 Quasi-Newton

The quasi-newton method, often referred to as *the Secant Method*, uses information of previous solution vectors and out-of-balance force vectors during the increment in order to accomplish a better approximation. Unlike the Regular Newton-Raphson method, the Quasi-Newton method does not establish completely new stiffness matrix every iteration.

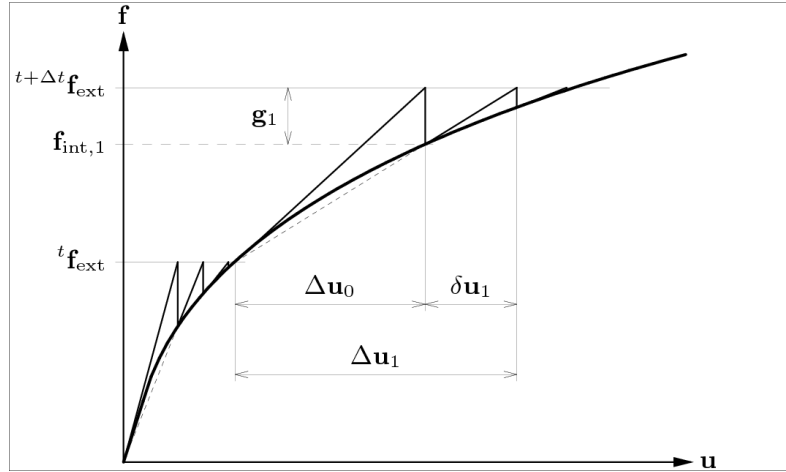


Figure 19 - Quasi-newton iteration, (TNO DIANA [18])

Quasi-Newton usually converges slower than regular Newton-Raphson, but faster than Modified Newton-Raphson.

The Quasi-Newton relation can be expressed as:

$$K_{i+1} \delta u_i = \delta g_i \quad (3.4)$$

Where g_i represents the change in out-of-balance force vector related to the increment:

$$\delta g_i = g_{i+1} - g_i \quad (3.5)$$

Now, with a stiffness matrix K_i that fulfills the requirements from eq. (3.4), the iterative displacement can be calculated from

$$\delta u_i = K_i^{-1} g_i. \quad (3.6)$$

Three different variations of the Quasi-Newton method are implemented in Diana10. These three are called *Broyden*, *Broyden-Fletcher-Goldfarb-Schanno* (BFGS) and *Chrisfield* methods. By substitution it can be shown that the matrices stated below satisfy the Quasi-Newton relation

$$K_{i+1} = K_i + \frac{(\delta g_i - K_i \delta u_i) c^T}{c^T \delta u_i} \quad (3.7)$$

$$K_{i+1} = K_i + \frac{(\delta g_i - K_i \delta u_i) c^T + c(\delta g_i - K_i \delta u_i)^T}{c^T \delta u_i} - \frac{(\delta g_i - K_i \delta u_i)^T \delta u_i c c^T}{(c^T \delta u_i)^2} \quad (3.8)$$

3.1.4 Broyden

If c is substituted with δu and K_{i+1} is inverted, the Broyden method results in:

$$K_{i+1}^{-1} = K_i^{-1} + \frac{(\delta u_i - K_i^{-1} \delta g_i) \delta u_i^T K_i^{-1}}{\delta u_i^T K_i^{-1} \delta g_i} \quad (3.9)$$

3.1.5 Broyden-Fletcher-Goldfarb-Schanno(BFGS)

Eq. (3.9) yields the following relation:

$$K_{i+1}^{-1} = \left(I + \frac{\delta u_i \delta g_i^T}{\delta u_i^T \delta g_i} \right) K_i^{-1} \left(I - \frac{\delta g_i \delta u_i^T}{\delta u_i^T \delta g_i} \right) + \frac{\delta u_i \delta u_i^T}{\delta u_i^T \delta g_i} \quad (3.10)$$

The relation stated in eq. (3.10) is known as the BFGS method.

For the BFGS method the secant stiffness matrices are not calculated explicitly. Instead the iterative displacements δu are calculated directly by substituting eq. (3.9) or eq. (3.10) into eq. (3.6). By use of eq. (3.9) and eq. (3.10), the correct secant stiffness matrix can be calculated from an update vector and K_0 . K_0 denotes the stiffness matrix that is used at the beginning of the increment.

3.1.6 Chrisfield method

According to Chrisfield [5], it has been developed a range of “more efficient Modified Newton-Raphson iterations or Secant-Newton techniques”, and these are relatable to the BFGS procedure presented in the previous section. These techniques were suggested in order to avoid increasing computational time required for Broyden or BFGS methods.

All three Quasi-Newton methods can be utilized irrespectively of the stiffness matrix K_0 . K_0 can in this case be the tangential stiffness matrix as used in Figure 19, but it could just as well be the linear elastic stiffness matrix. With respect to convergence rate, these methods usually lay between the convergence rate of the Regular Newton Raphson and the Modified Newton Raphson schemes. (TNO DIANA, [18]). This is also valid for the time consumption. For Broyden and BFGS schemes, the increase in number of iterations result in an increase in time consumption and memory.

3.1.7 Linear and constant stiffness iteration

These iteration methods can be applied if the methods described above, i.e. Newton-Raphson become unstable.

Linear stiffness iteration

This iteration method uses the linear stiffness matrix at every iteration. This method might have the slowest convergence, but it is very “cheap” with respect to computational time since the stiffness matrix only need to be established once. The Linear Stiffness method is useful when it is desired that the linear stiffness matrix remains symmetric where the tangential stiffness matrix would become un-symmetric.

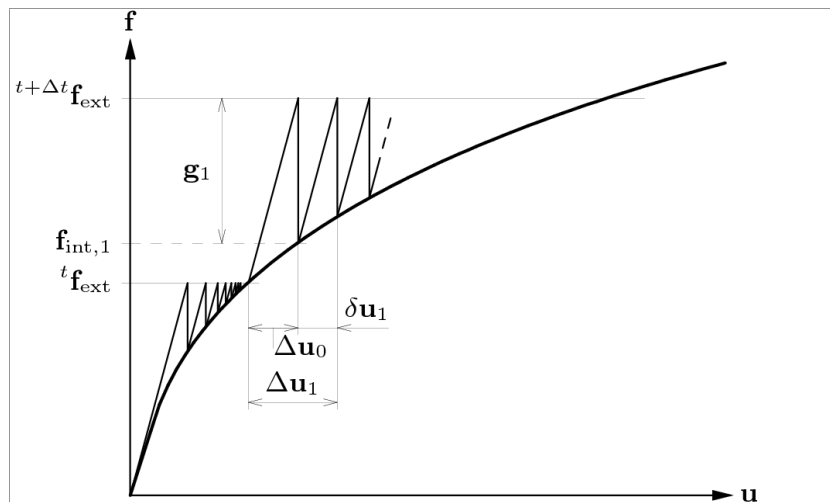


Figure 20 - Linear Stiffness iteration, (TNO DIANA [18])

Constant stiffness

The Constant Stiffness method utilizes the stiffness matrix obtained from the previous increment. This means that if Newton-Raphson iterations are used during the first phase of an analysis, and Constant Stiffness iterations are used in the second phase, the stiffness in the latter would be equal to the stiffness calculated in the last step of the first analysis phase. If Constant Stiffness iterations are used for all steps it corresponds to the Linear Stiffness Method.

3.1.8 Line Search

There are variations that can be combined with ordinary iteration procedures in order to improve the Finite Element Solution. In DIANA10, it is possible to enable both *Line Search* and *Continuation Iteration*. The Line Search option is well suited for situations involving rapid changes in tangent stiffness, i.e. in a reinforced concrete analysis where the concrete cracks or the reinforcement starts to yield. The basic idea of the line search method is to apply an improvement to the original incremental displacement vector by scaling it by a multiplier, and in that way arrive at the point of lowest potential energy along the search direction. (De Borst et.al. [7]). Continuation Iteration is well suited for continuous deformation processes. The Line Search method does not only accelerate the iterative process, but they may also provide convergence where it would be impossible to obtain

convergence without line search. (Mathisen [14]). This option is highly recommended and it may be applied in all types of Newton methods, i.e. standard, modified and quasi Newton methods.

3.2 Convergence criteria

A convergence criterion is a measurement of the accuracy of the obtained solution, or how well the obtained solution satisfies equilibrium. In nonlinear finite element analysis, the convergence criteria are based on some norm of either displacements, residuals, force or energy. The convergence criteria have the ability to terminate a step when convergence occurs, but they are also capable of controlling that the iterative procedures stop during a step if a certain amount of iterations have been exceeded or the iterative procedures leads to divergence. Also, in DIANA10, the analyst is provided with the option that the iterative procedures continue although convergence is not obtained within the respective step.

When setting up the analysis with the convergence criteria, one should proceed with caution. According to Mathisen [14], the displacement based convergence criterion is in general not advisable due to the fact that a slow convergence rate can lead to a misleadingly satisfaction of the criteria. On the other hand, the residual based criteria are by far more reliable than the displacement criteria as they monitor that equilibrium has been obtained within a prescribed tolerance in the current increment. The energy based criterion combined with both displacement criterion and residual criterion is possible, although the energy criterion should not be applied when line search is used.

Convergence criteria and tolerances should be set up and chosen in such a way that the solution is accurate, and at the same time “economical”. The balance lies between a “too strict” and a “too loose” convergence criteria. With a strict criterion, the results obtained will be very accurate, but at the same time the computational time needed to obtain this “unnecessarily” accurate solution may be large. With a loose criterion the results will be inaccurate. The number of load steps also play an important role when it comes to accuracy.

3.3 Load versus Displacement Control

The process where the load is applied to the structure in a number of steps is called *load control*. Another way of analyzing the response of the structure is to prescribe displacements in increments. This is called *displacement control*. These prescribed displacements cause a development of stresses within the specimen. These stresses will in turn result in nodal forces at the nodes where the displacements are prescribed. (De Borst et.al.[7]). By summing all of the nodal forces the total reaction force is obtained. The total reaction force equals the external load that would be caused by the prescribed displacement.

For many cases a prescribed displacement will be the natural choice. When there is no preference for either of the two from a physical point of view, the latter, displacement control, is often to be preferred. The main reasons why displacement control is preferred are:

- For displacement control there is often faster convergence in the iterative procedure than for load control. This is related to the fact that the tangential stiffness matrix is better conditioned for the displacement control option.
- The tangential stiffness matrix becomes singular at a limit point in the load-displacement diagram for load control. This will happen not only for global failure, but also for maximum local along the curve as seen in figure 21. For displacement control however, the tangential stiffness matrix does not become singular.

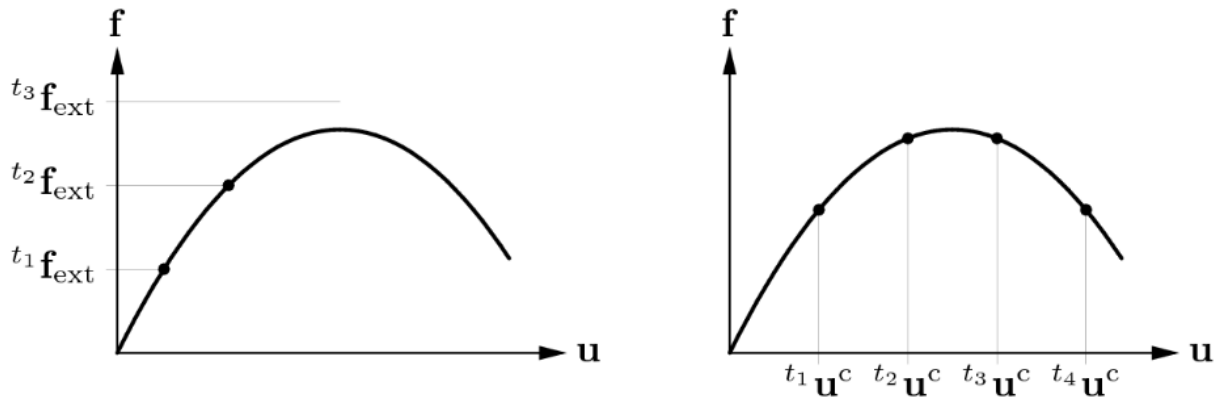


Figure 21 – Load control and displacement Control, (TNO DIANA [18])

An important difference, and an advantage for displacement control with respect to load control, is that load control requires the inversion of the matrix \mathbf{K} . On the other hand, for displacement control, only the reduced stiffness matrix has to be inverted.

When applying displacement control to the analysis, the external force vector is not increased directly. In order to obtain a proper prediction of the initial displacements, we must incorporate the prescribed displacements in the external force vector. By rewriting eq. (3.4) and splitting the displacement increment vector into two parts, the effective force may be calculated. We now get the following relation:

$$\begin{bmatrix} \mathbf{K}^{uu} & \mathbf{K}^{uc} \\ \mathbf{K}^{cu} & \mathbf{K}^{cc} \end{bmatrix}_0 \begin{Bmatrix} \Delta \mathbf{u}^u \\ \Delta \mathbf{u}^c \end{Bmatrix}_0 = \begin{Bmatrix} \mathbf{g}^u \\ \mathbf{g}^c \end{Bmatrix}_0 \quad (3.11)$$

The unknown displacement $\Delta \mathbf{u}^u$ is calculated by the first row from eq. (3.11):

$$\Delta \mathbf{u}_0^u = (\mathbf{K}^{uu})^{-1} \{-\mathbf{K}^{uc}_0 \Delta u^c + \mathbf{g}_0^c\} \quad (3.12)$$

In eq. (3.15), the term $(-\mathbf{K}^{uc}_0 \Delta u^c)$ is considered as the *effective force vector*. The iterative increments of the prescribed displacements in subsequent iterations are zero, and for that reason the effective force vector vanishes.

For the finite element analyses performed in this thesis, the displacement control option was found to be the more reliable compared to load control, hence displacement control was used in the analyses of the concrete panels.

4. Calculation of crack width and crack spacing

This section describes how cracking of concrete is being dealt with by different regulations. Two codes were used to illuminate the rules that apply for cracking in reinforced concrete. By considering two different codes, more data that could be compared with the calculation of crack widths based on the results from the nonlinear analyses would be obtained.

4.1 Eurocode 2

Rules regarding cracking of reinforced concrete is described in chapter 7 in Eurocode 2 [16]. It is stated that cracking shall be calculated in order to prevent that the structure's functionality or resistance is injured, or that it leads to an unacceptable appearance.

In section 7.3.4 in Eurocode 2, it is given formulas for how to calculate the crack width, w_k :

$$w_k = s_{r,max} (\varepsilon_{sm} - \varepsilon_{cm}) \quad (4.1)$$

$s_{r,max}$: Is the maximum crack spacing.

ε_{sm} : Denotes the average strain in the reinforcement including the effect of applied deformations where the influence of an increase in stiffness between cracks are taken into account.

ε_{cm} : Is taken as the average strain in the concrete between cracks.

The value of $\varepsilon_{sm} - \varepsilon_{cm}$ can be calculated as follows:

$$\varepsilon_{sm} - \varepsilon_{cm} = \frac{\sigma_s - k_t \frac{f_{ct,eff}}{\rho_{p,eff}} (1 + \alpha_e \rho_{p,eff})}{E_s} \geq 0,6 \frac{\sigma_s}{E_s} \quad (4.2)$$

σ_s : The stress in the longitudinal reinforcement under the assumption of a cracked cross-section.

α_e : The relationship between the modulus of elasticity in steel and concrete, E_s/E_{cm}

$\rho_{p,eff}$: With bar reinforcement only: $\rho_{p,eff} = A_s/A_{c,eff}$

$A_{c,eff}$ Effective tension area of the concrete.

k_t : A factor that is dependent on the duration of the loading.

- $k_t = 0,6$ short term loading
- $k_t = 0,4$ long term loading

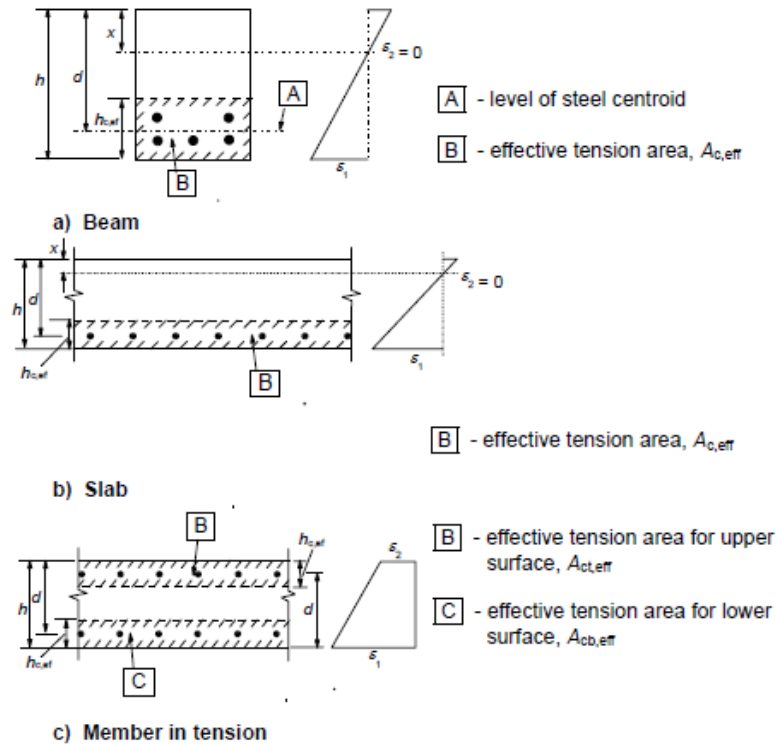


Figure 22 - Effective tension area. (Eurocode 2, [16])

The maximum crack spacing, $s_{r,max}$ is calculated by:

$$s_{r,max} = k_3 c + k_1 k_2 k_4 \frac{\phi}{\rho_{p,eff}} \quad (4.3)$$

ϕ : Bar diameter.

c : The cover of the longitudinal reinforcement.

k_1 : Coefficient which takes into account the bond properties of the bonded reinforcement:

- $k_1 = 0,8$ for high bond bars.
- $k_1 = 1,6$ for bars with effectively plain surfaces e.g. prestressing reinforcement.

k_2 : Coefficient that takes into account the strain distribution

- $k_2 = 0,5$ for bending
- $k_2 = 1,0$ for pure tension

k_3, k_4 : Values for these coefficients should be taken from the National Annex. The recommended values are however 3,4 and 0,425, respectively

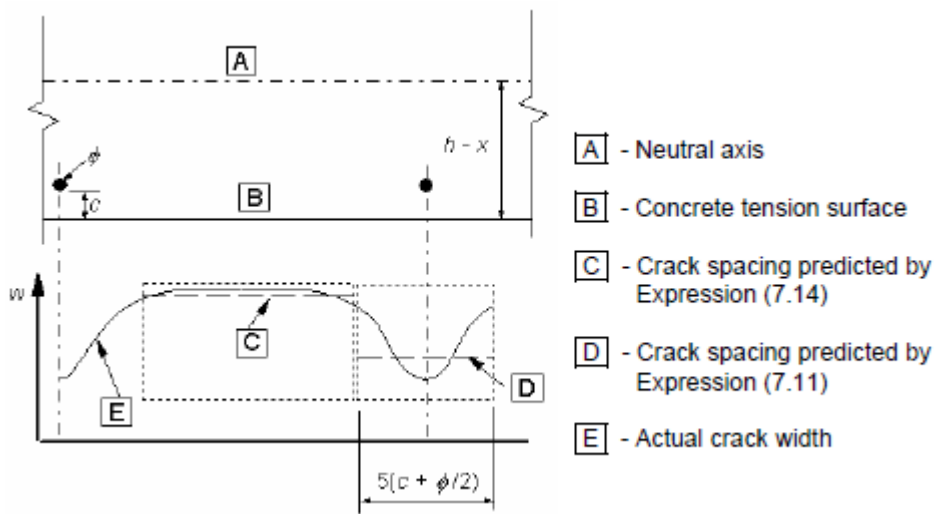


Figure 23 - Crack width at concrete surface relative to distance from reinforcing bar (Eurocode 2,[16])

In the case that the spacing of the bonded reinforcement exceeds $5 \left(c + \frac{\phi}{2} \right)$ or there is no bonded reinforcement within the tension zone, one can calculate an upper bound of the crack width with the assumption of a maximum crack spacing:

$$s_{r,max} = 1,3 (h - x) \quad (4.4)$$

For members with orthogonal reinforcement, or where the angle between the axes of principal stress and the direction of the reinforcement is significant, the crack spacing $s_{r,max}$ may be calculated as follows:

$$s_{r,max} = \frac{1}{\frac{\cos \phi}{s_{r,max,y}} + \frac{\sin \phi}{s_{r,max,z}}} \quad (4.5)$$

Where:

ϕ : is the angle between the direction of the principal tensile stress and the reinforcement in the y-direction.

$s_{r,max,y}, s_{r,max,z}$: the crack spacing calculated in the y-direction and the z-direction respectively, from eq. (4.3).

4.2 fib Model code 2010

“It should be ensured that, with adequate probability, cracks will not impair the serviceability and durability of the structure” (fib Model Code 2010, [11]).

Cracks do not necessarily indicate a lack of durability or serviceability in reinforced concrete structure. Cracking may be inevitable in reinforced concrete structures due to tension, shear, bending or torsion caused by direct loading or restraint of imposed deformations. The design of crack widths can satisfy requirements regarding functionality, durability or appearance.

The calculation of crack width is based on the basic case of a prismatic reinforced concrete bar subjected to pure tension only. In total, four stages of behavior are distinguished during the increase of tensile strain:

- Uncracked stage
- Crack initiation stage
- Crack stabilizing stage
- Yielding of steel stage

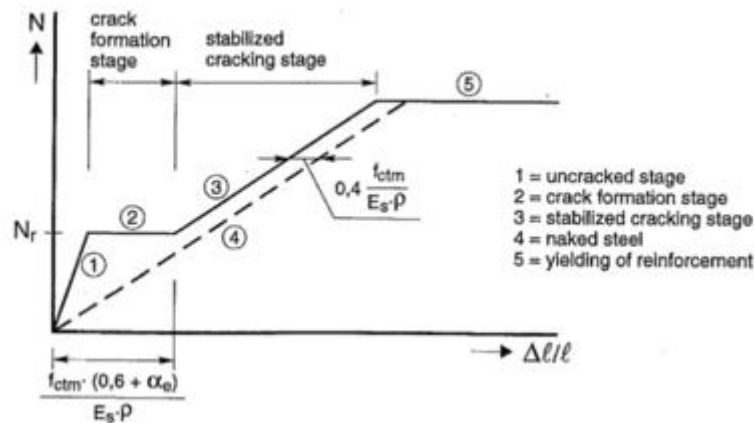


Figure 24 - Load-strain relation centrally reinforced member subjected to tension (fib Model Code 2010 [11])

Figure 24 describes a simplified representation of the cracking behaviour. In stage (2) the normal tensile force does not increase because of “fall-back behaviour” when new cracks develop. In this stage, the maximum crack width is obtained any time that the tensile force reaches the cracking load. If such a large amount of cracks has developed that there are no more undistributed areas, the tensile strength of the concrete between the cracks cannot be reached anymore, and this results in no new crack development. This initiates the crack stabilizing stage, stage (3). For calculation of the crack it is necessary to determine which stage that applies, whether it is the crack formation stage or the stabilized cracking stage, which is the stage where no new cracks develop, but the existing cracks propagate. The figure above shows a simplified representation of the different cracking stages, and according to this simplification, the stabilized cracking stage is applicable when the load N is larger than the cracking load N_r . For imposed deformation, the crack formation stage is applicable when the strain satisfies

$$\varepsilon \leq \frac{f_{ctm} (0,6 + \alpha_e)}{E_s \rho} \quad (4.6)$$

Where:

α_e : the modular ratio, $\alpha_e = \frac{E_s}{E_c}$.

f_{ctm} : the mean tensile strength [MPa].

If eq. (4.6) is not fulfilled, the stabilized cracking stage applies. If only imposed deformation occurs, the crack formation stage applies.

The cracking load, N_r is taken as follows:

$$N_r = A_c f_{ctm} (1 + \alpha_e \rho_{s,eff}) \quad (4.7)$$

In Figure 24, the crack formation stage is represented by a horizontal curve, corresponding with the constant cracking force, N_r . This curve would more accurately be represented by an inclined curve, within the range of $f_{ct,0.05}$ to $f_{ct,0.95}$. Many uncertainties are involved when calculating the crack widths, e.g. accuracy regarding reinforcement placement, real tensile strength of the concrete etc., and therefore this approximation with the horizontal curve is considered to be accurate enough.

For all stages of cracking, the design crack width may be calculated according to:

$$w_d = 2l_{s,max} \cdot (\varepsilon_{sm} - \varepsilon_{cm} - \varepsilon_{cs}) \quad (4.8)$$

$$l_{s,max} = k \cdot c + \frac{1}{4} \cdot \frac{f_{ctm}}{\tau_{bm}} \cdot \frac{\phi_s}{\rho_s} \quad (4.9)$$

Where:

$l_{s,max}$: De-bonding length. Length where slip between concrete and steel occurs: within this length, steel and concrete strains occur, and these will contribute to the crack width.

ε_{sm} : Average steel strain over the length $l_{s,max}$.

ε_{cm} : Average concrete strain over the length $l_{s,max}$.

ε_{cs} : Concrete strain caused by shrinkage

k : Factor that takes into account the influence of concrete cover. As a simplification, this factor can be set equal to 1,0.

c : Concrete cover

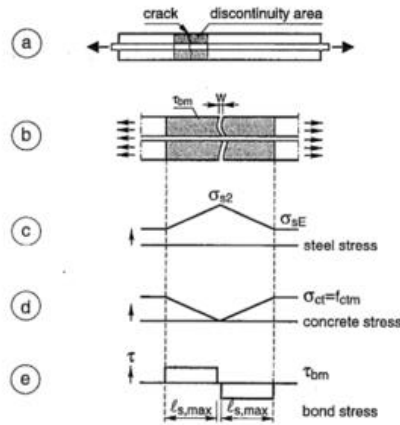


Figure 25 - Transmission of forces in a distributed area next to a crack, (fib Model Code 2010 [11])

Part (a) of figure 25 shows a *centrally reinforced tensile member with crack*. Part (b) describes the *discontinuity area*. Further the *steel stress development in discontinuity area* is shown in part (c). *Concrete stress development in discontinuity area and development of bond stress in discontinuity area* are presented in part (d) and part (e), respectively.

In general, the value for the maximum crack width may be calculated by the following expression

$$w_d = 0,5 \cdot \frac{\Phi_s}{\rho_{s,ef}} \cdot \frac{f_{ctm}}{\tau_{bm}} \cdot (\sigma_s - \beta \cdot \sigma_{sr} + \eta_r \cdot \varepsilon_r \cdot E_s) \quad (4.10)$$

$$\sigma_{sr} = \frac{f_{ctm}}{\rho_{s,ef}} (1 + \alpha_e \rho_s) \quad (4.11)$$

$$\rho_{s,ef} = \frac{A_s}{A_{c,ef}} \quad (4.12)$$

, where:

- σ_s : Steel stress in a crack.
- σ_{sr} : Maximum steel stress in a crack in stage 2 (crack formation stage).
- $A_{c,ef}$: Effective area of concrete.
- τ_{bm} : Mean bond strength between concrete and reinforcement.
- α_e : Modular ratio (E_s / E_c)
- β : Coefficient to assess main strain over the length $l_{s,max}$
- η_r : Coefficient that takes into account the influence of shrinkage

Values for τ_{bm} , β and η_r depend on the loading conditions and the relevant cracking stage and are stated in the table below:

Table 4 – Values for τ_{bm} , η_r and β for deformed reinforcing bars. (fib Model Code 2010 [11])

Loading type	Crack formation stage	Stabilized cracking stage
Short term, instantaneous loading	$\tau_{bm} = 1,8f_{ctm}(t)$ $\beta = 0,6$ $\eta_r = 0$	$\tau_{bm} = 1,8f_{ctm}(t)$ $\beta = 0,6$ $\eta_r = 0$
Long term, repeated loading	$\tau_{bm} = 1,35f_{ctm}(t)$ $\beta = 0,6$ $\eta_r = 0$	$\tau_{bm} = 1,8f_{ctm}(t)$ $\beta = 0,4$ $\eta_r = 1,0$

4.2.1 Reinforcement with an angle to the principal stress axis

When a member is reinforced in two orthogonal directions, and the cracks are expected to develop in an angle that is much larger than the angle of the reinforcement, one may assess approximations when calculating the value for the length, $l_{s,max}$. The following expression may be assessed:

$$l_{s,max} = \frac{1}{\frac{\cos(\theta)}{l_{sx,k}} + \frac{\sin(\theta)}{l_{sy,k}}} \quad (4.13)$$

And following the calculation of the crack width:

$$w_d = 2 \cdot l_{s,max,\theta} \cdot (\varepsilon_{\perp} - \varepsilon_{c,\perp}) \quad (4.14)$$

Where:

θ : The angle between the reinforcement in x-direction and the direction of the principal tensile stress.

$l_{sx,k}$, $l_{sy,k}$: Slip lengths in orthogonal directions. These two can be calculated from eq. (4.9).

ε_{\perp} , $\varepsilon_{c,\perp}$: Total mean strain and the total mean concrete strain.

Part II: Modeling

General

Part two of this thesis will be about all the modeling challenges and decisions that were made. Both of the two models will be described. In order to get an overview over the entire modelling procedure, the geometry, supports/boundary conditions, finite element mesh and load attachment of the two panels will be described. Next, the material properties chosen in the two different models will be presented.

5. Concrete panels TP1 and TP2

5.1 Python scripting

The compatibility with python scripts is one of the new features implemented in DIANA10. Another new feature in DIANA10 is that both pre-processing and post-processing may be carried out in the same working environment. The new post-processor is called DIANA Native. The modelling procedure was mainly performed with the use of *python-scripting*. The reason for this is that it makes editing of geometry, material parameters, analysis settings etc. more convenient. With the use of *python-scripting*, changing parameters becomes easier and the analyst has full control over what is happening with the model. All the python scripts used in this thesis is attached in Appendix A.

Python was used to establish the numerical models. In earlier versions of DIANA10 the .dat file was normally used to change parameters. Instead of importing a .dat-file, you can now run a python script and the model will be built up piece by piece on screen. When importing a .dat file in DIANA10 you end up in a state where you can no longer edit the geometry. After running a python script, you can still edit geometry and material properties with the user interface. Python scripting has a huge advantage over the .dat-file method at this point.

The TP1 panel with horizontal reinforcement was modeled only with the use of python-scripts. The process of parameter study would go like this. The original python script was made. The script was run in DIANA10, and would appear on screen. The user interface could then be used to change aspects of the model like geometry, supports, loads and so on. DIANA10 writes python codes in the command console every time a parameter is changed. The python code would then be copied and pasted into the original python script. After changing several parameters, it would simply be a matter of commenting out the code that was unwanted in the current version of the model. When a model was ready to be analyzed, a second python script would be prepared. This script would contain all the analysis settings that were needed. This would include the load steps, iteration method, post processing and other necessary settings. Running this second script would make DIANA10 start the analysis and when it finished it would write the displacement and reaction forces to two separate text files. Results from the text files were copied into excel and a graph was made to represent the load displacement curve.

For TP2 with diagonal reinforcement the same procedure was followed, but the tying functions were impossible to implement into the python scripts. Instead, the model had to be exported to a .dat file, the tying commands were written manually, and then imported back into DIANA10. After that, a script with analysis settings could be run to start the analysis.

5.2 Geometry

TP1

The concrete panel denoted TP1 is the panel with horizontal reinforcement only. “TP” is short for “Tension Panel”, and the dimensions of the panel are: $B \times H \times T = 630 \times 630 \times 100 \text{ mm}$. The geometry of panel TP1 with reinforcement positions is shown in figure 26. The concrete panel was modelled as one single sheet. The reinforcement bars were modeled as seven lines, starting and ending on the edge of the sheet. Although the modelling was performed in two dimensions, a thickness has to be prescribed nonetheless. This thickness is then prescribed to the element geometries.

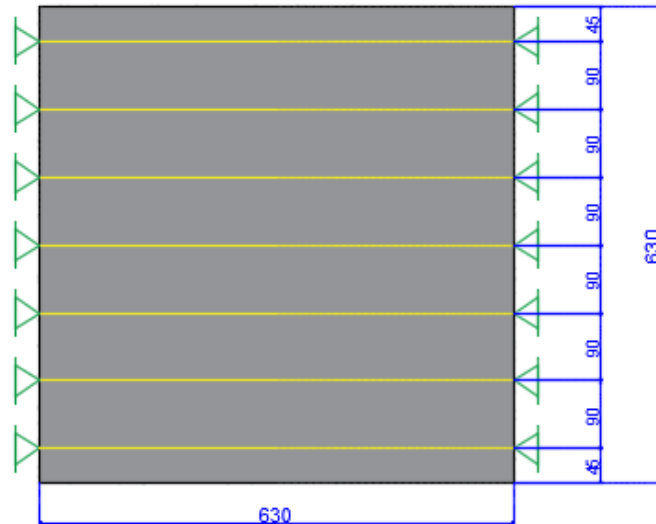


Figure 26 - Geometry TP1

TP2

The panel denoted TP2 is the panel with the orthogonal reinforcement grid oriented in a 45-degree angle. Both of the panels have the same external dimensions, it is only the reinforcement layout that differs. As for TP1, the reinforcement spacing $P2$ is also 90 mm. Figure 27 shows the geometry of panel TP2. A for loop was used to place all of the bars at the right places.

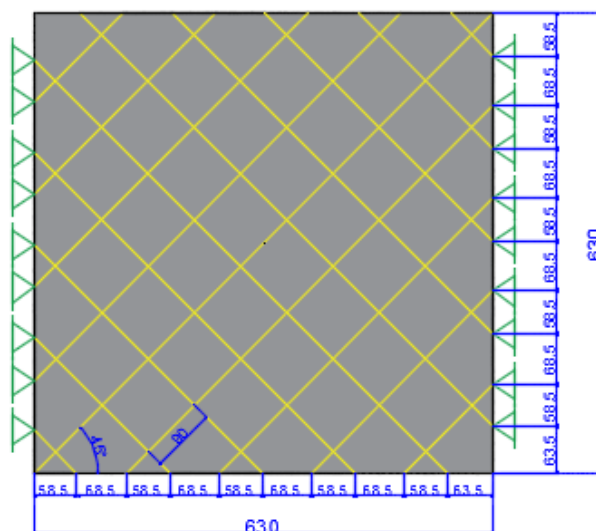


Figure 27: Geometry TP2

5.3 Supports and tyings

TP1

All the reinforcement bars of TP1 are restrained against translation in the global x- and y-direction. When assigning bond-slip reinforcement, the reinforcement bars obtain degrees of freedom for themselves, unlike for the default setting of embedded reinforcement, in which the reinforcement bars have no degrees of freedom. The fact that the reinforcement bars obtain own degrees of freedom after meshing makes it possible to attach a loading directly to the reinforcing bar.

TP2

For TP2, the support conditions are a bit more complicated. Figure 27 shows which reinforcement start or end node that is restrained against translation in x- and y- direction. The other start and end nodes are not exactly pinned, which would mean that translation can take place. Instead they are tied to nearby concrete nodes with an option called *tyings*. In DIANA [18], tyings are defined as linear constraints. These linear constraints are user specified linear dependencies between degrees of freedom of the system of equations. These linear dependencies are specified in the input table “TYINGS” in the .dat file. A Single point tying was used for the reinforcement nodes on the upper and lower edge of the panel. A recipe for assigning tyings between the reinforcement and the concrete nodes can be found in “Modelling Script TP2”.

5.4 Mesh and element types

In the finite element models for TP1 and TP2 the same element sizes and element types are used. For a 2D analysis of this case with tension loading only, there are mainly two choices for element type that seem relevant. The first one is a four node linear element with added incompatible displacement modes. The incompatible displacement modes are added to the shape functions of the element with the function *bubble* in DIANA10. This is an element data property, which is related to integration schemes of the element. The bubble-function adds four incompatible strain modes to the elements. The purpose of adding the bubble-function to the 4-noded quadrilateral linear element is to prevent shear locking in the elements, and to make sure that the obtained solution is not too stiff. The second option is the 8 node quadratic element. The 8-noded element has in total 16 degrees of freedom opposed to the 4-noded element with only 8 degrees of freedom. In a fine mesh the increasing number of degrees of freedom requires many more equilibrium equations, and the computational time also increases. Only 4-noded elements with bubble-function were used in the analyses because of good performance and low computational cost.

The meshing was done with an element size that was set to $h/60$, resulting in an element size of 10,5 mm. this decision was in compliance with Hendriks et.al [12], who recommends a maximum element size:

$$\min\left(\frac{l}{50}, \frac{b}{50}\right).$$

5.5 Loads

The load is applied in the x-direction on the right hand side in the reinforcement end-nodes, as seen in figure 28. In order to recreate the laboratory experiment performed by Dyngeland [8] in the best and most accurate way possible, it was chosen to attach the loading to the reinforcement bars only. Furthermore, to ensure an as stable analysis as possible, displacement control was used, i.e. attaching a prescribed displacement to the reinforcement end nodes. As mentioned earlier, when using bond-slip reinforcement, independent reinforcement nodes are created after the meshing procedure is performed, and it is then possible to attach a loading to these particular nodes. If embedded reinforcement is used, the reinforcement bars obtain no degrees of freedom, and no load can be attached directly to the reinforcement.

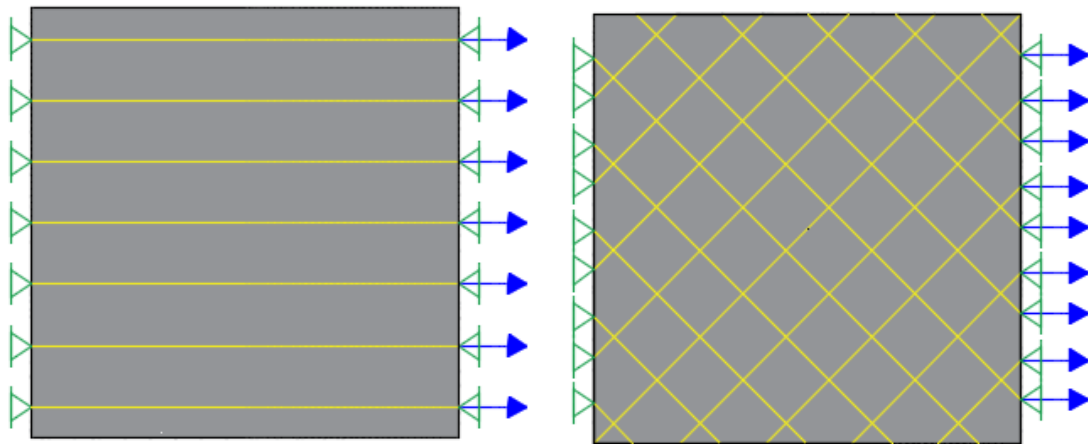


Figure 28 - Load attachment TP1 and TP2

5.6 Material properties

In this section follows an overview over which material properties that were used for both concrete and steel in the two numerical models for the concrete panels TP1 and TP2. The concrete is given properties regarding behavior in tension and compression. The reinforcement is assigned a yield strength and hardening parameters.

5.6.1 Reinforcement

In Dyngeland [8], KS400 reinforcement was used in both tension panels. The elastic modulus E_s of the reinforcement was set to 210000 MPa. The yield stress f_y was set to 403 MPa. There were no measurements of the ultimate strength of the reinforcement. Graphs describing the stress-strain relation for KS400 was found in Svenska Cementföreningen [15]. Base on those graphs a simplified bilinear stress-strain relation shown in Figure 29

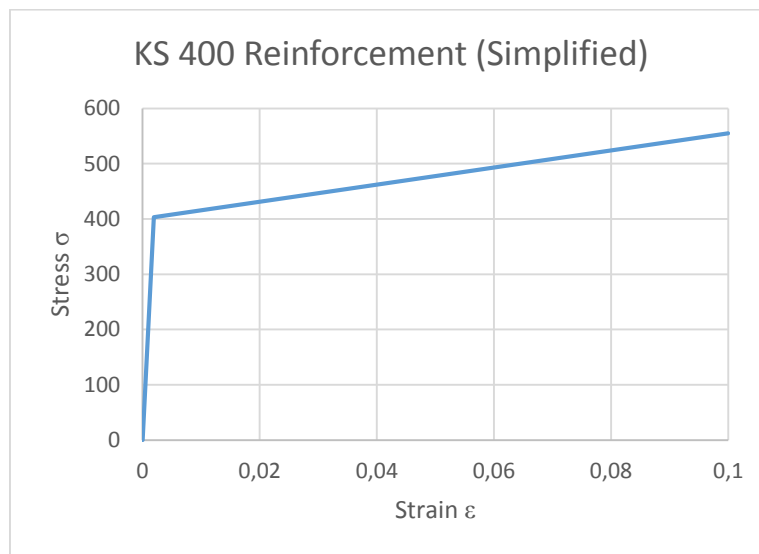


Figure 29: Stress-Strain relation KS400

Table 5: Tabulated values Stress-strain curve KS400

KS400	
Elastic Modulus E_s	210000 Mpa
Yield Strength f_{yd}	403 Mpa
Ultimate strength f_u	555 Mpa
Ultimate strain ϵ_u	0,1

5.6.2 Bond slip reinforcement

A user defined bond-slip model was chosen for the reinforcement. The bond-slip curve was calculated according to fib Model Code 2010 [11]. It was assumed good bonding conditions, and the stress-slip diagram below was calculated by eq. (2.96) -eq. (2.99), see 2.8.2. Also, the cubic bond-slip relation by Dörr was also investigated. The cubic bond-slip formulation will be compared with the fib Model Code 2010 bond-slip formulation. For this bond-slip model the values for the slip and bond stress had to be calculated. In the area of 0 mm slip to 1,0 mm slip, values for the slip and bond stress were calculated for every 0,1 mm. This gave a nice shape on the bond stress-slip curve. For the fib Model Code 2010 bond-slip model requires the clear distance between ribs to be supplied. According to Svenska Cementföreningen [15], for 8 mm bars, the rib distance is 6,0 mm.

For the concrete panel TP1 and TP2, the following user defined bond-slip curves were used:

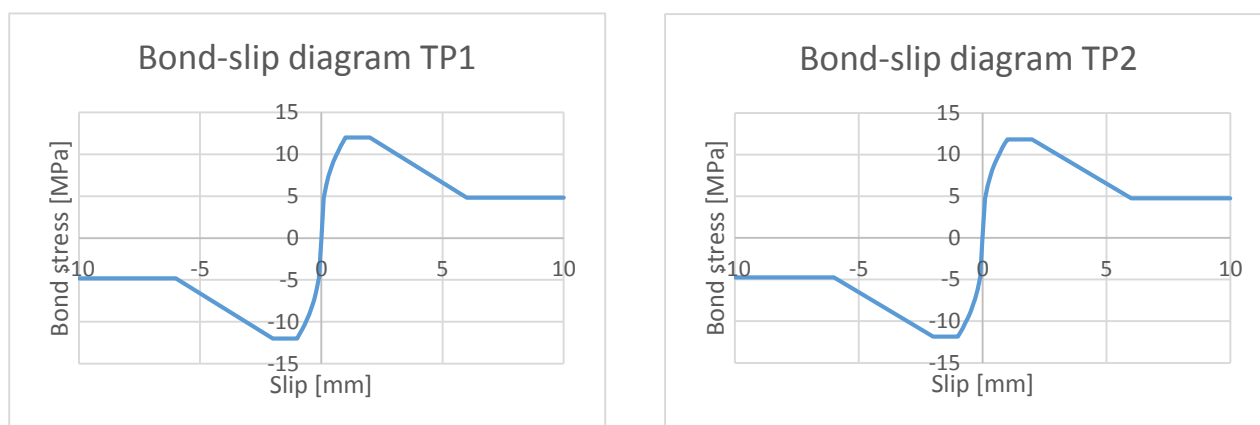


Figure 30: Bond-slip Diagram TP1 and TP2

The bond-slip diagrams in figure 33 are defined by the tabulated values seen in table. 6.

Table 6: Tabulated values Bond-slip diagram TP1 and TP2

Slip [mm]	Bond stress [MPa]	
	TP1	TP2
0	0	0
0,1	4,78	4,71
0,2	6,30	6,21
0,3	7,41	7,31
0,4	8,32	8,20
0,5	9,09	8,97
0,6	9,78	9,64
0,7	10,4	10,25
0,8	10,98	10,82
0,9	11,50	11,34
1,0	12,0	11,83
2,0	12,0	11,83
6,0	4,80	4,73
10,0	4,80	4,73

The bond-slip diagrams are also defined with negative slip values and negative bond stresses. These values correspond with the values stated in table 6, only with a negative sign.

The cubic bond-slip curve proposed by Dörr is a predefined curve in DIANA10.

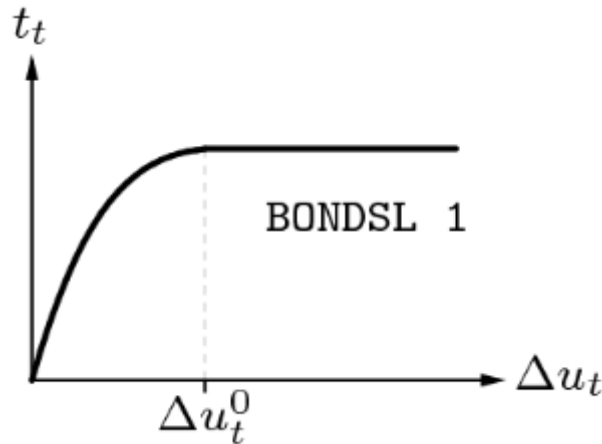


Figure 31: Cubic bond-slip curve (TNO DIANA [18])

The value at which the curve reaches its plateau had to be defined. The recommended value for Δu_t^0 from DIANA [18] is 0.06 mm. The maximum value for the shear traction t_t equals $1,9 \cdot f_t$, where f_t is the tensile strength of the concrete.

Bond slip was introduced to the numerical model by defining a bond slip material. “Bond-slip reinforcement” was selected from the “Reinforcement and pile foundations” material class. Either the user defined slip curve or the Dörr formulation was applied. The bond slip reinforcement also needed to be set to either truss or beam elements. This was done using the following python code.

```
for i in range (1,len(STARTNODEREINF)+1):
    ZZZZ='Element data {}'.format(ELEMENTDATANUM)
    ELEMENTDATANAME.append(ZZZZ)
    addElementData( ELEMENTDATANAME[i-1] )
    setParameter( DATA, ELEMENTDATANAME[i-1], "INTERF", "TRUSS")
    setParameter( DATA, ELEMENTDATANAME[i-1], "BEGINN", STARTNODEREINF[i-1] )
    setParameter( DATA, ELEMENTDATANAME[i-1], "ENDNOD", ENDNODEREINF[i-1] )
    assignElementData( ELEMENTDATANAME[i-1], SHAPE, ASBARS[i-1] )
    ELEMENTDATANUM=ELEMENTDATANUM+1
```

As well as element type, start and end nodes had to be applied. This is to mark the start and end of the reinforcement bars. The python script above shows how it was done.

5.6.3 Shear stiffness and normal stiffness

Regardless of the bond-slip model that is being used, DIANA10 demands values for certain relations, namely the shear stiffness $DSSX$ and the normal stiffness $DSNY$. According to TNO DIANA [18], $DSSX$ is the linear stiffness modulus D_{11} , which sets the relation between the shear traction t_t and the relative shear displacement Δu_t in the x-direction of the reinforcement. This stiffness modulus

has the annotation stress per length, e.g. N/mm^3 . Furthermore, the linear stiffness modulus $DSNY$, or D_{22} , sets the relation between the normal traction t_n and the relative normal displacement Δu_n in the y-direction of the reinforcement. The annotations are the same as for $DSSX$. $DSNY$ is interpreted as the stiffness related to crushing of the concrete by the reinforcing bar. $DSSX$ is interpreted as the slope of the bond slip curve at zero slip. The value for $DSSX$ is calculated as the slope between zero and the first sampling point in the bond slip curve from fib Model Code 2010. This results in $DSNY$ being much larger than $DSSX$.

The values for $DSSX$ for the two panels with the bond-slip model from fib Model Code 2010 were taken as:

$$DSSX_{P1} = \frac{4,78}{0,1} = 47,8 \frac{N}{mm^2} \quad (5.1)$$

$$DSSX_{P2} = \frac{4,71}{0,1} = 47,1 \frac{N}{mm^2} \quad (5.2)$$

For the cubic bond-slip formulation, the shear stiffness is calculated at the plateau of bond-slip curve, which corresponds to a slip of 0,06. In TNO DIANA [18], formulas for calculating $DSSX$ for the cubic formulation are given by:

$$DSSX_{P1} = 5 \frac{1,9 \cdot f_t}{\Delta u_0^t} = 5 \cdot \frac{1,9 \cdot 2,51}{0,06} = 397 \frac{N}{mm^2} \quad (5.3)$$

$$DSSX_{P2} = 5 \frac{1,9 \cdot f_t}{\Delta u_0^t} = 5 \cdot \frac{1,9 \cdot 2,44}{0,06} = 386 \frac{N}{mm^2} \quad (5.4)$$

The normal stiffness is assumed to be equal regardless of bond-slip formulation. In an older DIANA manual, release 9.4.2, formulas for the normal stiffness are stated as:

$$k_n = \frac{E}{l_{fr}} \quad (5.5)$$

Where E denotes the modulus of elasticity of concrete and l_{fr} the free length.

This free length was found hard to relate to. Together with supervisor Max Hendriks an alternative approach for the normal stiffness has been applied.

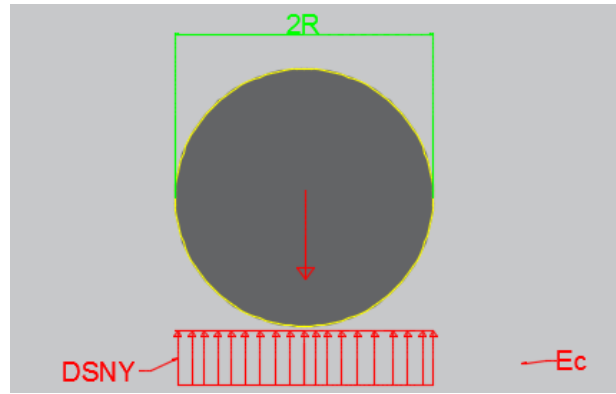


Figure 32: Illustration DSNY

Figure 32 illustrates the thought behind the normal stiffness. The figure shows a reinforcing bar surrounded by concrete. DSNY is assumed as the concrete resistance of the reinforcement penetrating and crushing the concrete. DSNY was calculated as follows per reinforcement bar:

$$DSNY = \frac{E_c}{2R} \cdot 10^3 \frac{N}{mm^2} \frac{mm^2}{mm} \quad (5.6)$$

A great deal of uncertainty was related to DSSX and DSNY. For this reason, a sensitivity study of these two inputs was carried out. This can be read about in section 8.1.

5.6.4 Concrete

Different choices for material properties available in DIANA10 were presented in section 2.6. For the concrete, both a rotating total strain crack model and a fixed total strain crack model was assigned in the modelling process in order to compare these two models.

Table 7 - Material Properties panel P1 and P2

Property	TP1	TP2	Annotation
Modulus of elasticity E_c	21900	23625	MPa
Tensile strength f_t	2,51	2,44	MPa
Compressive strength f_c	23,50	22,40	MPa
Tensile fracture energy G_F	0,129	0,128	N/mm
Compressive fracture energy G_c	32,25	31,94	N/mm

Table 7 shows the concrete material properties for panel TP1 and TP2. The modulus of elasticity, the tensile strength and the compressive strength were taken from Dyngeland [8], where cylinder strength, cube strength and modulus of elasticity was determined by testing. Only one tensile test was performed in total. The tensile strength for the other specimen was calculated from the average compressive strength and the ratio between tensile and compressive strength.

The tensile fracture energy was calculated by eq. (2.80), see 2.7.1 , and divided with a factor 10^3 in order to obtain the annotation [N/mm].

$$G_{F,P1} = 73 \cdot 23,50^{0,18} \cdot 0,001 = 0,129 \text{ N/mm} \quad (5.7)$$

The same applies for TP2:

$$G_{F,P2} = 73 \cdot 22,40^{0,18} \cdot 0,001 = 0,128 \text{ N/mm} \quad (5.8)$$

The compressive fracture energy depends on the tensile fracture energy, as stated in 2.7.2. For concrete panel TP1, the compressive fracture energy is calculated by:

$$G_{c,P1} = 250G_{F,P1} = 32,25 \text{ N/mm} \quad (5.9)$$

And for the concrete panel TP2, the compressive fracture energy is calculated by:

$$G_{c,P1} = 250G_{F,P2} = 31,94 \text{ N/mm} \quad (5.10)$$

The values for the compressive fracture energy are valid for the parabolic curve in compression.

The behavior of concrete in tension was chosen to follow the exponential curve. The tensile fracture energy from eq. (5.7) and eq. (5.8) was used. The area under the exponential curve is equal to the tensile fracture energy divided by the crack band width. The default mesh size was set to $H/60$, but a mesh size of $H/100$ was also investigated. The two mesh sizes would result in two different crack bandwidths as stated in the equations below.

$$h = \sqrt{2A} = \sqrt{2 \left(\frac{630}{60} \right)^2} \approx 14,85 \quad (5.11)$$

$$h = \sqrt{2A} = \sqrt{2 \cdot \left(\frac{630}{100} \right)^2} \approx 8,91 \quad (4.12)$$

Analyses with both fixed and rotating total strain crack model were carried out in order to study the difference. When the fixed option was used, properties for the shear behaviour was assigned to the concrete. A constant shear retention function was assumed with $\beta = 0,01$. (TNO DIANA [18]). For the rotating crack model, a shear retention function is not needed.

Part III: Analysis and results

6. Reference model

In this section follows a description of the reference models. These reference models were established in order to study the effect of changing variables, for instance the normal stiffness DSNY and the shear stiffness DSSX.

The reference models for TP1 and TP2 were modeled with the following inputs:

Mesh properties

- Mesh order
 - 4-noded linear quadrilateral elements with bubble function
- Element size $H/60$

Material properties

- Total strain crack model
 - Rotating crack model
- Exponential curve in tension
 - Fracture energy calculated according to fib Model Code 2010 [11]
- Parabolic curve in compression
 - Compressive fracture energy based on tensile fracture energy
- Reduction due to lateral cracking: Reduction model proposed by *Vecchio and Collins*
- Poisson's ratio reduction: Reduction model *Damage Based*
- Stress Confinement: Confinement model proposed by *Selby and Vecchio*
- Reinforcement: Bond-slip reinforcement
 - Bond-slip relation from fib Model Code 2010
 - TP1 - DSSX and DSNY calculated by eq. (5.1) and eq. (5.6), respectively.
 - TP2 - DSSX and DSNY calculated by eq. (5.2) and eq. (5.6), respectively.

Analysis settings

- Iteration method: Quasi Newton, Broyden
- Load step size: 0,01mm
- Number of load steps
 - TP1: 200 load steps
 - TP2: 400 load steps
- Convergence criteria
 - Force based, tolerance: 0,01
 - Residual based, tolerance: 0,01
- Line Search option switched on
- Solver: *Sparse Cholesky*
- Total strain based cracking, tangent: *Consistent*

For the parameter study, the following input in the numerical models was changed:

Mesh

- Element sizes
 - H/20
 - H/100

Material properties

- Total strain crack model
 - Fixed crack model
- Reinforcement: Bond-slip
 - Cubic function by Dörr
 - DSSX
 - DSNY

Naming scheme

Here follows an overview over the different versions of the panels:

- Reference - TP1/TP2 reference model
- Cubic - TP1/TP2 with cubic bond-slip
- Fixed - TP1/TP2 with fixed crack model
- H/20 - TP1/TP2 with mesh H/20
- H/100 - TP1/TP2 with mesh H/100
- xHyH - TP1/TP2 with high DSSX and high DSNY
 - DSSX is given the same value as DSNY, calculated from eq. (5.6)
- xLyL - TP1/TP2 with low DSSX and low DSNY
 - DSNY same value as DSSX, calculated from eq. (5.1) or eq. (5.2)
- xHyL - TP1/TP2 with high DSSX and low DSNY
 - DSSX calculated from eq. (5.6) and DSNY calculated from eq. (5.1) or eq. (5.2)

6.1 Loading procedure

Both panels were subjected to a prescribed displacement loading of total 4,0 mm. The total loading procedure of TP1 was divided into two parts. First, 100 steps of 0,01 mm per step were prescribed to the model, followed by 100 steps of 0,03 mm per step, resulting in a total displacement of 4,0 mm after 200 load steps. TP2 was prescribed 400 load steps of 0,01 mm displacement per step. Figure 35 illustrates the two different loading procedures.

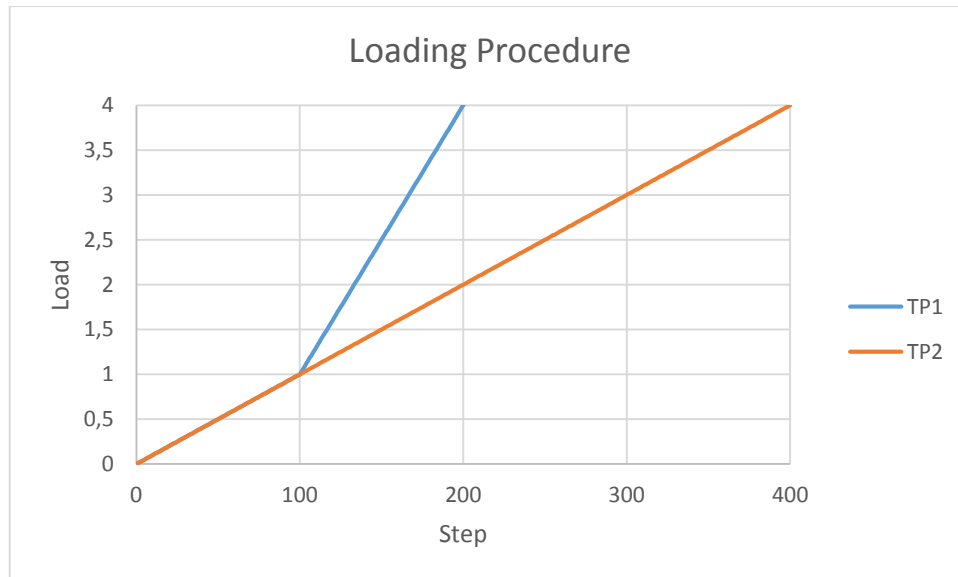


Figure 33: Loading Procedure TP1 and TP2

7. Results

In this chapter the analysis results for TP1 and TP2 will be presented. To start with, the results from the reference models will be presented. The two reference models were described in section 6. Furthermore, relevant results from the parameter study will be presented. For the reference cases, the following analysis output will be highlighted:

- Load-displacement curve
- Stress-average strain curve
- Total displacement
- Cauchy total stresses σ_1
- Total strains
- Crack widths
- Reinforcement stresses
- Reinforcement interface relative displacement

The analysis output stated above will be presented for a certain number of points along the load-displacement curve. Typical for these points is that they reflect a change in the global behavior of model, e.g. crack initiation or reinforcement yielding.

The load-displacement curve represents the relation between displacement loading and the reaction forces at the reinforcement start node. For each step, DIANA10 writes a displacement and a total reaction force in the x-direction. The total reaction force is the sum of the reaction forces acting in every reinforcement start node, i.e. all the reinforcement nodes at the left side of the panels.

In order to assess the global behavior of TP1 and TP2, stress-average strain curves were plotted and compared with the experimental stress-average strain curves from Dyngeland [8]. The panels with horizontal reinforcement are denoted S1 and S2. The panels with orthogonal reinforcement are denoted S3 and S4. TP1 was plotted against an average of S1 and S2, and TP2 was plotted against an average of S3 and S4.

7.1 TP1 Reference model

In this section follows the results of the reference analysis for panel TP1.

7.1.1 Load-displacement curve

Figure 34 shows the load-displacement curve for the reference model for TP1. The orange curve represents the numerical solution, while the blue curve represents the experimental results. By comparing the two curves the global behavior of the model can be evaluated. It is seen that the initial stiffness is a bit off.

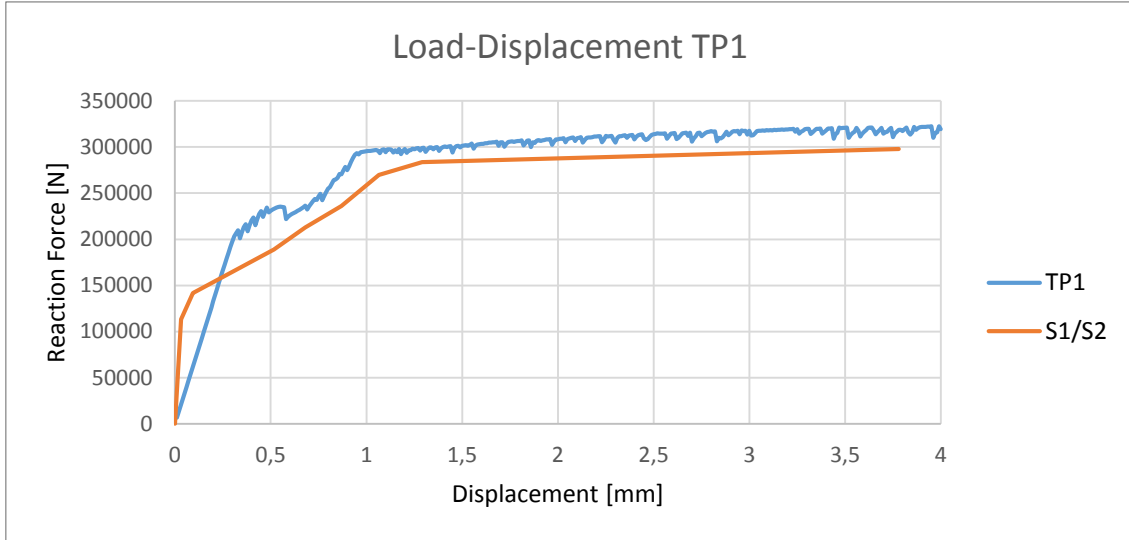


Figure 34: Load-displacement TP1 vs. S1/S2

7.1.2 Stress-Average strain

The values on the y-axis in the stress-average strain curve is established by dividing the total reaction force due to prescribed displacement load by the total area of the panel:

$$\sigma_i = \sum_{i=1}^7 \frac{F_{xi}}{A_{tot}} \quad (7.1)$$

Where F_{xi} reaction force in reinforcement start node i and A_{tot} is the total area. ($A_{tot} = 63000mm^2$). The strain was calculated by the following formula:

$$\varepsilon_i = \frac{\Delta u_i}{L} \quad (7.2)$$

Where Δu_i is the prescribed displacement in load step i , and L is the length of the panel.

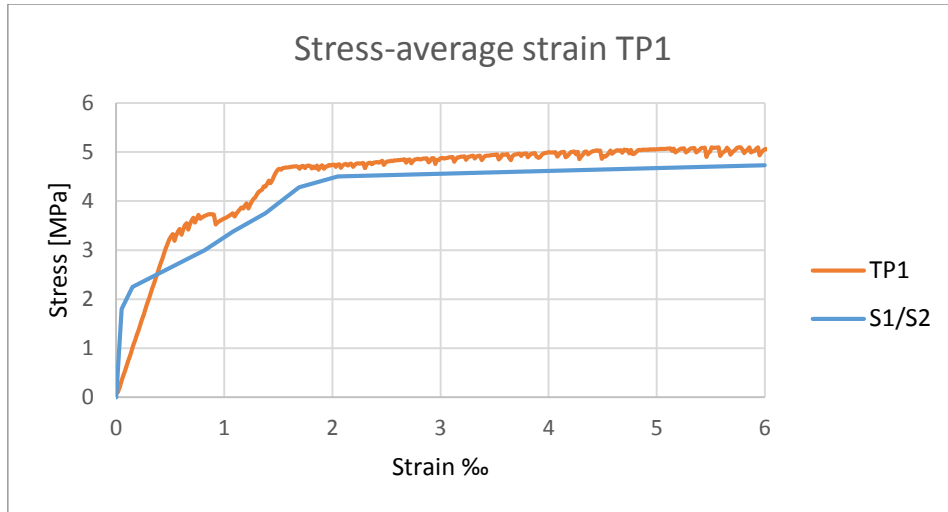


Figure 35: Stress-average strain curve TP1 vs. S1/S2

7.1.3 Plots panel TP1 – reference analysis

In Figure 36 three circles are marked. These circles correspond to the load steps that are investigated. At the first point crack initiation occurs, i.e. the tensile strength of the concrete is exceeded somewhere in the panel. The second point corresponds to an experimental stress level which is stated in Table 10. In the laboratory experiments, the average crack widths and spacing were documented at this stress level, which is set to approximately 3,66 MPa. For the reference test, a stress level of 3,66 MPa corresponded to a load step just after crack initiation where no stabilized crack patterns had developed. For that reason, the second point corresponds to the experimental strain of 1,3 ‰, which takes place in load step 82 for the reference test. In the third point, the yield stress in all bars is exceeded.

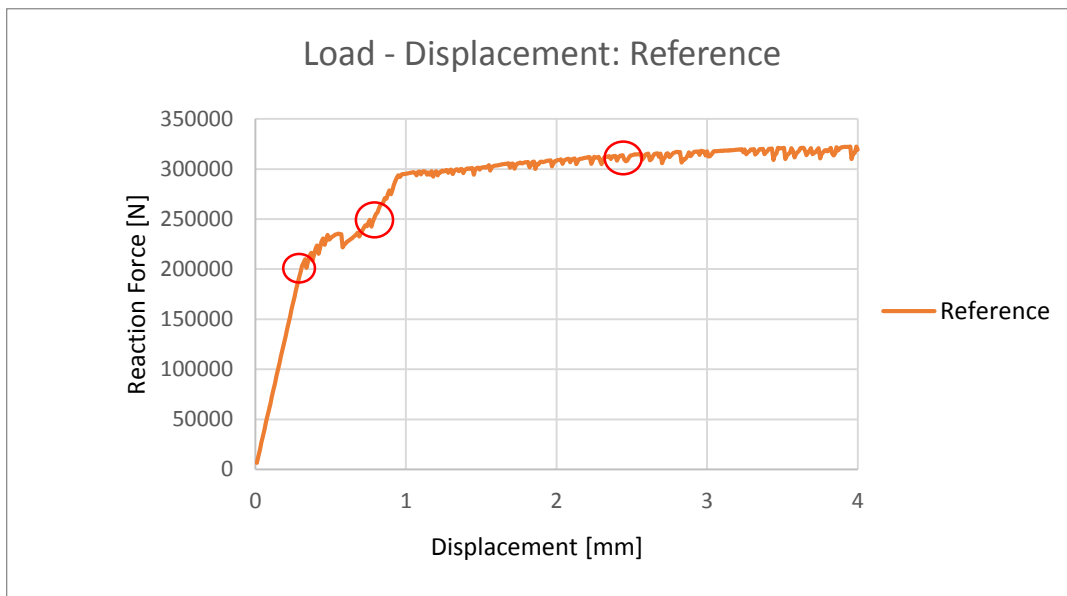
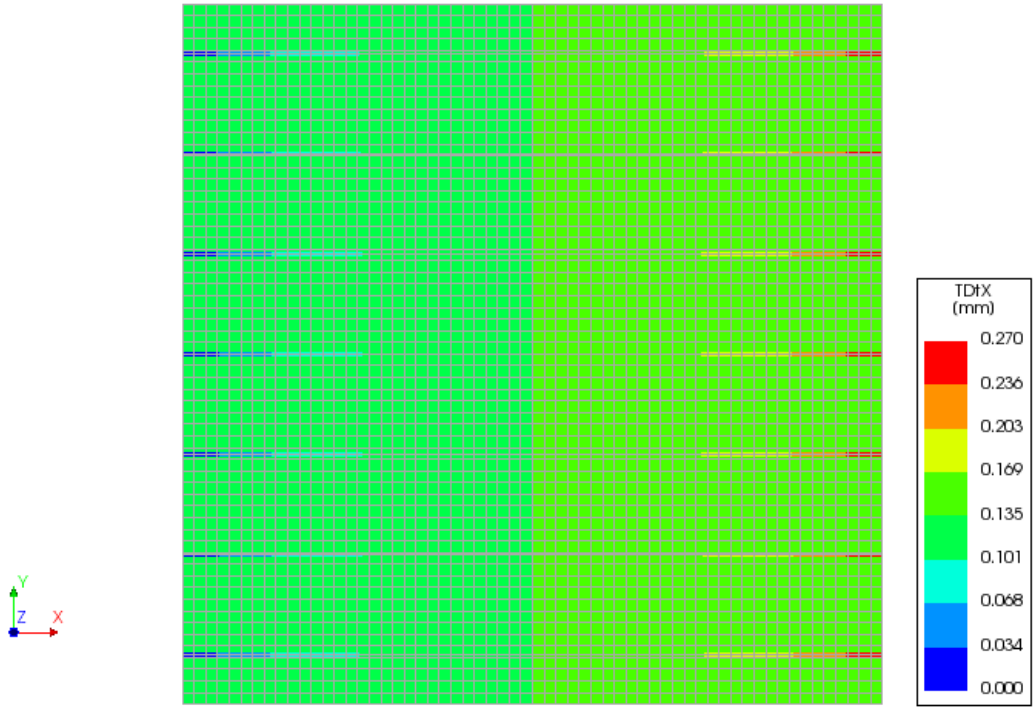


Figure 36: Load-displacement TP1 reference - interesting points

1. Load Step 27

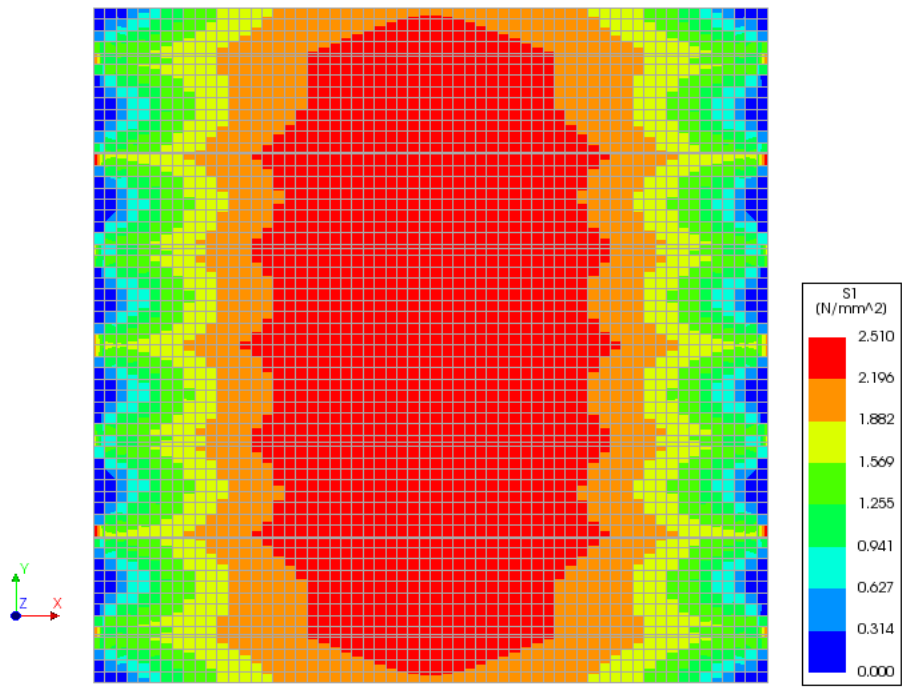
Total displacement

Nonlinear analysis
Load-step 27, Load-factor 27.000
Total Displacements Tdtx



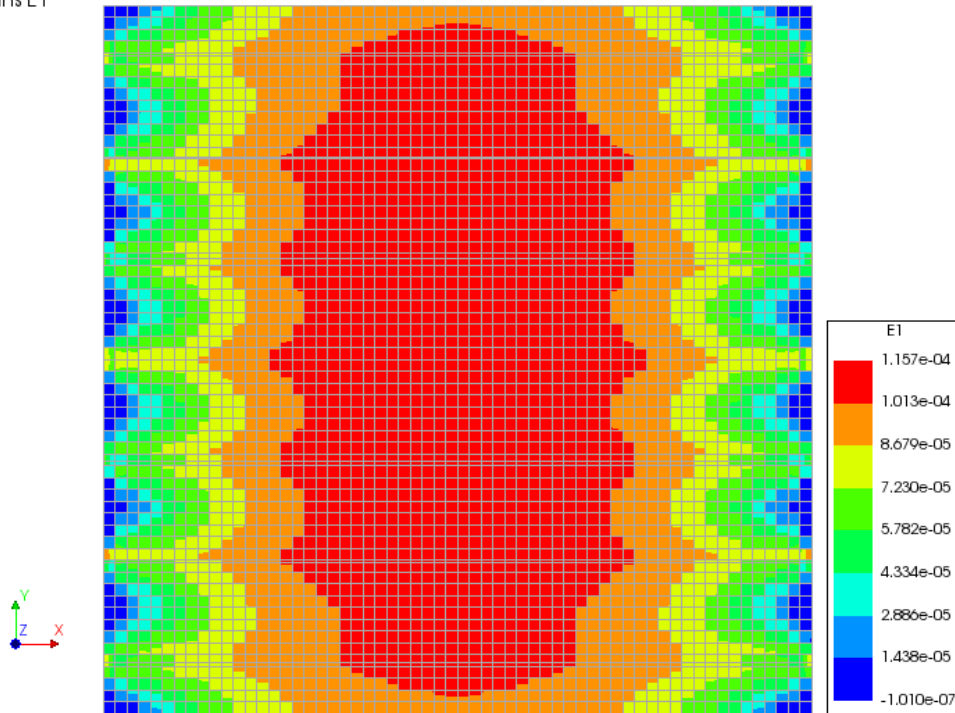
Cauchy total stresses

Analysis1
Load-step 27, Load-factor 27.000
Cauchy Total Stresses S1



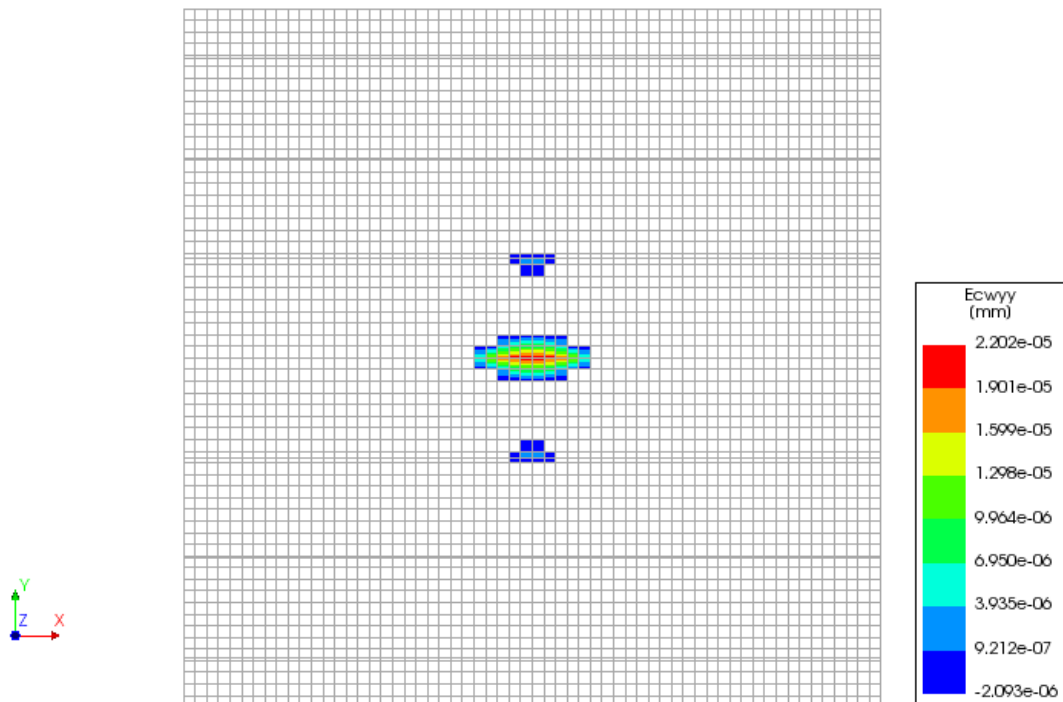
Total Strains

Nonlinear analysis
Load-step 27, Load-factor 27.000
Total Strains E1



Crack widths

Nonlinear analysis
Load-step 27, Load-factor 27.000
Crack-widths Ecwyy



Reinforcement Stresses

Nonlinear analysis
Load-step 27, Load-factor 27.000
Reinforcement Cauchy Total Stresses SXX



Reinforcement interface relative displacement

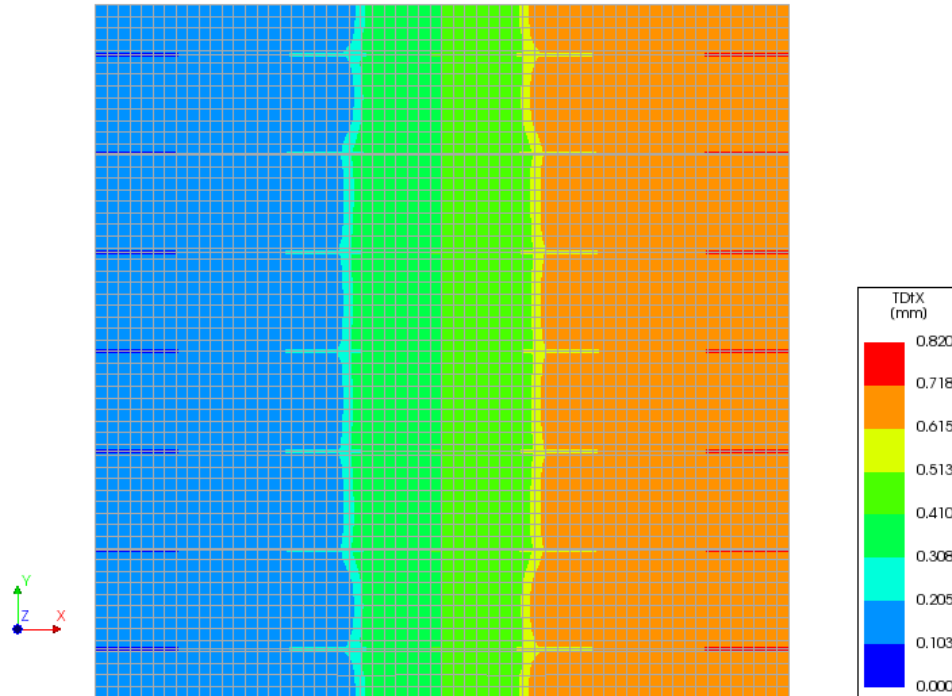
Nonlinear analysis
Load-step 27, Load-factor 27.000
Reinforcement Interface Relative Displac DUSx



2. Load step 82

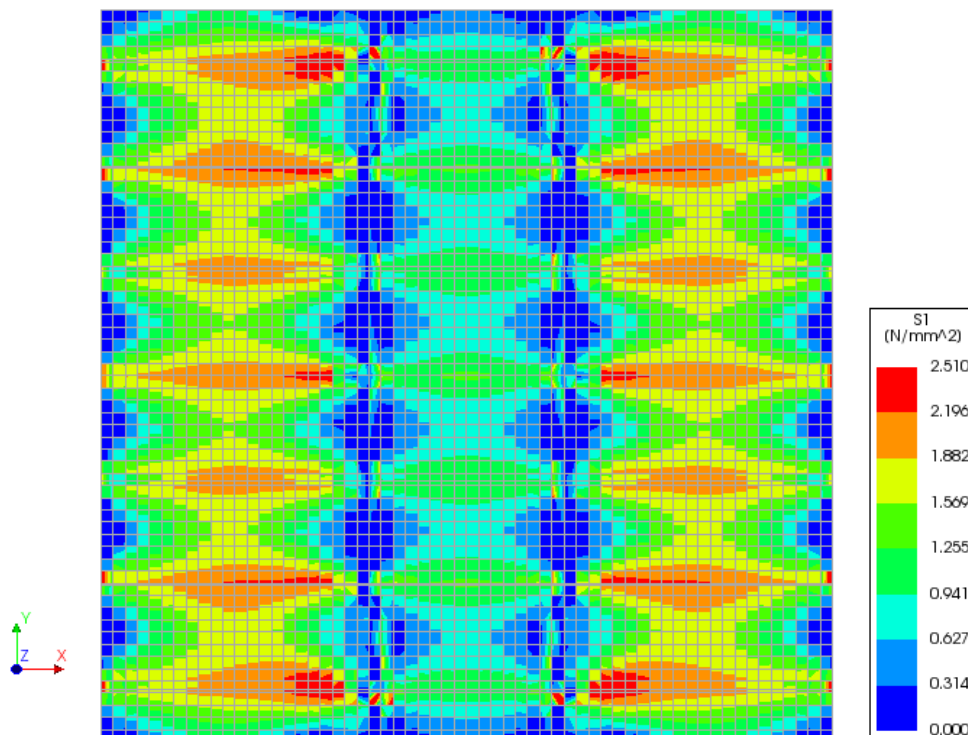
Total displacement

Analysis1
Load-step 82, Load-factor 82.000
Total Displacements TdTX



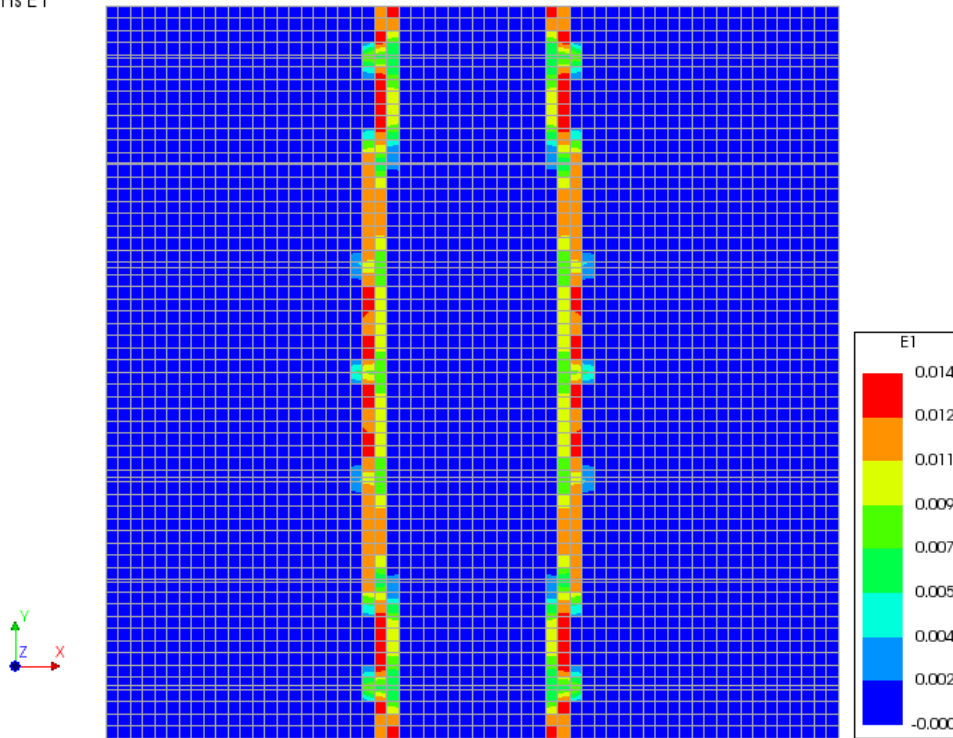
Cauchy total stresses

Analysis1
Load-step 82, Load-factor 82.000
Cauchy Total Stresses S1



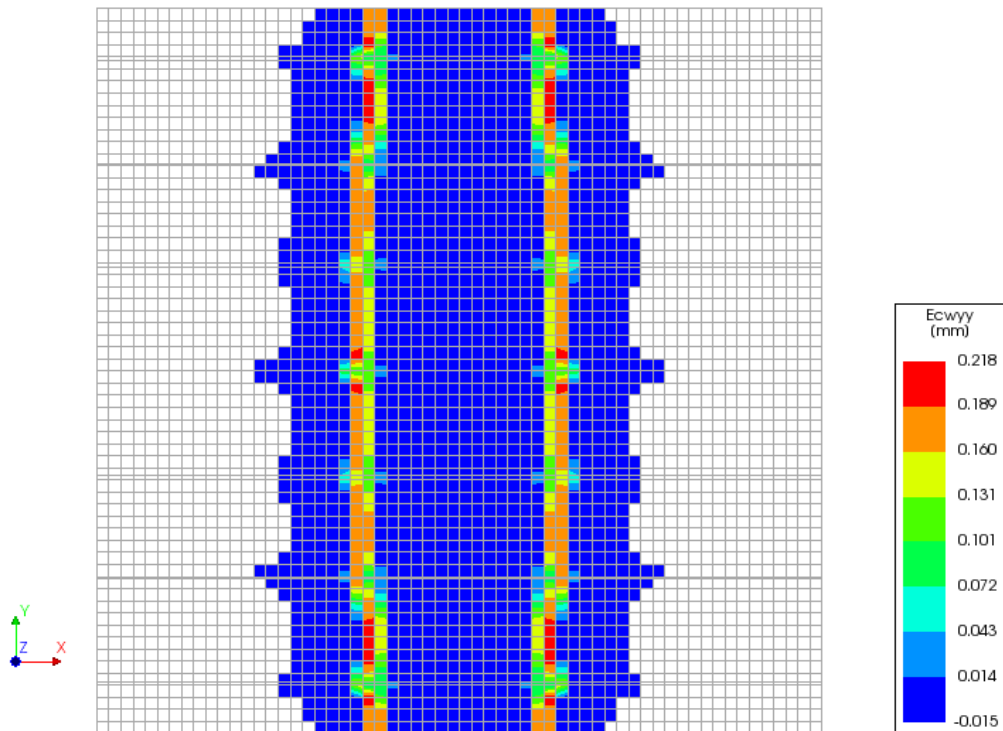
Total Strains

Nonlinear analysis
Load-step 82, Load-factor 82.000
Total Strains E1



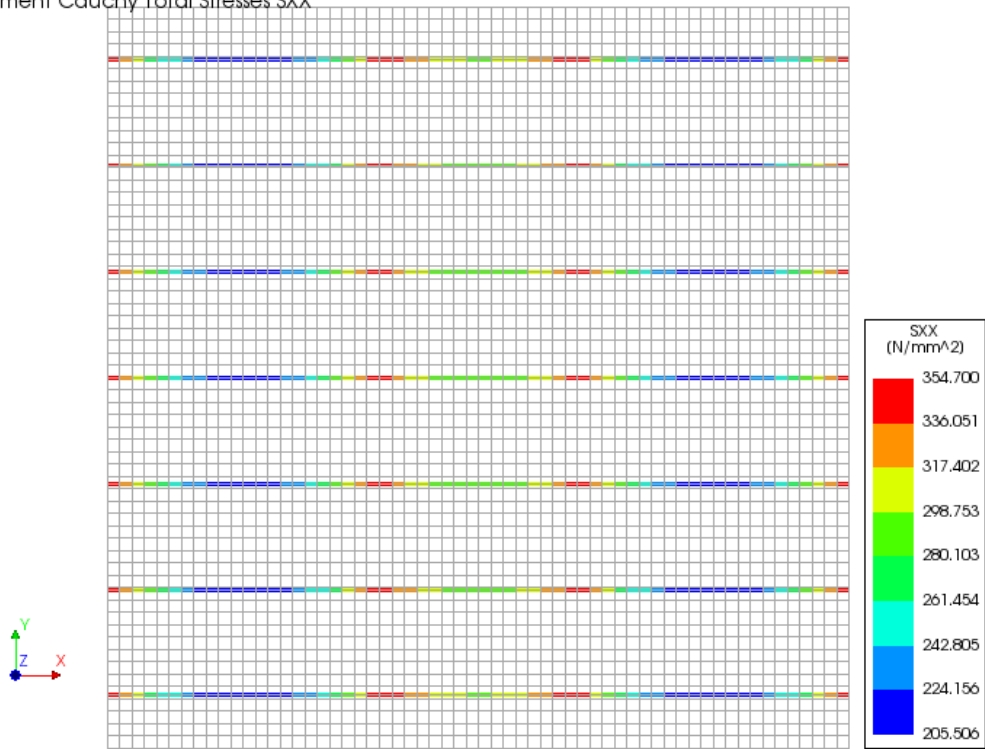
Crack widths

Analysis1
Load-step 82, Load-factor 82.000
Crack-widths Ecwyy



Reinforcement Stresses

Nonlinear analysis
Load-step 82, Load-factor 82.000
Reinforcement Cauchy Total Stresses SXX



Reinforcement interface relative displacement

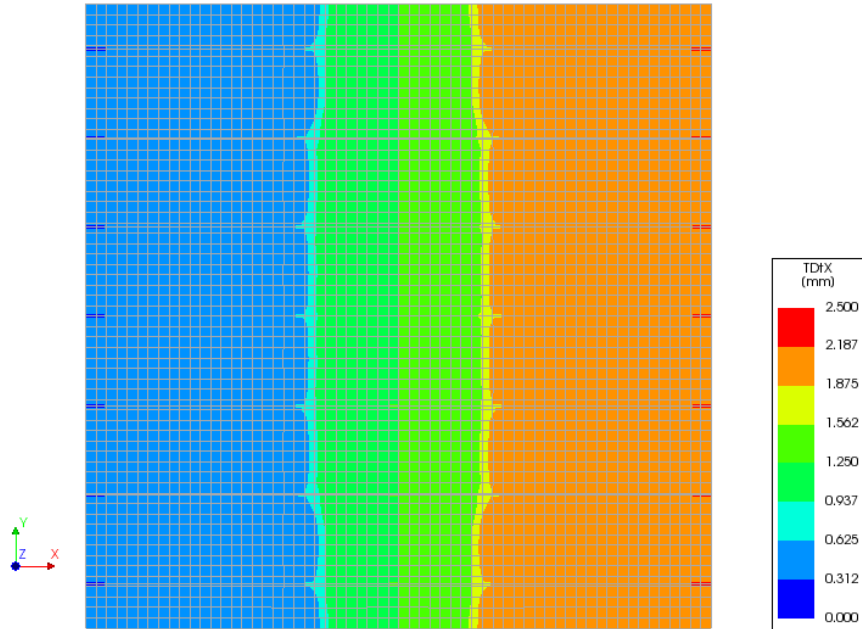
Analysis1
Load-step 82, Load-factor 82.000
Reinforcement Interface Relative Displac DUSx



3. Load step 150

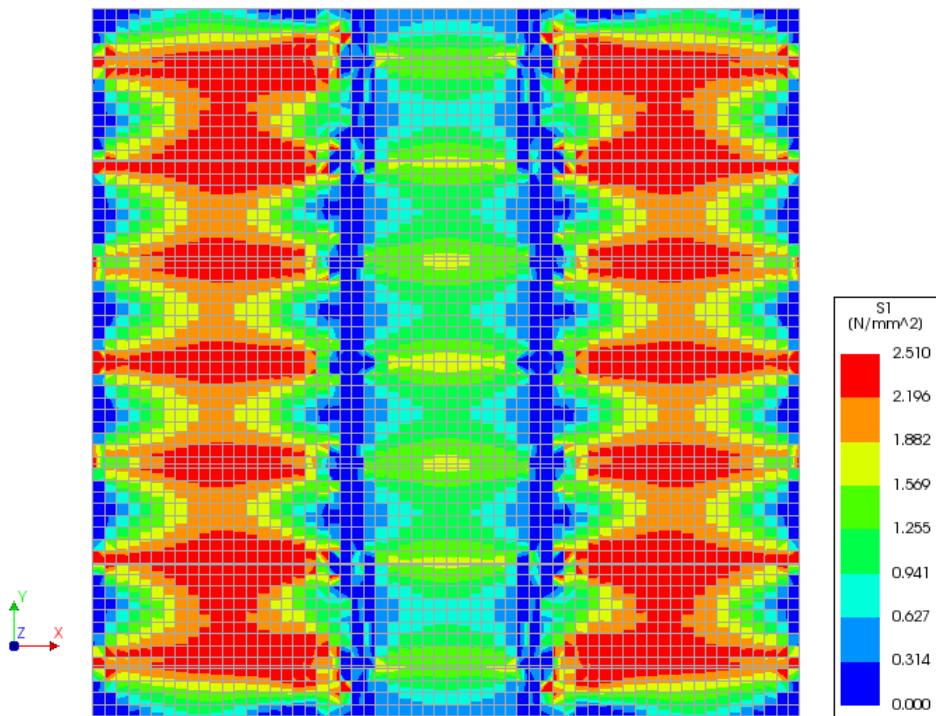
Total displacement

Analysis1
Load-step 150, Load-factor 250.00
Total Displacements TDX



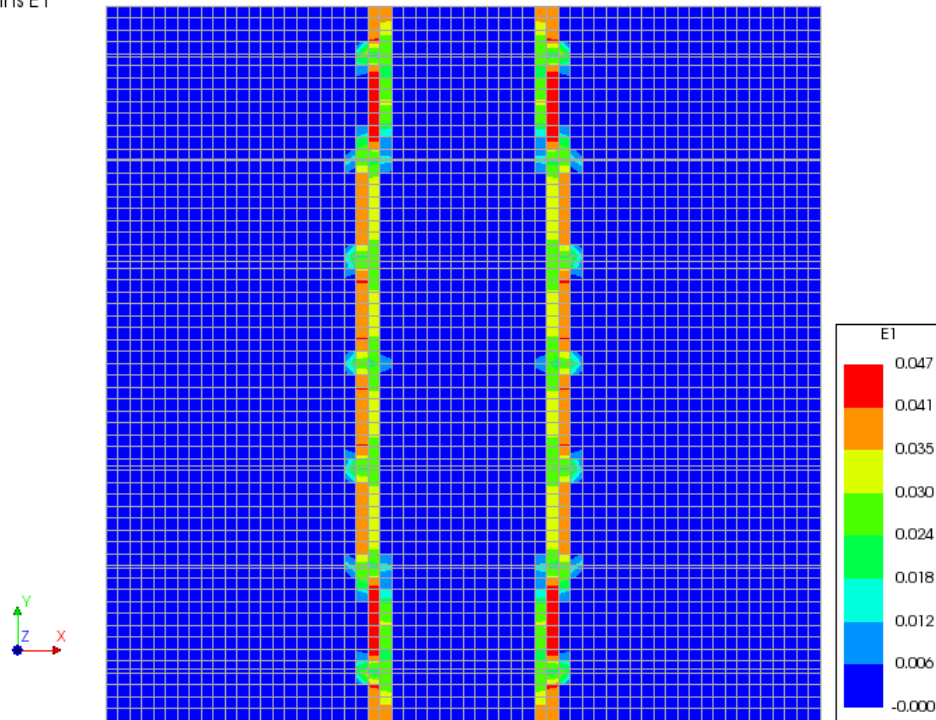
Cauchy total stresses

Analysis1
Load-step 150, Load-factor 250.00
Cauchy Total Stresses S1



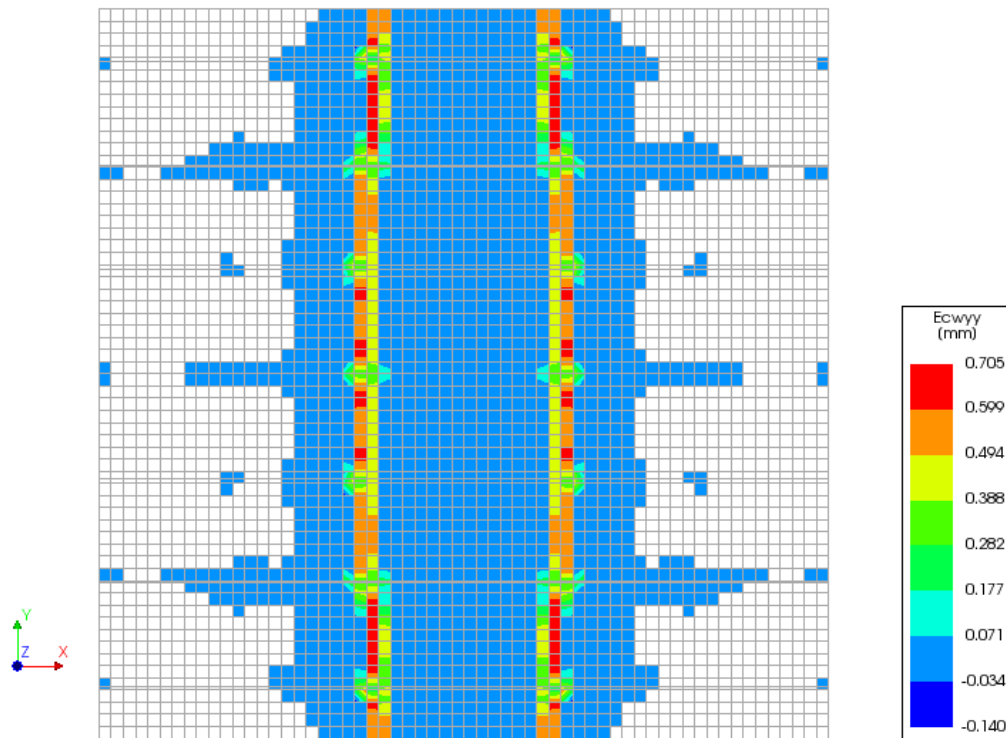
Total Strains

Nonlinear analysis
Load-step 150, Load-factor 250.00
Total Strains E1



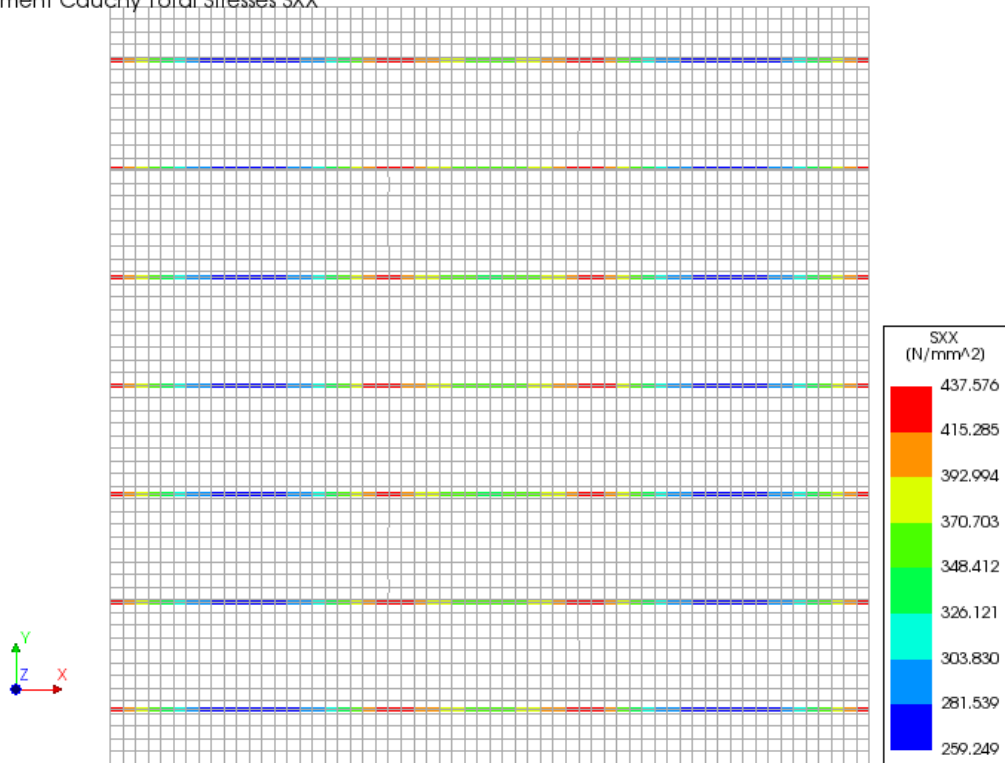
Crack widths

Analysis1
Load-step 150, Load-factor 250.00
Crack-widths Ecwyy



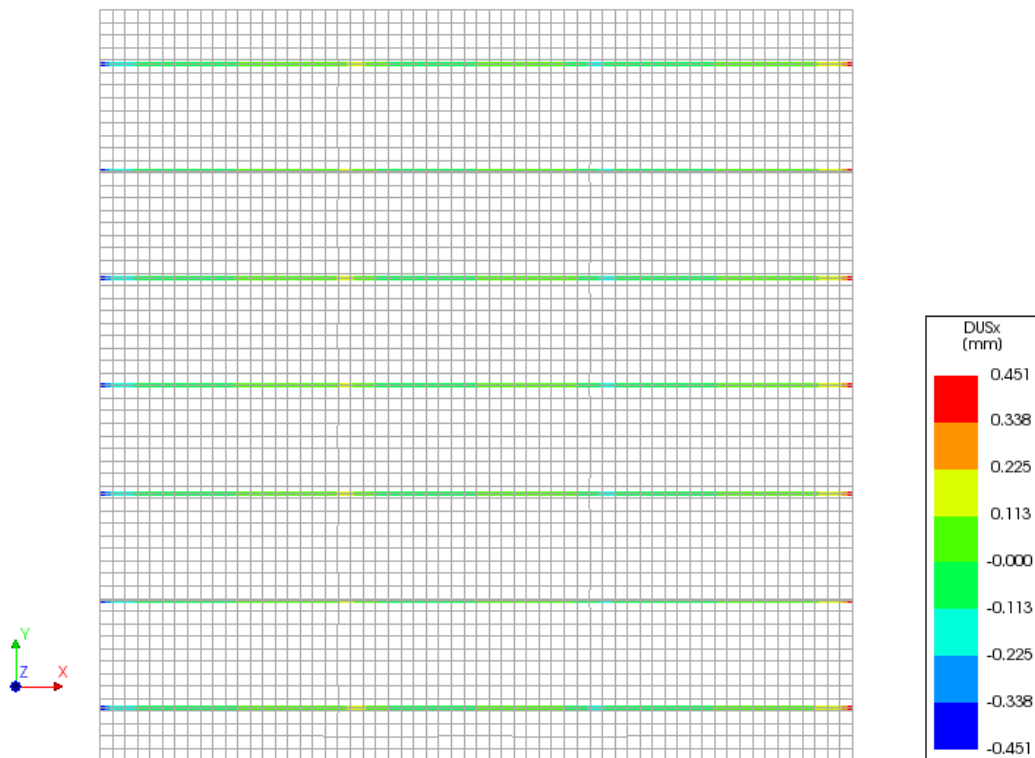
Reinforcement Stresses

Nonlinear analysis
Load-step 150, Load-factor 250.00
Reinforcement Cauchy Total Stresses SXX



Reinforcement interface relative displacement

Analysis1
Load-step 150, Load-factor 250.00
Reinforcement Interface Relative Displac DUSx



Load step 27

At load step 27, cracks start to propagate in the panel as a result of the tensile stresses exceeding the tensile strength of the concrete. In the load-displacement curve, this point marks the end of the linear domain, where the concrete behaves in a linear elastic manner. From the Total Cauchy Stress contour plot it is seen that the maximum principal stresses in the middle of the panel, σ_1 , equals 2,639 MPa, which is larger than the tensile strength of the concrete ($f_t = 2,51$ MPa). As a result of this, cracks start to propagate in the middle of the panel. Furthermore, it is seen that the maximum reinforcement stresses are located at the reinforcement start and end nodes, and equal approximately 243 MPa. The yield strength of the reinforcing bars was set to: $f_y = 403$ MPa. A slip between the reinforcement and the concrete is also seen, and indicates that the bond-slip formulation indeed has been implemented into the model. The slip is largest at the start and end of the reinforcing bars, where we also have the largest interface tractions.

Load step 82

Load step 82 corresponds to the experimental strain state in which a stabilized crack pattern would develop, and average crack widths and crack spacing were assessed. For the numerical model of TP1, a stabilized crack pattern has developed at this load step. With reference material properties and numerical solution method, two distinct cracks propagate in the panel. By comparing the crack strain plot with the plot for the reinforcement stresses, it is seen that the largest reinforcement stresses occur at the locations where the two cracks propagate. This seems plausible given the fact that in a crack, all the cross sectional forces must be carried by the reinforcement. The slip is largest at the cracks, and this also seems reasonable, given the fact that large relative displacements between reinforcement and concrete nodes will take place in a crack.

Load step 150

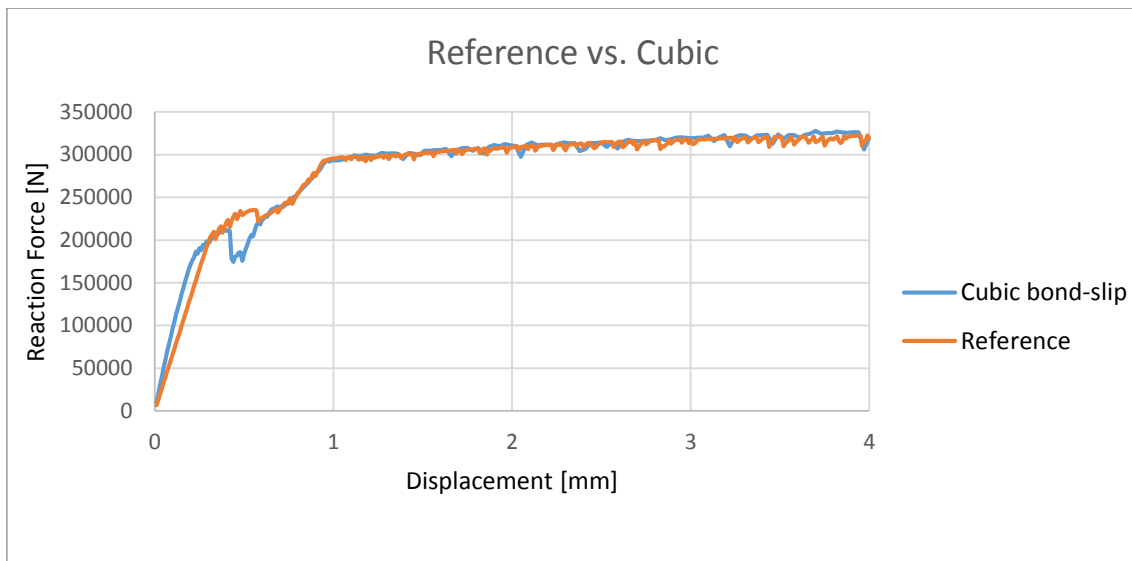
In load step 150, which corresponds to a displacement of 2,5 mm, yielding occurs in all the reinforcing bars, which indicates a hardening domain where the reinforcement is responsible for the capacity of the panel. The crack pattern stabilizes around load step 82 for the reference test, and from load step 82 load step 150, no new crack patterns develop. There is only seen a widening of the existing cracks.

In order to compare the crack patterns obtained from the nonlinear finite element analyses to those obtained experimental, mean crack spacing and crack widths were calculated. The numerical average crack widths can be found in Table 8.

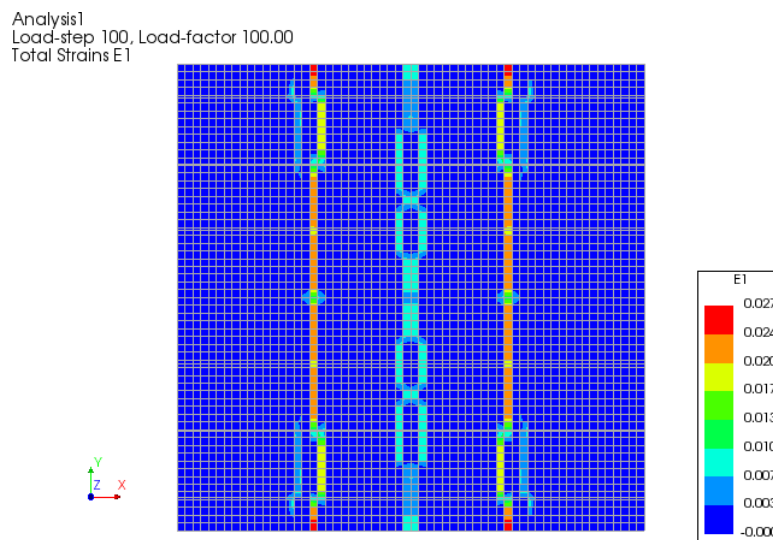
7.2 Parameter study TP1

TP1 with cubic bond-slip

In this section the results from the cubic bond-slip analysis will be presented.

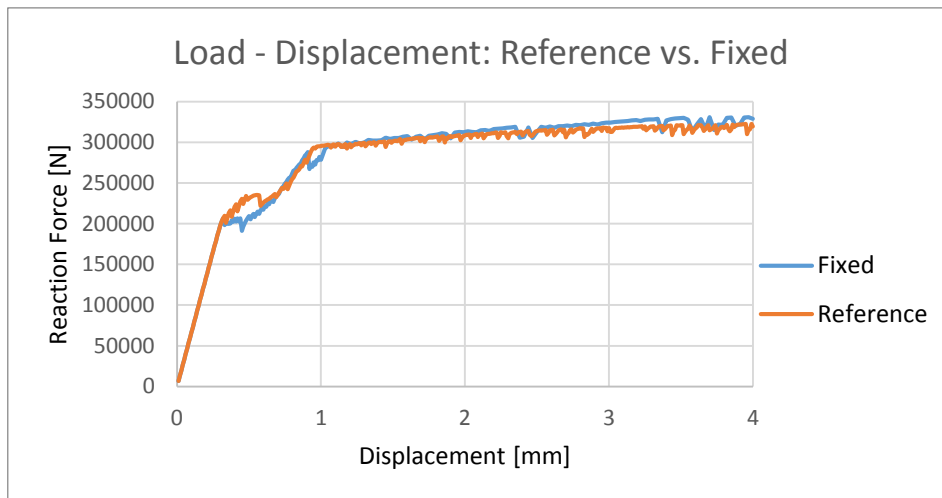


As seen from the load-displacement curve, the global behavior is quite similar when comparing fib Model Code bond-slip formulation with the cubic bond-slip formulation. In the load-displacement curve for the cubic bond-slip formulation, a drop in reaction force occurs around 0,44 mm as a result of no convergence in step 44.

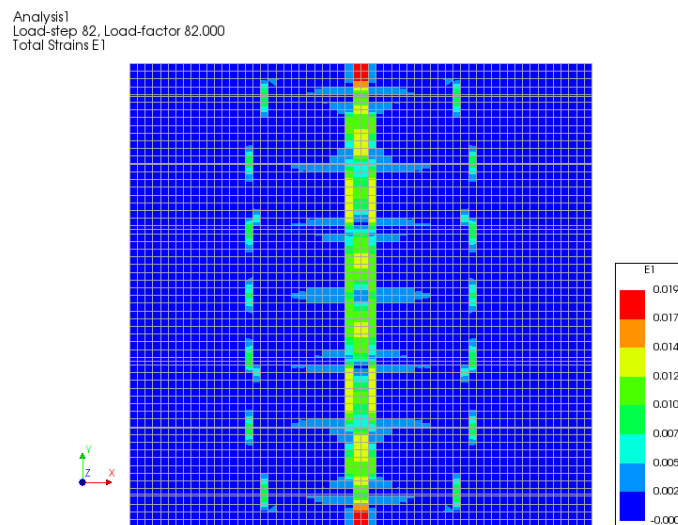


The figure above illustrates the total concrete strains at load step 100, where a stabilized crack pattern finally starts to develop. When comparing this plot with the total strain plot from the reference model in 7.1.3, it is noted that an additional crack propagates in the middle of the panel.

TP1 with fixed crack model



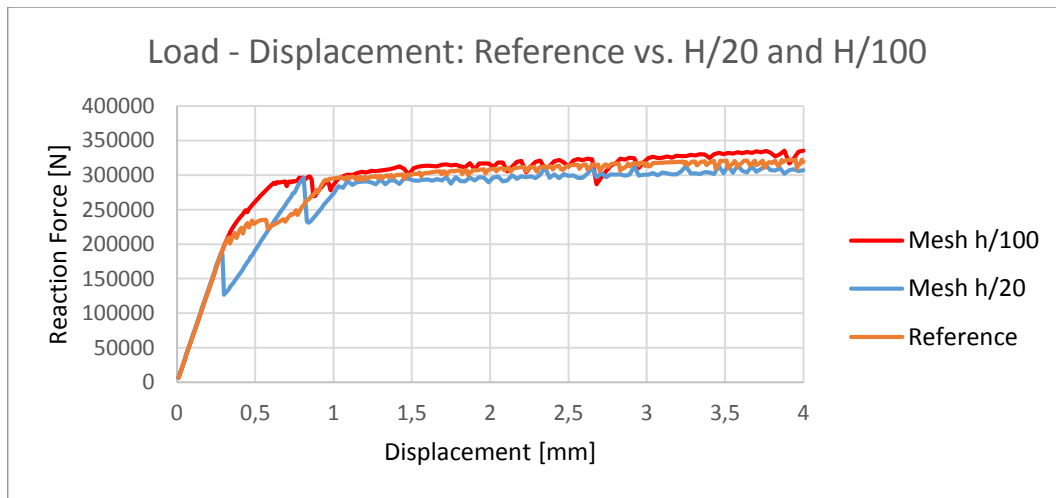
As seen from the load-displacement curve above, the global behavior of the panel quite similar for the fixed crack model compared with the rotating crack model. The load-displacement curve for the fixed crack model flattens out around crack initiation unlike the load-displacement curve for the rotating crack model.



For the fixed crack model, the crack pattern of the panel looks quite different than the crack pattern obtained with a rotating crack model. For the fixed crack model, an additional crack propagates in the middle of the panel.

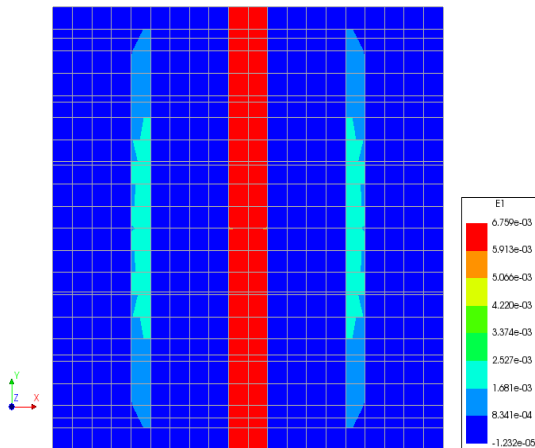
TP1 with mesh H/20 and H/100

The mesh sensitivity study that was carried out included in addition to the reference mesh H/60, two additional mesh sizes of H/20 and H/100.

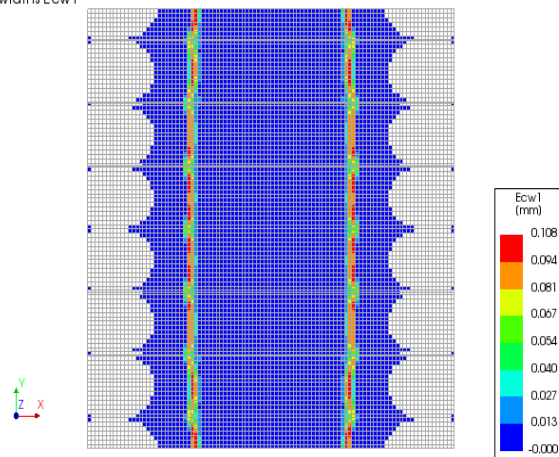


It seems that the numerical model for panel TP1 to some extent is mesh sensitive given the load-displacement paths in the interval 0,3 mm to 1,0 mm. With mesh size H/20, which was considered as a course mesh, no distinct crack pattern developed, as seen in the picture to the left below.

Analysis1
Load-step 82, Load-factor 82.000
Total Strains E1



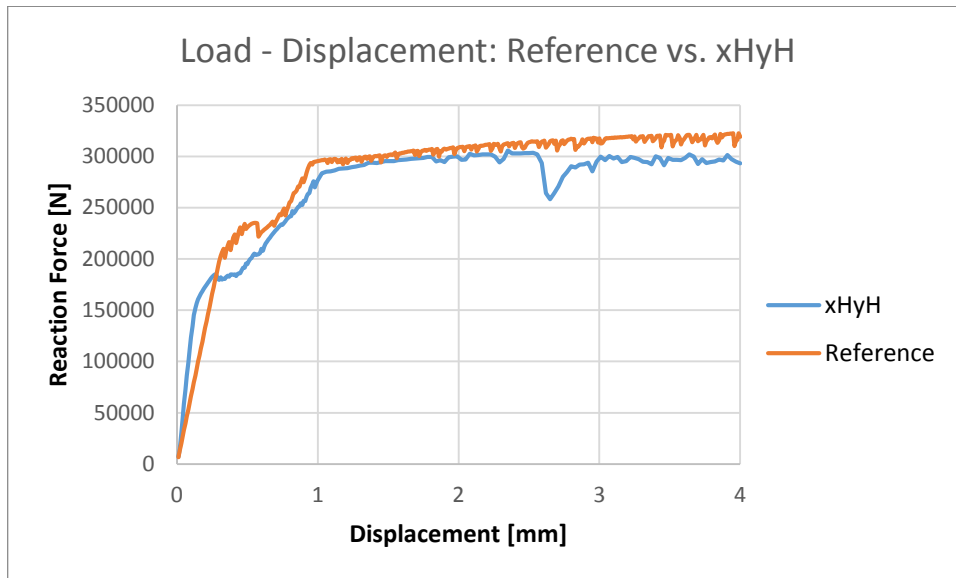
Analysis1
Load-step 88, Load-factor 88.000
Crack-widths Ecw1



The figure to the right shows the contour plot of the principal total strains $E1$ for load step 88 for mesh H/100, which is the first step with a stabilized crack pattern. Compared with the reference, the crack patterns are quite similar in appearance, but the total strains are smaller for the case with mesh H/100 at load step 88, compared with the total strains for the reference test at load step 82.

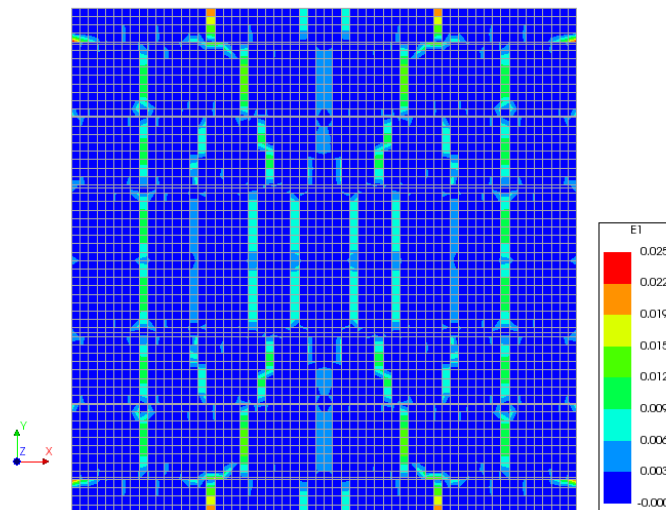
The reinforcing bars starts to yield around load step 97, which corresponds well with the reference test.

TP1 with high DSNY and high DSSX (xHyH)



From the load-displacement curve a sudden drop around 2,6 mm is observed. This is caused by no convergence at load step 153. It is also seen that the initial stiffness is higher for the case “xHyH” than for the reference case, as expected.

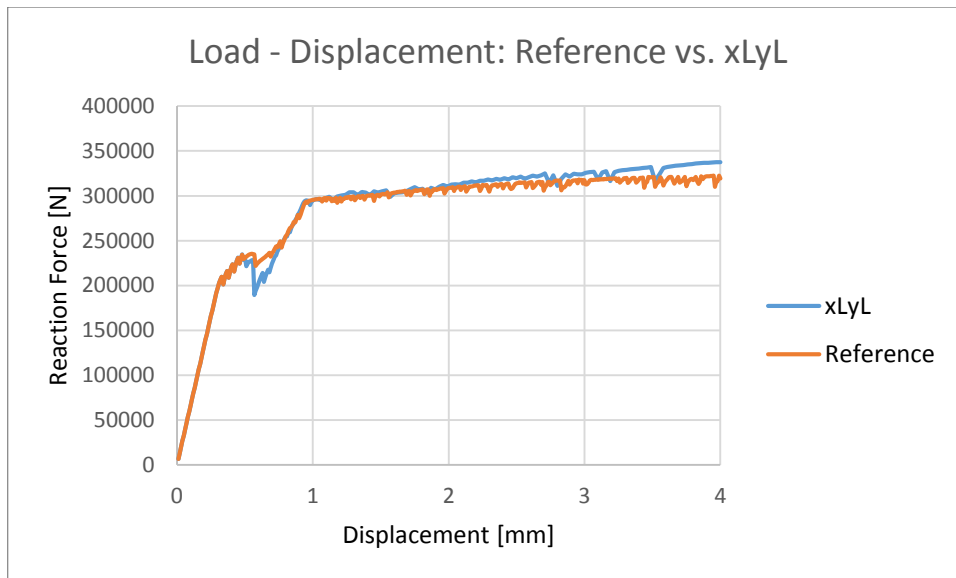
Analysis1
Load-step 82, Load-factor 82.000
Total Strains E1



As seen from the figure above, the crack pattern differs a lot from the crack pattern of the reference test. Instead of two distinct cracks it may now be observed 5-6 cracks in the panel.

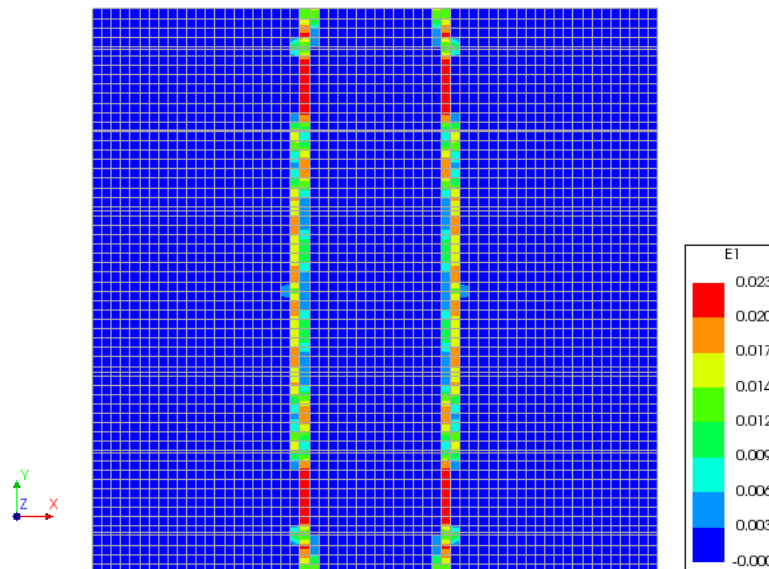
TP1 with low DSSX and low DSNY (xLyL)

As seen from the load-displacement curve, the global behavior of the reference test compared with the “xLyL” case seem to correspond rather well.



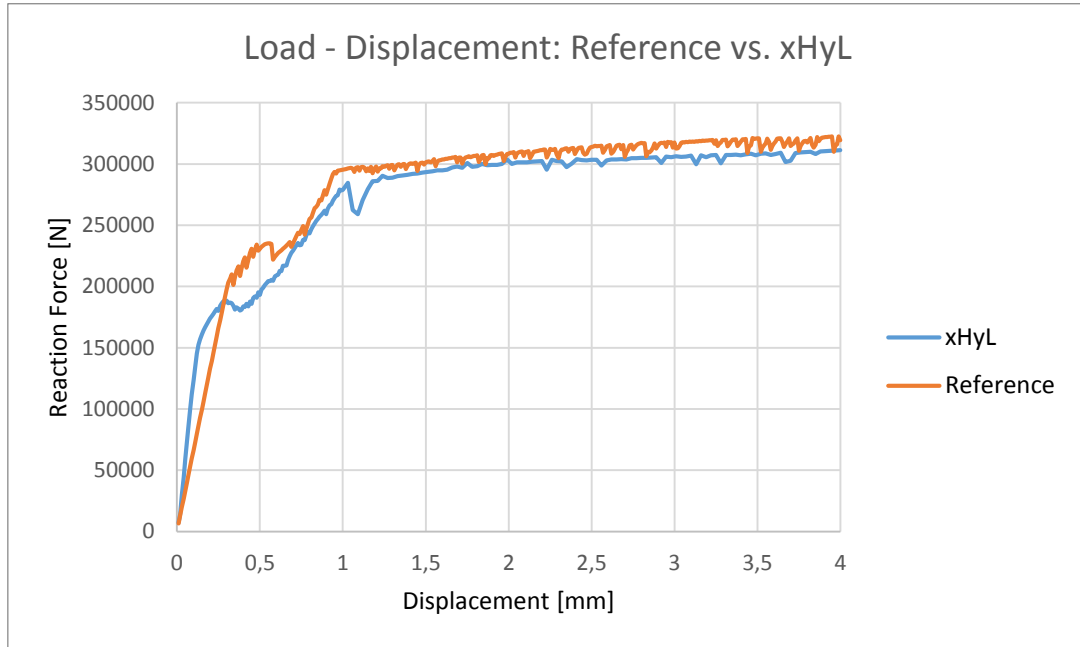
From the total strain plot shown below, it is observed that the crack pattern of the “xLyL” case looks very similar to the reference crack pattern. For the “xLyL” case, only two cracks propagate during the analysis, as for the reference case.

Analysis1
Load-step 88, Load-factor 88.000
Total Strains E1



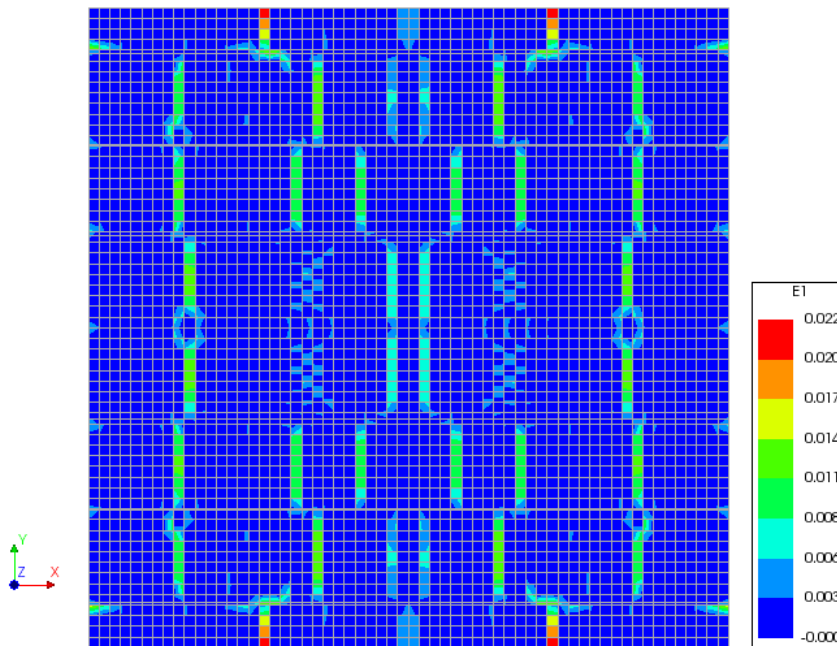
TP1 with high DSSX and low DSNY (xHyL)

From the load-displacement curve a quite different global behavior is observed for the “xHyL” case compared to the reference case. For the “xHyL” case, the slope of the load-displacement curve is steeper than for the reference case. An all over lower load response is also observed for the “xHyL” case.



From the total strain plot, a crack pattern that looks very similar compared with the “xHyH” case is observed.

Analysis1
Load-step 82, Load-factor 82.000
Total Strains E1



7.3 TP2 Reference model

In this section follows the results of the reference analysis for panel TP2.

7.3.1 Load displacement

The figure below describes the load-displacement curve for the reference model with orthogonal reinforcement. The reference panel is represented with an orange curve and the experimental results for the same panel is the blue curve. The initial stiffness seems to be a bit off, but after cracking the two curves corresponds better.

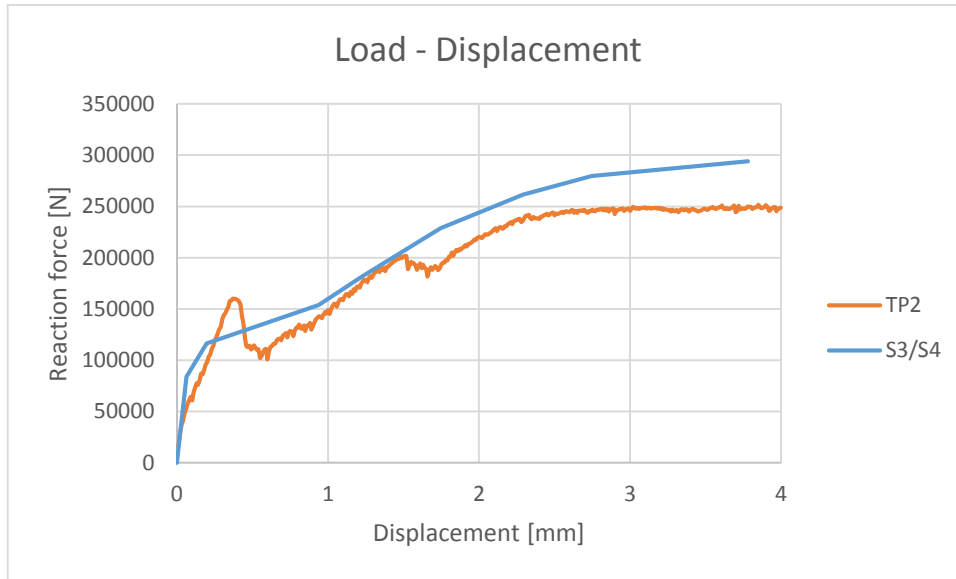


Figure 37: Load-Displacement TP2 vs. S3/S4

7.3.2 Stress – average strain

The values along the y-axis in the stress-average strain curve were established by dividing the total reaction force due to prescribed displacement load by the total area of the panel:

$$\sigma_i = \sum_{i=1}^{10} \frac{F_{xi}}{A_{tot}} \quad (7.3)$$

Where F_{xi} is the reaction force in start node i and A_{tot} is the total area ($A_{tot} = 63000 \text{ mm}^2$). The strain was calculated by the following formula:

$$\varepsilon_i = \frac{\Delta u_i}{L} \quad (5.4)$$

Where Δu_i is the prescribed displacement in load step i and L denotes the length of the panel.

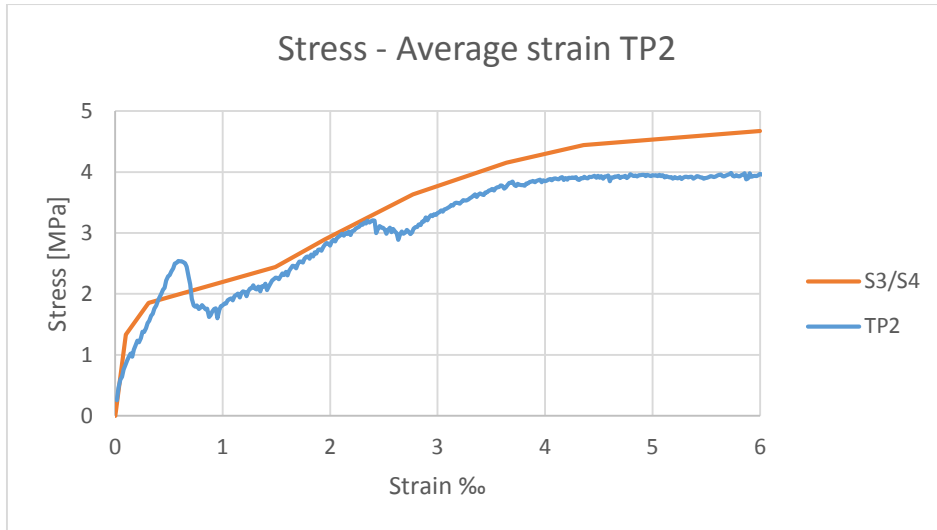


Figure 38: Stress-Average strain TP2 vs. S3/S4

7.3.3 Plots panel TP2 - reference

From the load displacement curve three points were selected to be looked at closer. These points are located at load step 55, 175 and 214.

Load step 55 where selected as it describes the panel right after the first period of cracking.

Load step 175 where selected as it describes the panel right after the second cracking period.

Load step 214 has stress level of 3,65 which represents the stress level where the experimental cracks were documented.

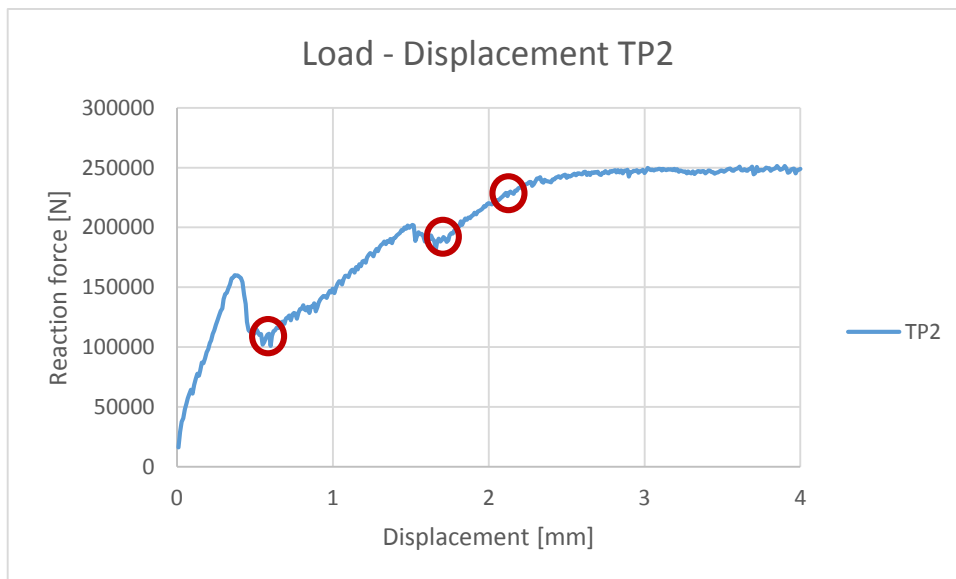
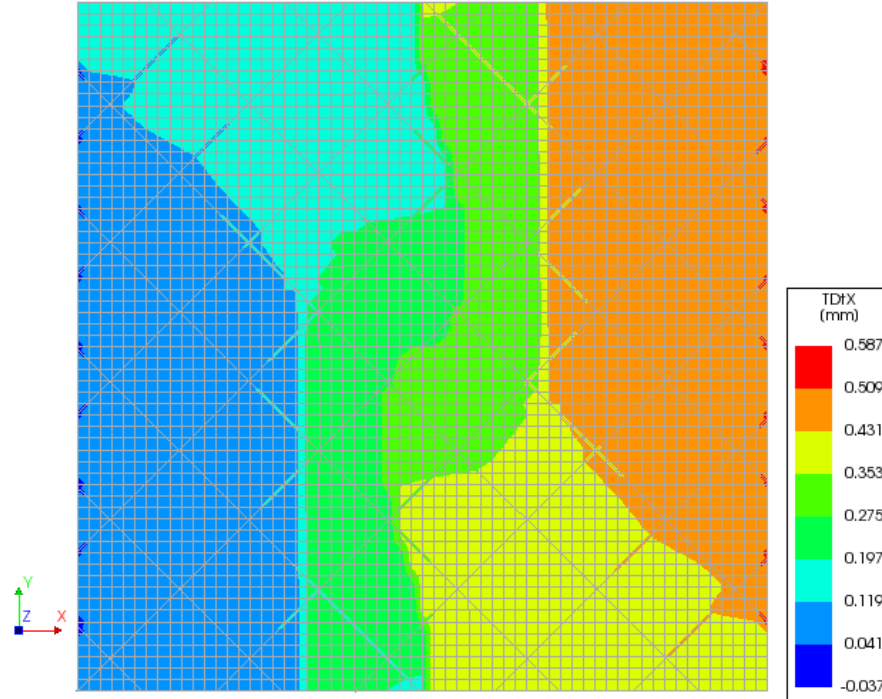


Figure 39: Load-displacement TP2 reference-interesting points

1. TP2 Reference model, load step 55

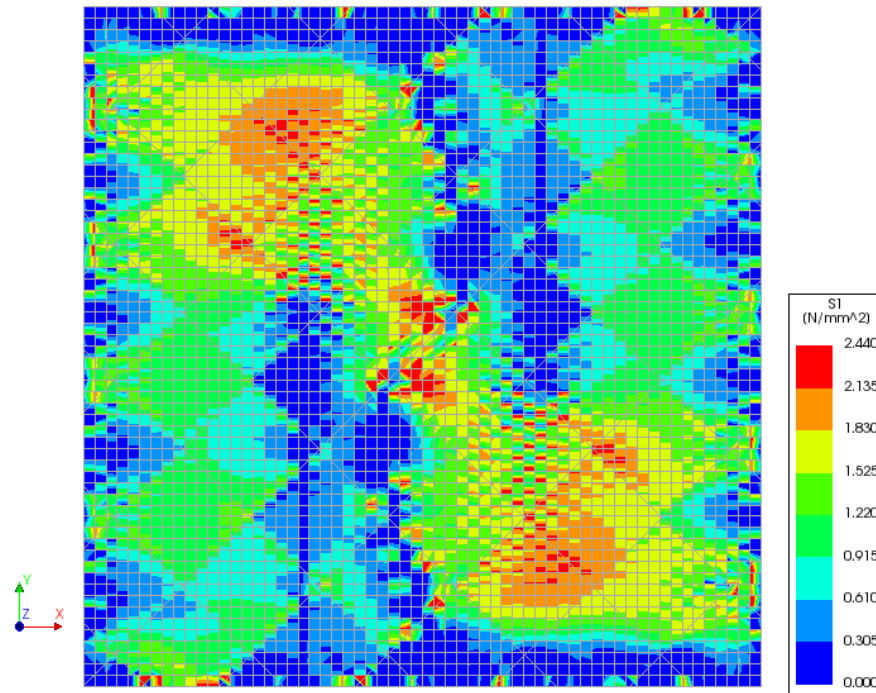
Total displacement

Nonlinear analysis
Load-step 55, Load-factor 55.000
Total Displacements TDtX



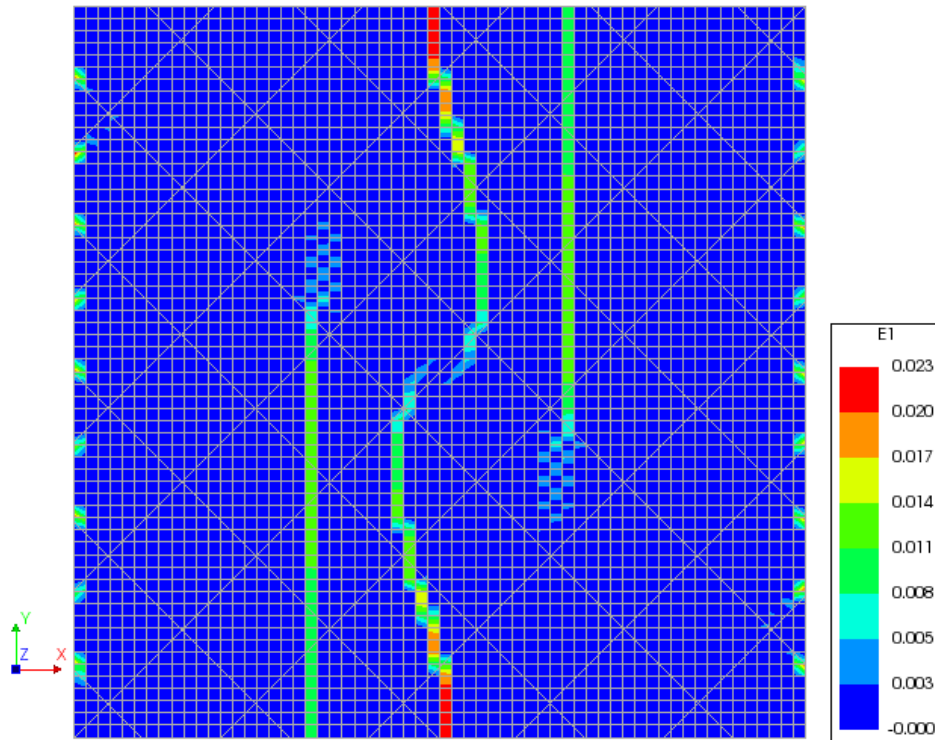
Cauchy total stresses

Analysis61
Load-step 55, Load-factor 55.000
Cauchy Total Stresses S1



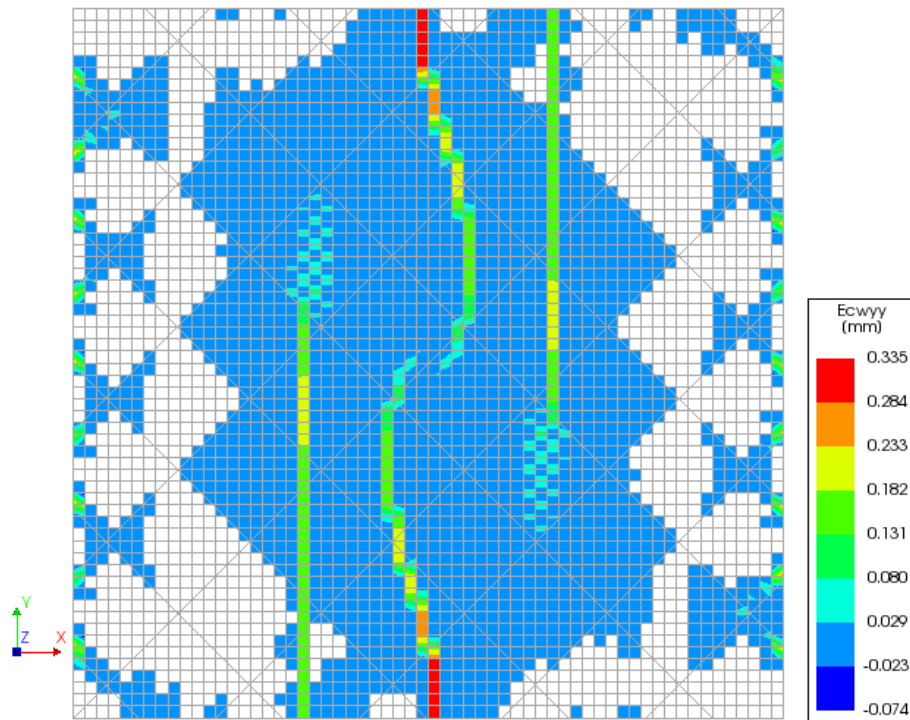
Principal strains

Nonlinear analysis
Load-step 55, Load-factor 55.000
Total Strains E1



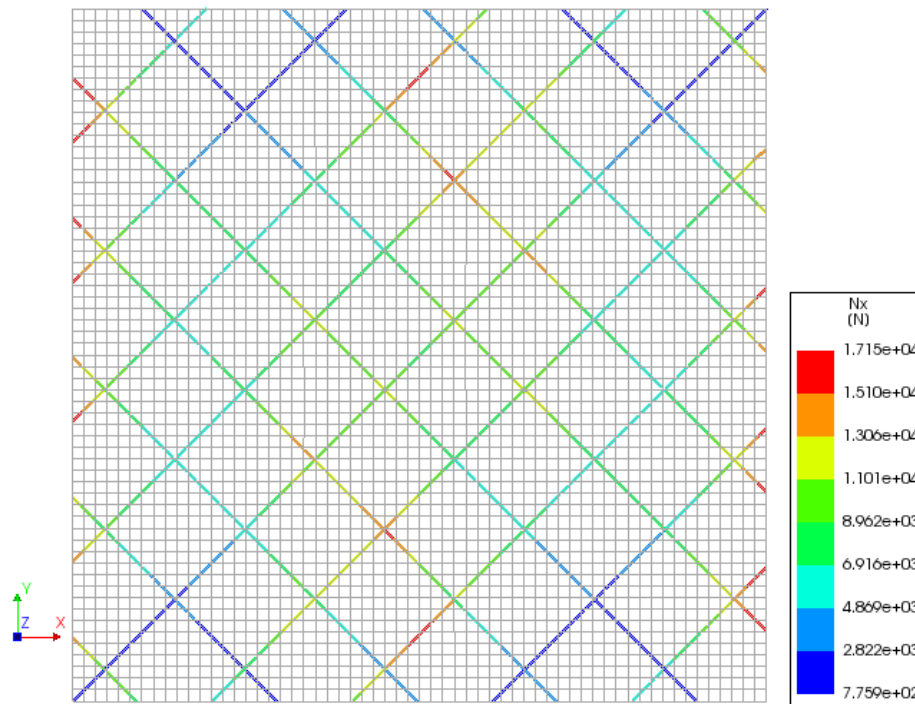
Crack widths

Nonlinear analysis
Load-step 55, Load-factor 55.000
Crack-widths E_{wyy}



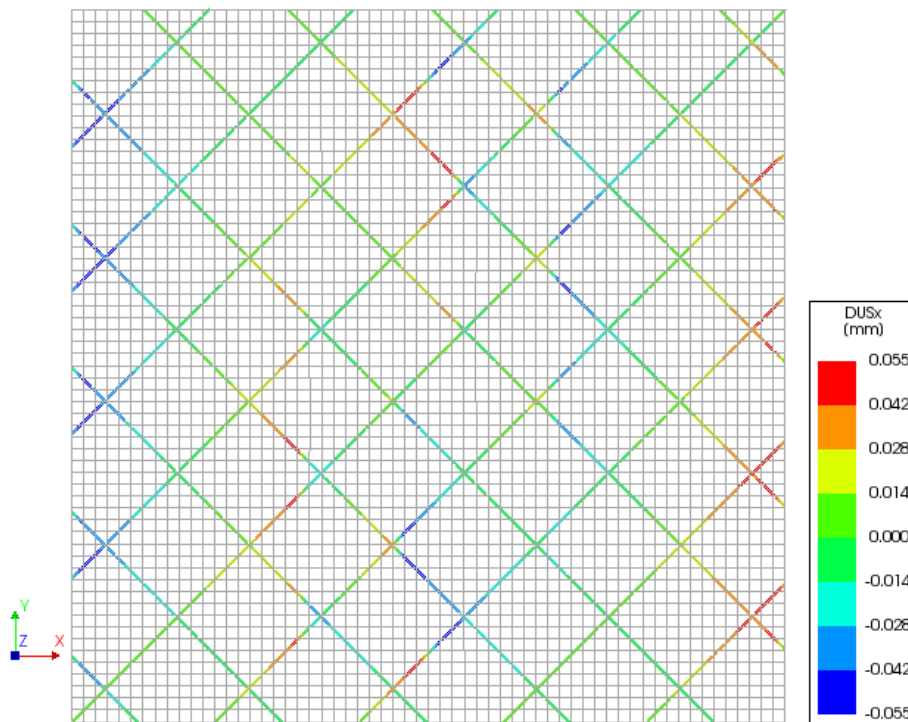
Reinforcement cross section forces

Nonlinear analysis
Load-step 55, Load-factor 55.000
Reinforcement Cross-section Forces Nx



Reinforcement interface relative displacement

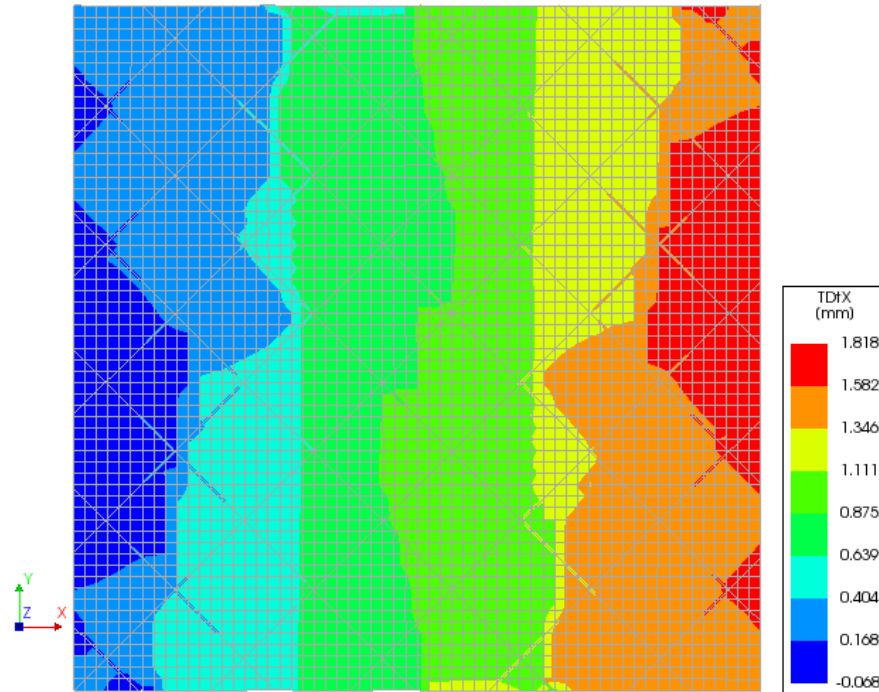
Nonlinear analysis
Load-step 55, Load-factor 55.000
Reinforcement Interface Relative Displac DUSx



2. TP2 Reference model, load step 175

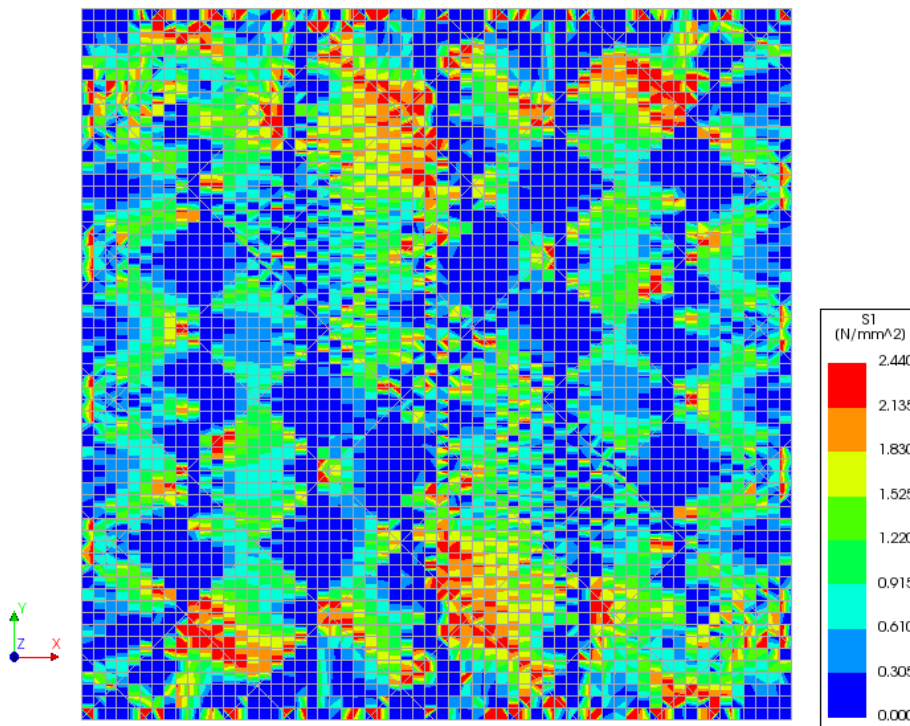
Total displacement

Nonlinear analysis
Load-step 175, Load-factor 175.00
Total Displacements TDtX



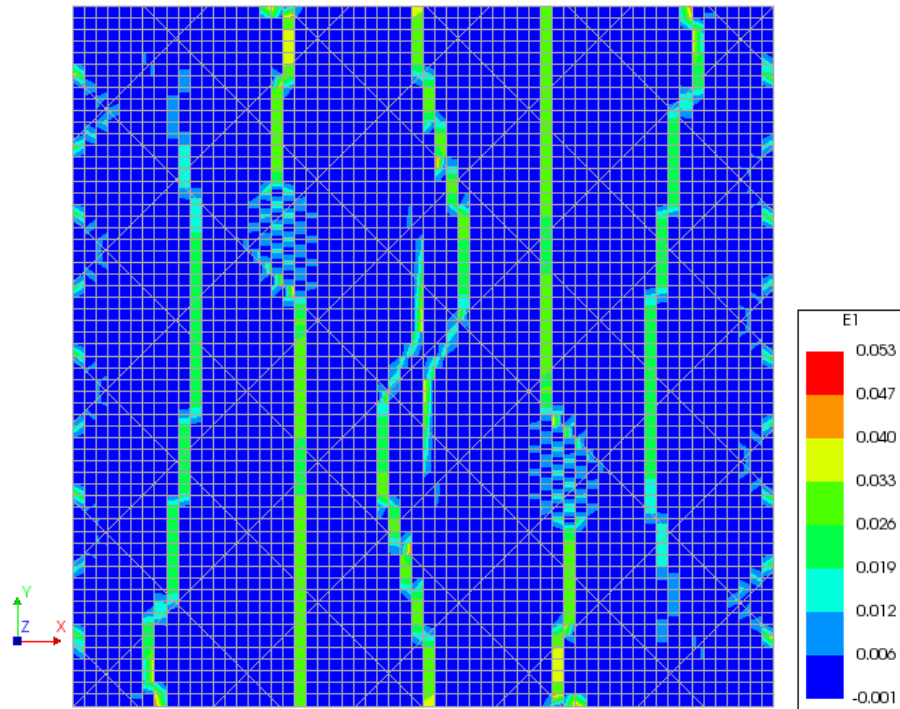
Cauchy total stresses

Analysis61
Load-step 175, Load-factor 175.00
Cauchy Total Stresses S1



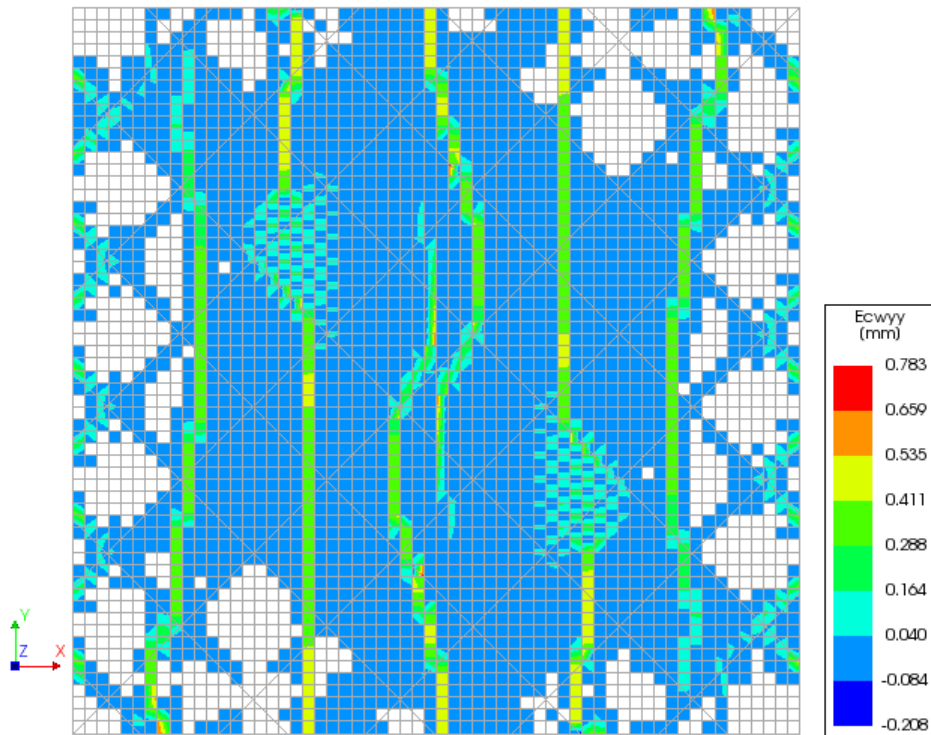
Principal strains

Nonlinear analysis
Load-step 175, Load-factor 175.00
Total Strains E1



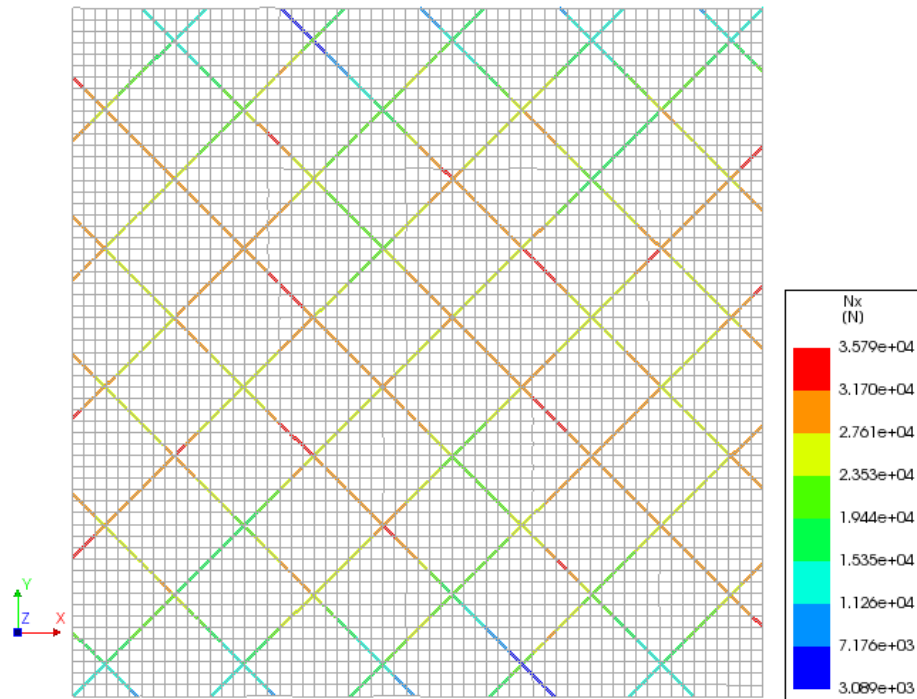
Crack widths

Nonlinear analysis
Load-step 175, Load-factor 175.00
Crack-widths Ecwyy



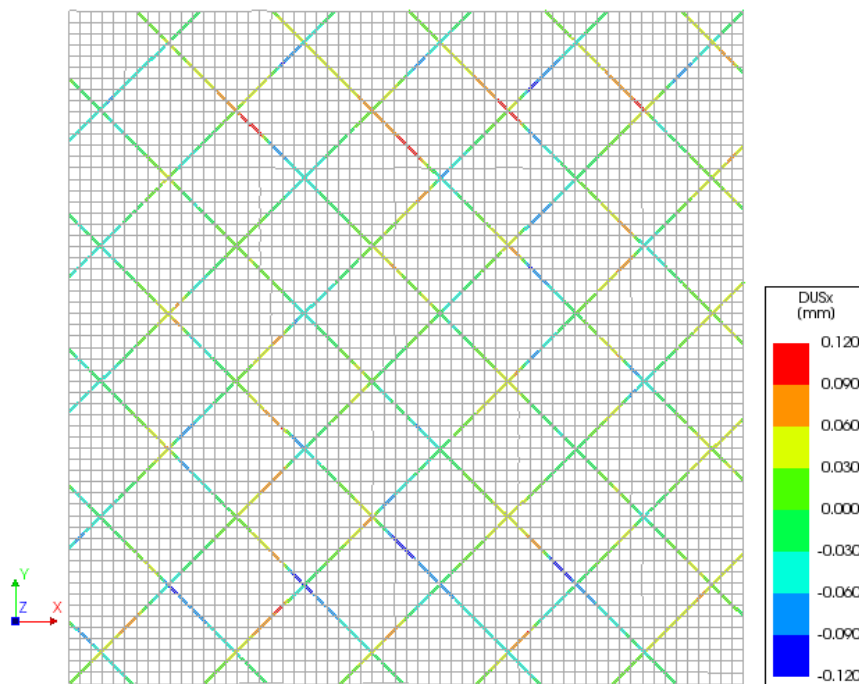
Reinforcement cross section forces

Nonlinear analysis
Load-step 175, Load-factor 175.00
Reinforcement Cross-section Forces Nx



Reinforcement interface relative displacement

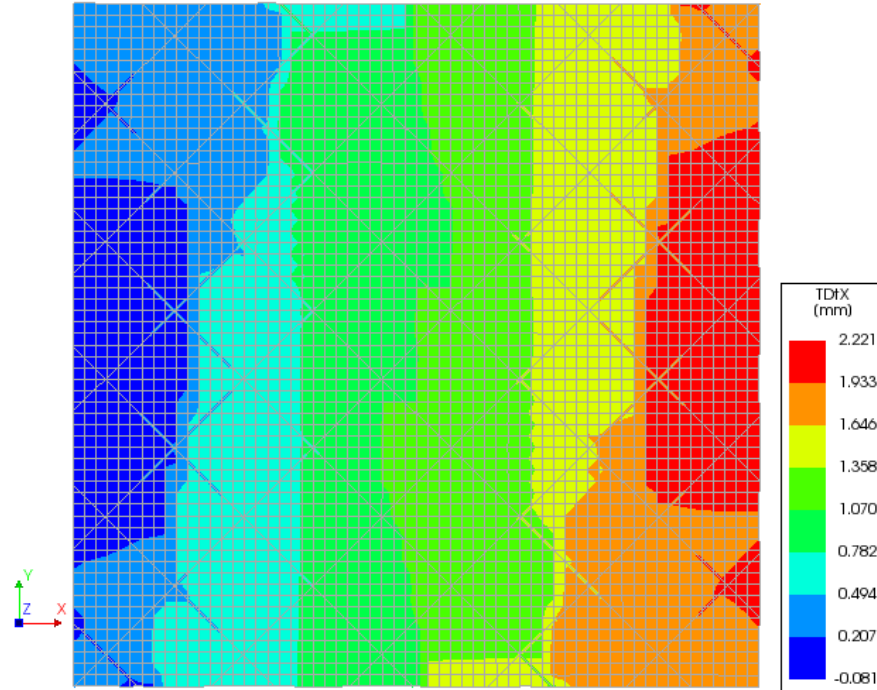
Nonlinear analysis
Load-step 175, Load-factor 175.00
Reinforcement Interface Relative Displac DUSx



3. TP2 Reference model, load step 214

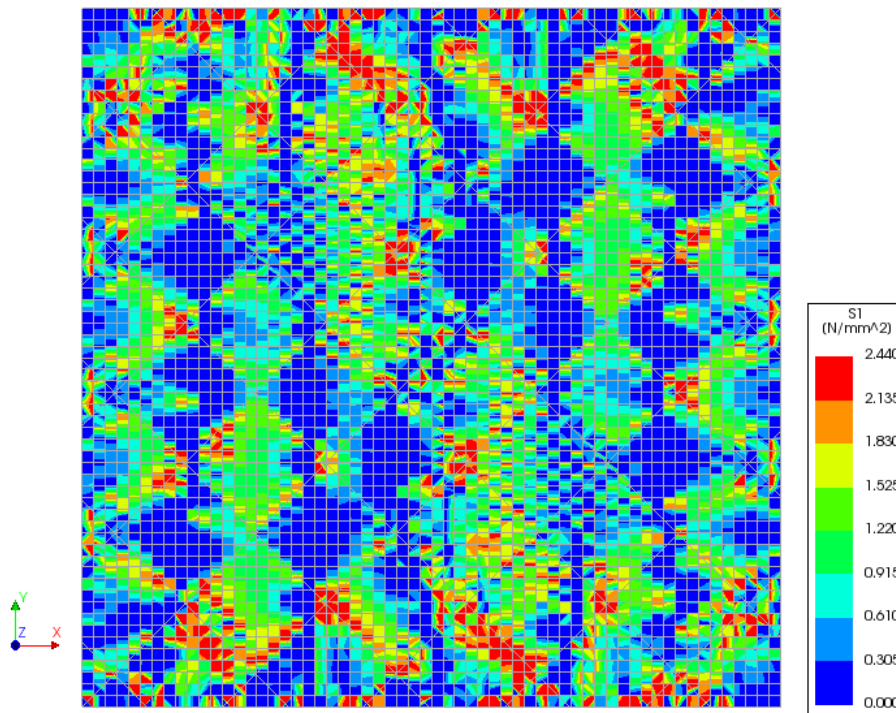
Total displacement

Nonlinear analysis
Load-step 214, Load-factor 214.00
Total Displacements TDtX



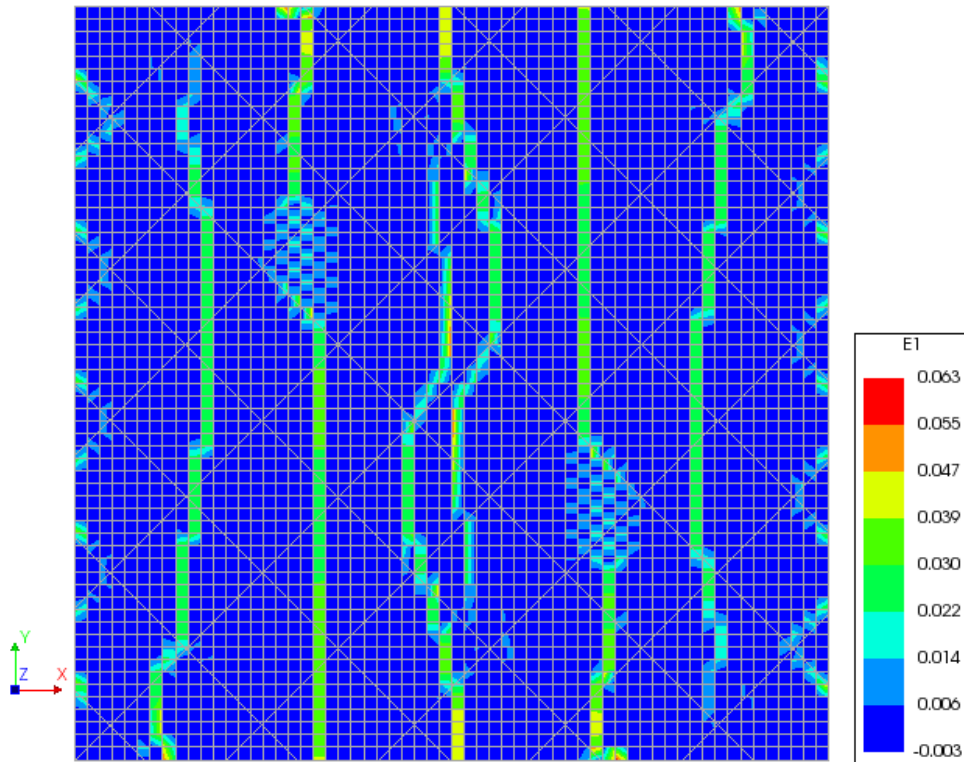
Cauchy total stresses

Analysis61
Load-step 214, Load-factor 214.00
Cauchy Total Stresses S1



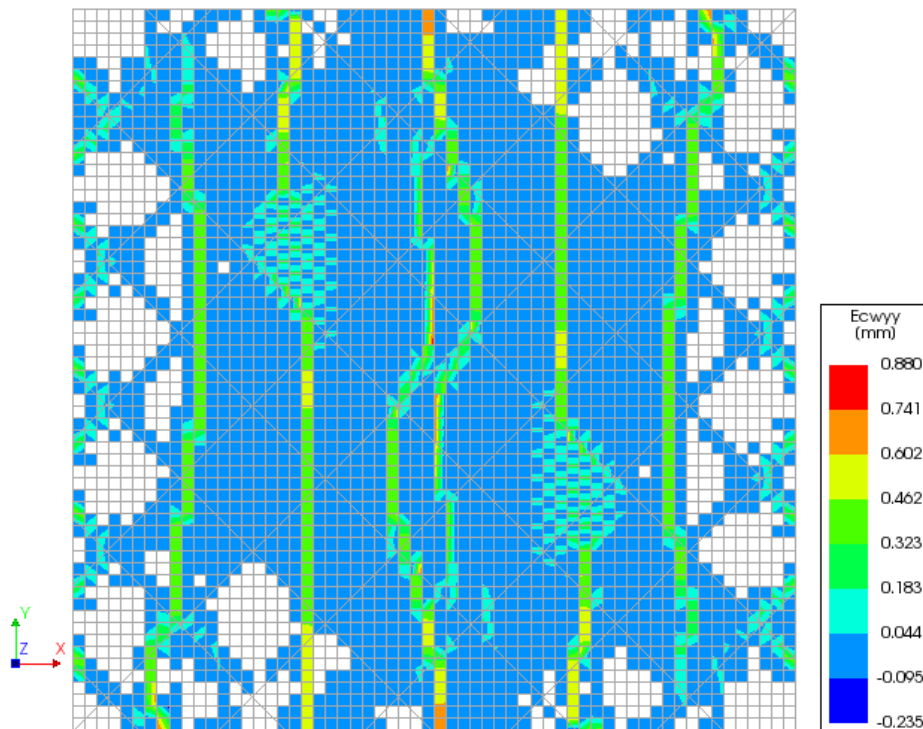
Crack strains

Nonlinear analysis
Load-step 214, Load-factor 214.00
Total Strains E1



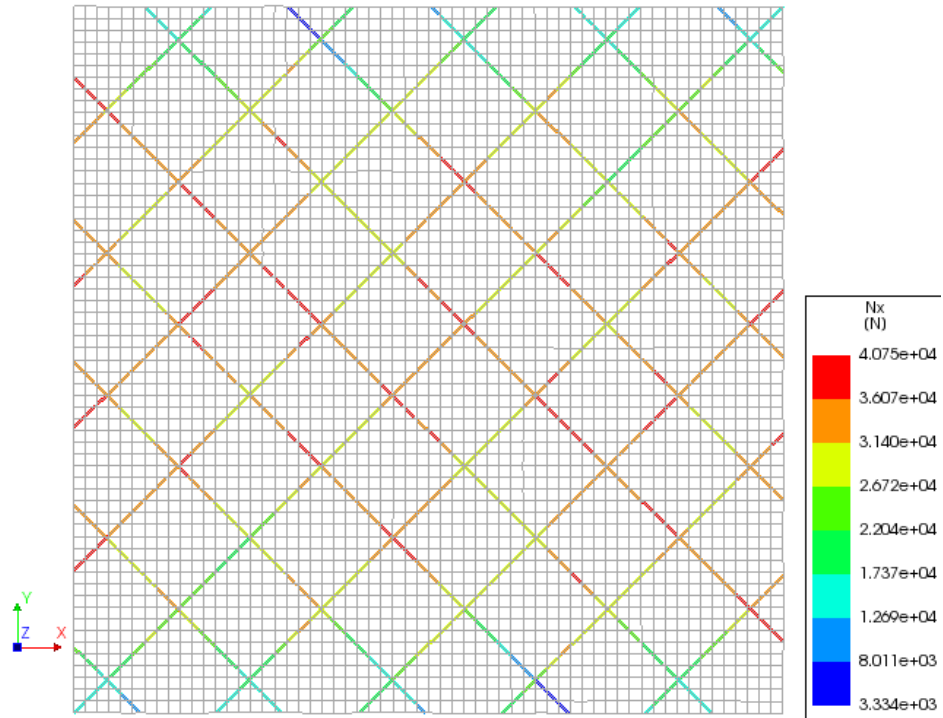
Crack widths

Nonlinear analysis
Load-step 214, Load-factor 214.00
Crack-widths Ecwyy



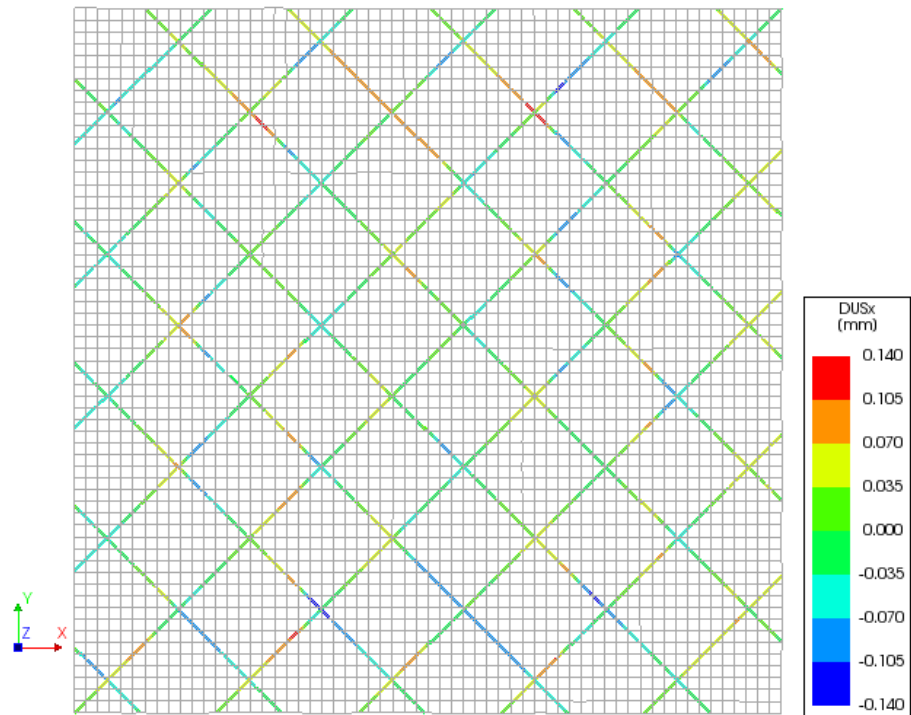
Reinforcement cross section forces

Nonlinear analysis
Load-step 214, Load-factor 214.00
Reinforcement Cross-section Forces Nx



Reinforcement interface relative displacement

Nonlinear analysis
Load-step 214, Load-factor 214.00
Reinforcement Interface Relative Displac DUSx



Load step 55

Load step 55 is the first step on TP2 that was investigated. The reason why this step is interesting is that the first period of cracking ends right before step 55. At this load step the total load on the panel is approximately 102 kN. This load corresponds to a stress level of 1,62 MPa and an average strain of 0,87 ‰. Crack initiation occur in the middle of the upper and lower concrete edge around load step 40. These cracks propagate in an arc towards the middle as two more cracks are initiated. The two latest cracks propagate from the center towards the concrete edge. On load step 55 the two latest cracks reach the concrete edge. As more load is applied, the crack pattern is fairly stable.

Load step 175

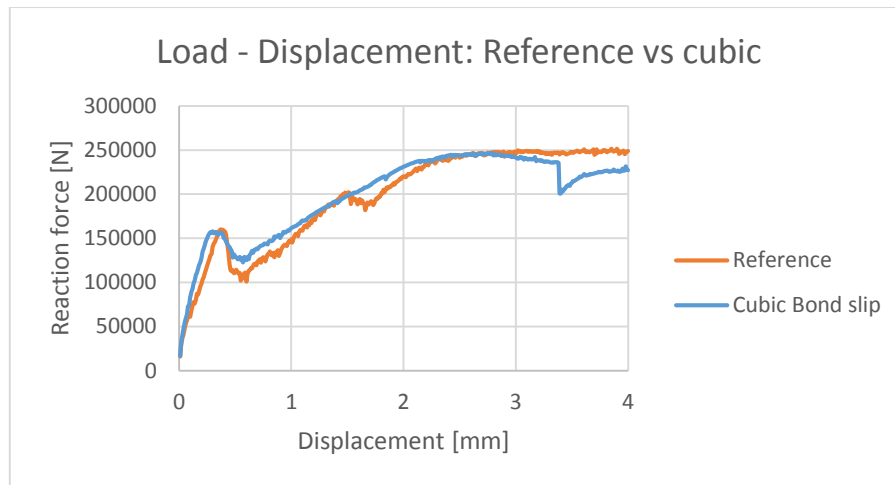
Load step 175 is the second step that was investigated. Before this load step, there has been new cracks developing and the crack pattern has stabilized. The applied loading is at this point approximately 194 kN. The corresponding stress and strain is 3,09 MPa and 2,79 ‰, respectively. The latest period of cracking starts around load step 150 and lasts until load step 175 where it stabilizes. Between load step 55 and 150 three distinct cracks are completely crossing the concrete panel. Right before step 150 two cracks are initiating. After step 150 these two crack initiations enter a period of rapid growth and at step 175 they have almost crossed the whole concrete panel.

Load step 214

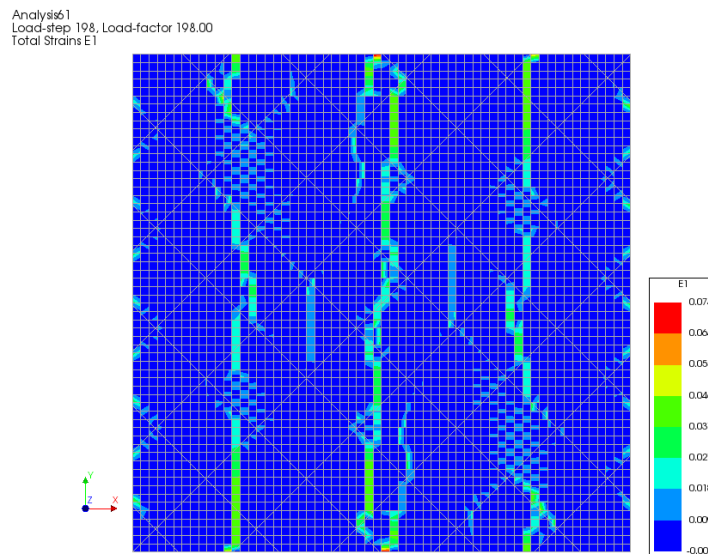
This load step corresponds to the stress level at which cracking results were documented in the experimental work of Dyngeland [8]. This stress level is 3,65 MPa and leads to a strain level of 3,34‰. The applied load at this time is 229kN. Not much has changed since load step 175, except for a little crack growth in the center of the panel.

7.4 Parameter study TP2

TP2 with cubic bond slip

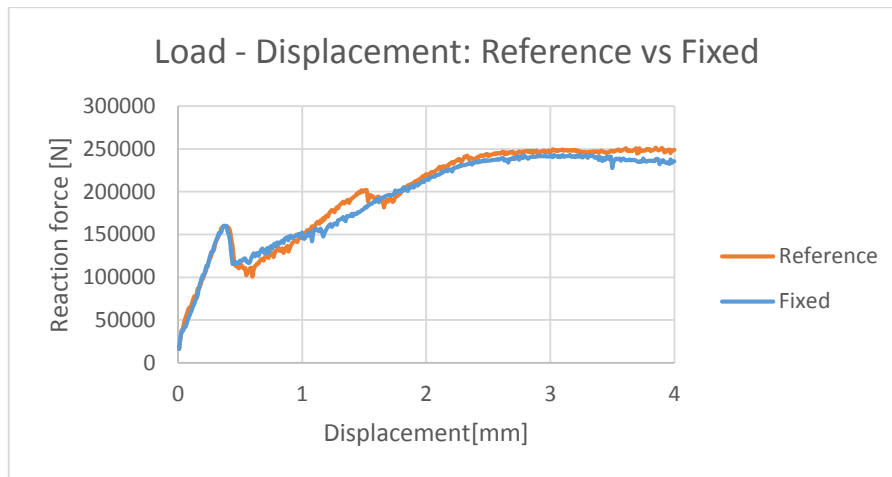


From the load displacement curve above it can be seen that the cubic bond-slip model has, to some extent, an influence with respect to the global behavior. The initial stiffness is slightly higher than for the reference model and instead of two periods of cracking, there is just one for the cubic bond slip model. The cubic bond-slip model is described in chapter 2.8.2 and DSSX is calculated in eq. (5.4).



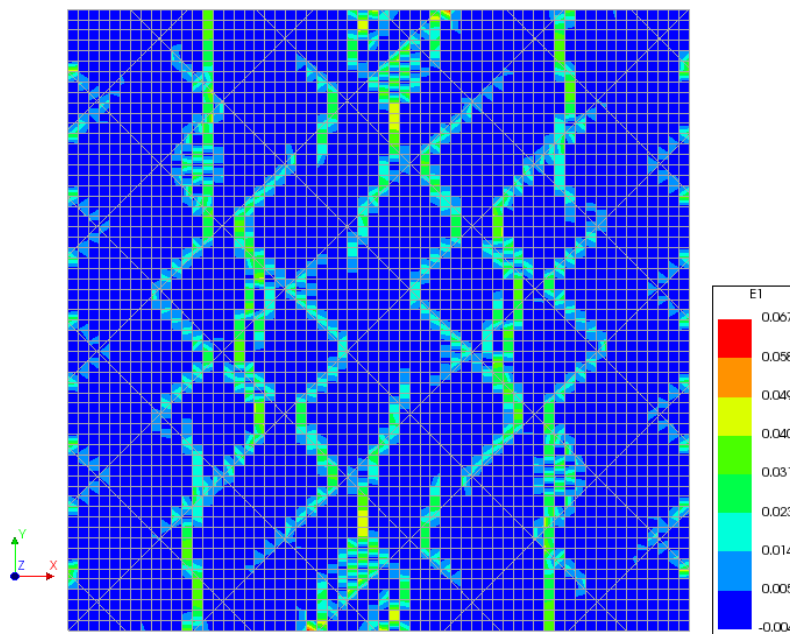
Above is a plot of the principle strain for the model with cubic bond slip formulation. After the first period of cracking between load step 35 and 75, there are three distinct cracks crossing the concrete panel. Because there are no second period of cracking the panel reaches a stress level of 3,65 MPa earlier than the reference panel. From load step 75 to 198 there has been crack growth in the three main cracks but also smaller parallel cracks have occurred.

TP2 with fixed cracking



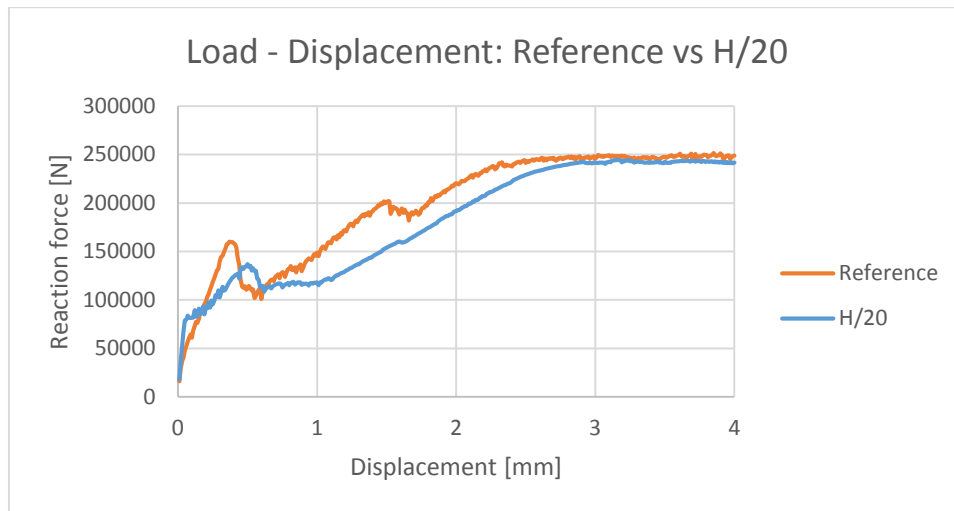
The beginning of the load displacement curve for the model with fixed cracking is almost identical to the reference model. Also after the first cracking period the curves are fairly similar. The model with fixed cracking reaches a stress level of 3,65 after 226 load steps and has a corresponding strain of 3,59‰.

Analysis61
Load-step 226, Load-factor 226.00
Total Strains E1



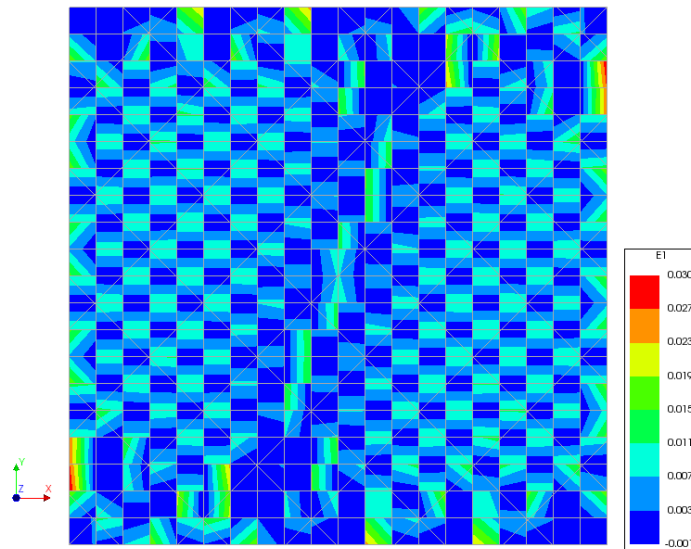
Above, a plot of the principle strain at load step 226 is shown. This model with fixed cracking has a completely different crack pattern than the other models that are studied. At load step 41, four individual cracks initiate, and by step 48 their combined length and position correspond to one crack over the height of the panel. As more load is applied there is a combination of crack width growth, crack propagation and initiation of new cracks. The crack pattern of this model is very chaotic and the number of cracks is hard to determine.

TP2 with mesh H/20



The load displacement curve for the model with mesh size of H/20 is quite different from the reference model curve. Initial stiffness is higher and the model enters a cracking period much earlier than the reference model. The cracking period seems to last much longer than for any other of the modes that have been studied. The duration of the cracking period makes the model appear softer although the stiffness after cracking is about the same for both models.

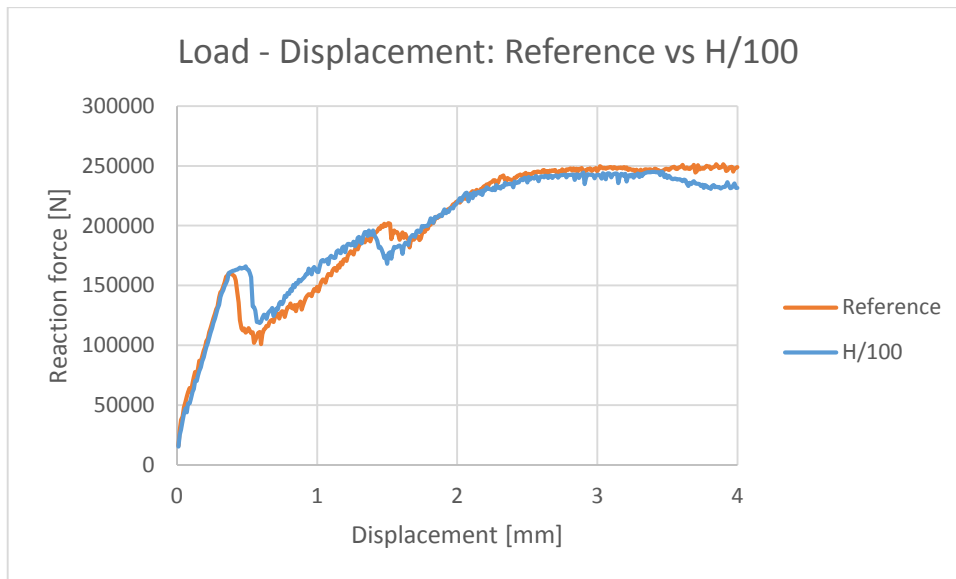
Nonlinear analysis
Load-step 252, Load-factor 252.00
Total Strains E1



Above is a plot of the principal strain in the H/20 model at load step 252. No proper crack pattern can be seen from any load step of this model. Instead of strain localization and crack initiation, strain increases from the left and right side and makes a checkered pattern inwards towards the middle. Around load step 60 there are some localization on the upper and lower edge but no proper crack develops from these points.

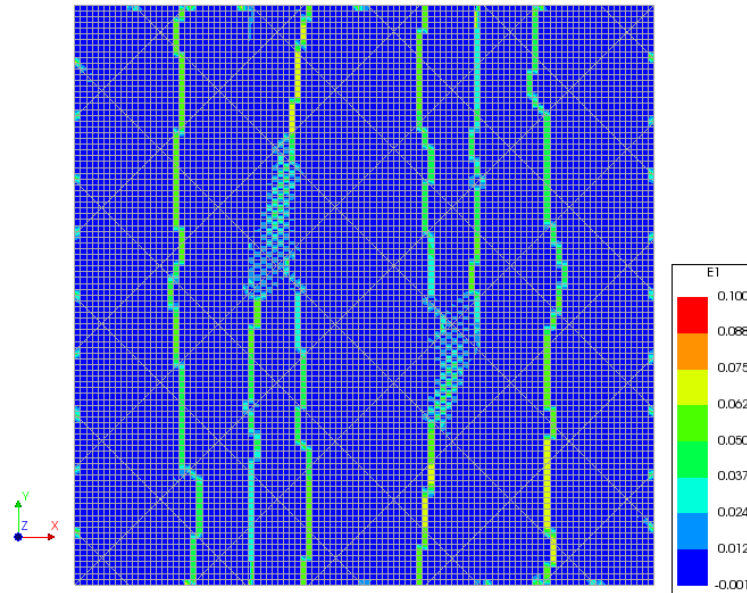
Because there is no proper crack pattern, this model with H/20 is neglected and will not be discussed any further.

TP2 with mesh H/100



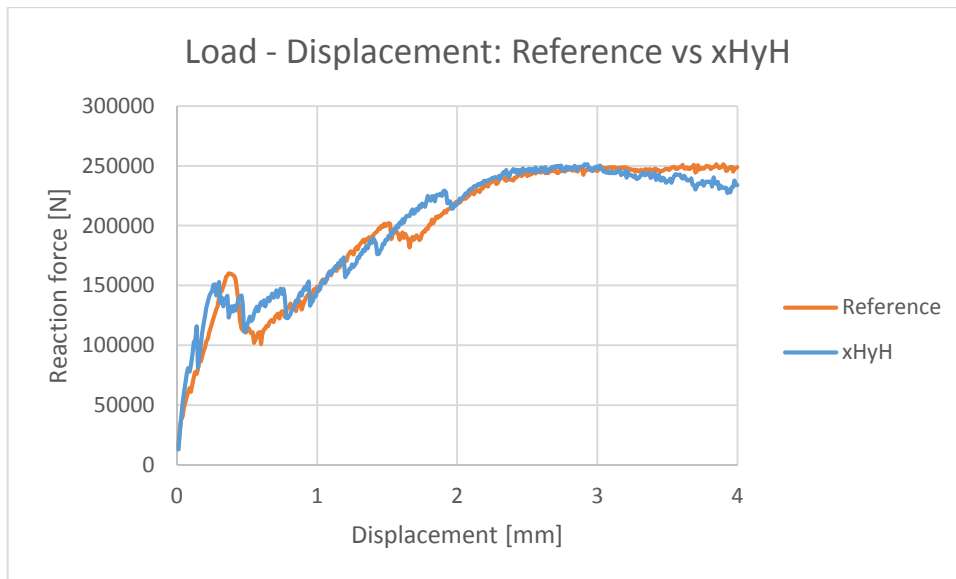
The load displacement curve for the reference panel and the H/100 panel looks very similar. They both have two periods of cracking occurring at about the same stress level. The behavior after cracking is also similar.

Analysis61
Load-step 219, Load-factor 219.00
Total Strains E1



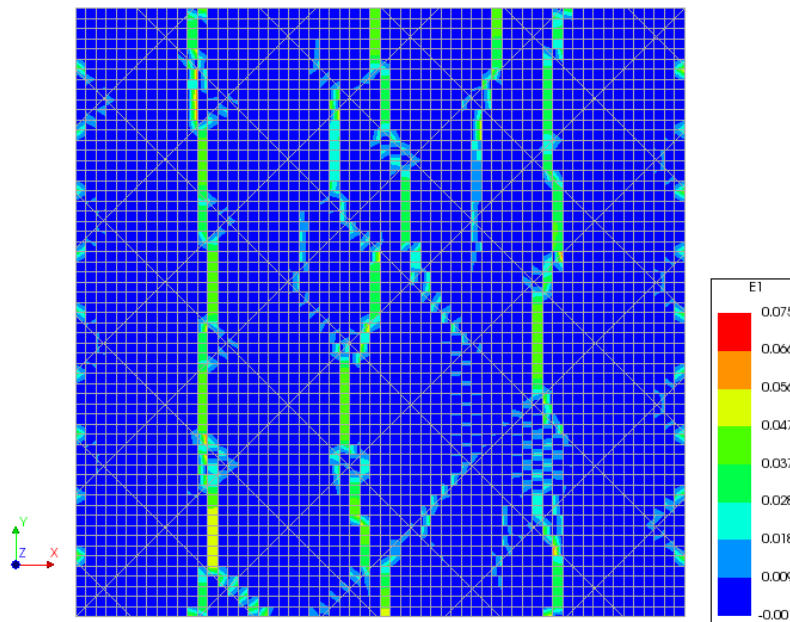
The principle strain plot is taken from load step 219 and clearly displays the formation of five cracks. After the first cracking period there are two complete cracks crossing the height of the panel. Between the cracking periods the crack width of the existing cracks is increasing. During the second cracking period, two of the cracks are merging in addition to the creation of two separate cracks crossing the panel on the left and right side.

TP2 with high DSSX and high DSNY (xHyH)



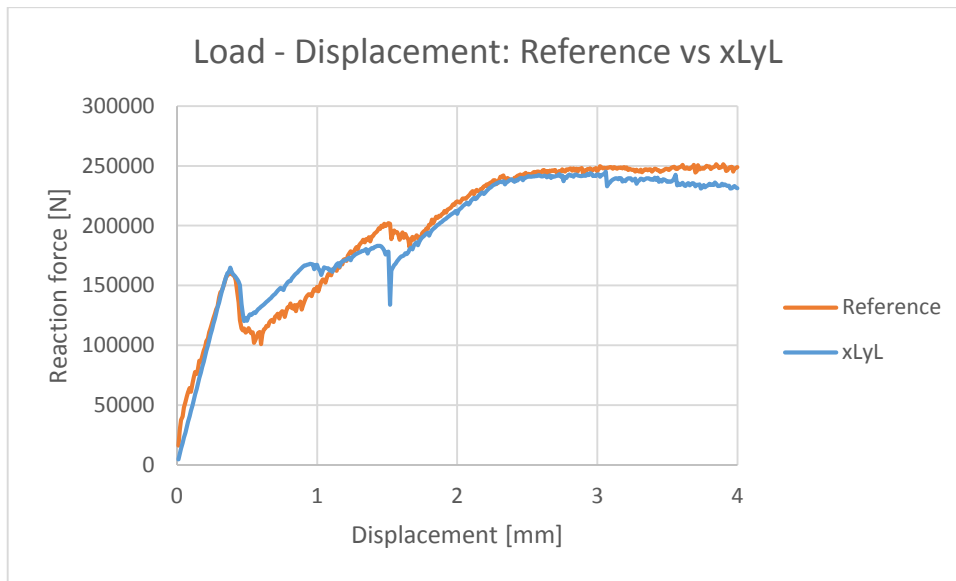
Compared to the reference curve, the model xHyH curve is very jagged. That is because those points are non-converging load steps. Despite the non-converged load steps the load displacement curves are not very different.

Analysis61
Load-step 209, Load-factor 209.00
Total Strains E1



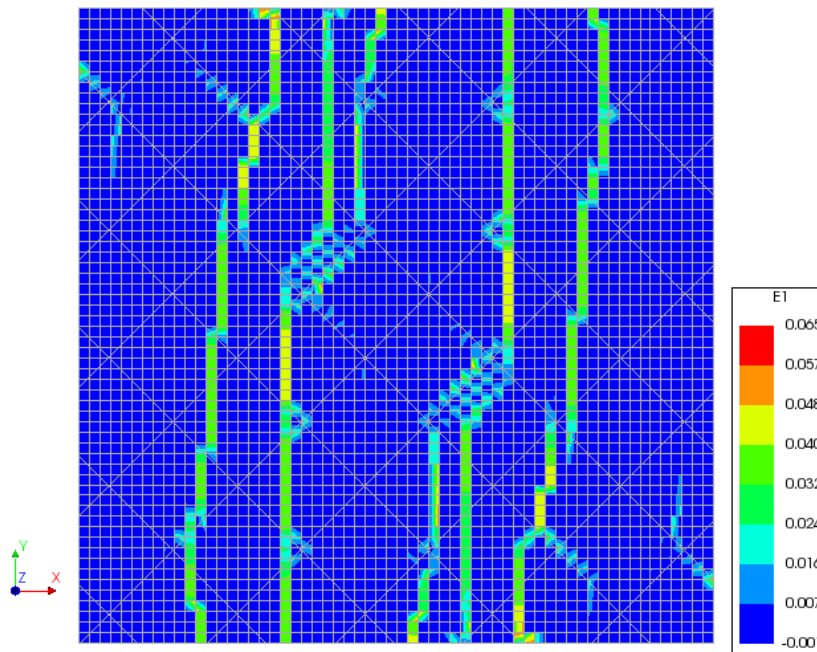
The principal strain plot from load step 209 is plotted above. The first crack initiation occurs around load step 30 and develops into three main cracks crossing the panel by load step 100. After load step 100 smaller cracks and cracks along the reinforcement bars develop.

TP2 with low DSSX and low DSNY (xLyL)



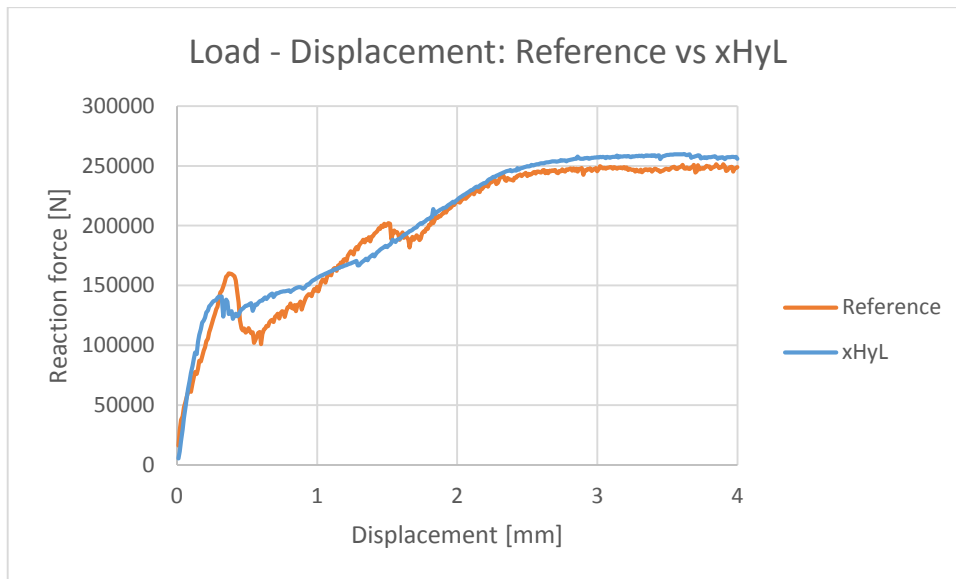
The initial stiffness of the two cases are almost identical. An all over corresponding global behavior is observed. All load steps have converged, even around load step 150 where it is seen a big drop in the reaction force.

Analysis61
Load-step 222, Load-factor 222.00
Total Strains E1



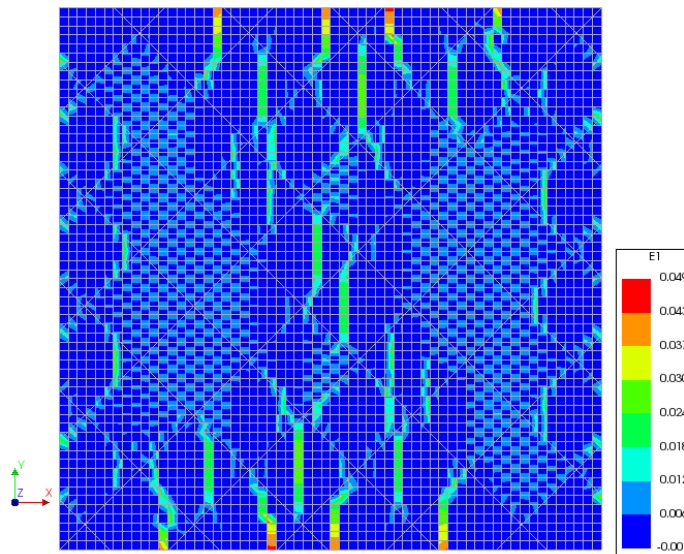
Principal strain plot from load step 222 is shown above. Between load step 42 and 46 two cracks initiate and propagate across the whole panel. Around load step 100, two previously initiated cracks propagate into two more cracks that crosses the panel on the outer left and right side. From this load step and until 222 two minor cracks slowly propagates and merges with the two first cracks.

TP2 with high DSSX and low DSNY (xHyL)



The load displacement curve from the reference and xHyL model can be seen above. Unlike the reference model, the xHyL only has one period of cracking. Overall the global behavior is quite similar.

Analysis61
Load-step 211, Load-factor 211.00
Total Strains E1



Principal strain from load step 211 is plotted above. It shows large areas with a checked pattern. These areas develop before any crack initiation from the concrete edges. Between load step 30 and 50, eight small cracks initiate and propagate at different places but no continuous cracks are formed. Onward towards step 211 new cracks develop but still no continuous crack develops.

7.5 Crack widths and crack spacing TP1 and TP2

Table 8 shows a listing of average crack widths and average crack spacing calculated from the finite element analyses of the panels. Method 1 is based on the total displacement at a given load step. Displacements “TDtX”, i.e. total displacement in x-direction, was collected for all concrete nodes along the left and right edges of each panel. An average displacement for each edge was then calculated by dividing all nodal displacements by the number of nodes along the respective edge. Lastly, the difference in average nodal displacement between left and right edge was divided by the number of observed cracks. Method 2 is based on the total concrete principal strain, which was sampled at the element integration points. All strains were collected and divided by the number of nodes per element times the number of elements. This would correspond to an average element principal strain. This average strain was multiplied with the crack bandwidth, resulting in an average crack width. This method works best with models where the strain is concentrated to one element width and not spread across a large area. Results from TP2 “xHyL” for example will underestimate the crack widths substantially. To avoid large areas of increased strain, only strain levels above 0,0067 were sampled. 0,0067 corresponds to a crack width of 0,1 mm when multiplied by the crack band width. This results in an average crack width for the cracks that have a width of 0,1 mm or higher.

Table 8: Average crack widths and spacing from Nonlinear Analyses

Specimen	Stress [MPa]	Average crack width, method 1 Displacement [mm]	Average crack width, method 2 [mm]	Average Spacing [mm]	Number of cracks
TP1 Reference	4,13	0,273	0,159	315	2
TP1 Cubic	4,13	0,248	0,196	210	3
TP1 Fixed	4,13	0,232	0,168	210	3
TP1 H/100*	4,28	0,273	0,158	315	2
TP1 xHyH	4,13	0,162	0,162	126	5
TP1 xLyL	4,13	0,265	0,194	315	2
TP1 xHyL	4,13	0,153	0,160	126	5
TP2 Reference	3.66	0,307	0,374	105	6
TP2 Cubic	3.66	0,567	0,268	210	3
TP2 Fixed	3.66	0,322	0,319	105	6
TP2 H/100	3.66	0,367	0,358	126	5
TP2 xHyH	3.66	0,355	0,369	126	5
TP2 xLyL	3.66	0,370	0,420	126	5
TP2 xHyL	3.66	0,313	0,194	105	6

*No stabilized crack pattern at stress level 4,13 MPa.

Table 9: Crack widths and spacing according to Eurocode 2 and fib Model Code 2010

Specimen	Average reinforcement strain*	Eurocode 2		fib Model code 2010	
		$s_{r,max}^{**}$ [mm]	w_d [mm]	$l_{s,max}^{***}$ [mm]	w_d [mm]
TP1 Reference	0,00167	219,16	0,37	79,62	0,27
TP1 Cubic	0,00170	219,16	0,37	79,62	0,27
TP1 Fixed	0,00147	219,16	0,32	79,62	0,23
TP1 H/100	0,00142	219,16	0,31	79,62	0,23
TP1 xHyH	0,00164	219,16	0,36	79,62	0,26
TP1 xLyL	0,00182	219,16	0,39	79,62	0,29
TP1 xHyL	0,00158	219,16	0,35	79,62	0,25
TP2 Reference	0,001664	115,60	0,19	44,49	0,15
TP2 Cubic	0,001656	115,60	0,19	44,49	0,15
TP2 Fixed	0,001746	115,60	0,20	44,49	0,16
TP2 H/100	0,001841	115,60	0,21	44,49	0,16
TP2 xHyH	0,001714	115,60	0,20	44,49	0,15
TP2 xLyL	0,001780	115,60	0,21	44,49	0,16
TP2 xHyL	0,001714	115,60	0,20	44,49	0,15

* Average strain in reinforcement in cracks, sampled from nonlinear analyses

** Maximum crack spacing.

*** Length where slip between concrete and steel occurs.

The table above shows the calculated crack widths for TP1 and TP2 according to Eurocode 2 and fib Model Code 2010. Both codes state that a certain distance is to be multiplied with an average strain. Eurocode 2 operates with a maximum crack distance, while fib Model Code 2010 uses a de-bonding length. The calculation of these may be found in Appendix B. The average strain consists of the average strain in the reinforcement minus the average strain in the concrete. The latter was neglected in the calculations due to difficulties regarding the sampling of the concrete strains between cracks.

Table 10 contains experimental average crack widths and spacing and average crack widths and spacing obtained from nonlinear analysis results. The average crack widths for TP1 and TP2 are taken as the average of Method 1 and Method 2 in Table 8.

Table 10: Experimental crack widths and spacing

Specimen	Stress level [MPa]	Average crack width [mm]	Spacing [mm]
S1	3,76	0,11	112
S2	3,56	0,08	99
S3	3,80	0,19	78
S4	3,49	0,20	77
TP1	3,66	0,22	315
TP2	3,65	0,34	105

Part IV: Evaluation and conclusion

8. Evaluation

In the previous chapter, results from the finite element analyses of the concrete panels TP1 and TP2 were presented. From the parameter study the most important aspects of the analyses were presented. For both panels, results from analyses of a reference test, cubic bond-slip, fixed crack model, mesh size $h/20$, mesh size $h/100$ and a “xHyH”-, “xLyL”- and “xHyL” case was presented. In this section follows an evaluation of the obtained results from the finite element analyses linked to the various numerical model inputs.

8.1 Bond-slip models

It seems that the fib Model Code 2010 bond-slip model, hereafter denoted MC10 bond-slip model, describes the interface between concrete and reinforcing steel in a more complex manner compared to the cubic bond-slip model. This is due to the fact that for the MC10 bond-slip model, the distance between the reinforcement ribs are taken into account.

TP1

When comparing the reference case with the cubic bond-slip case, a different crack behavior is observed. For the reference case, only two cracks develop during the entire loading procedure, while for the cubic bond-slip case, three cracks develop in the panel. Crack initiation starts at load step 27 for the reference case while for the cubic bond-slip case, crack initiation starts at step 20. This makes sense, since the initial stiffness of the cubic bond-slip curve is larger than the initial stiffness of the MC10 bond-slip curve, which results in a quicker transfer of force to the concrete. Reinforcement yielding occur approximately at the same load step for both cases. However, for the cubic bond-slip case, yielding occurs on three locations at the reinforcing bars, compared to the reference case where yielding only occurs on two locations. This indicates a development of an additional crack in the middle of the panel. A larger reinforcement interface relative displacement, i.e. the relative displacement between reinforcement and concrete nodes, is observed for the MC10 bond-slip model. This results in less transfer of force between reinforcement and concrete, resulting in slower crack initiation for the reference case.

The parameter study of DSSX and DSNY showed that different values for these stiffness moduli had a large impact on the crack patterns. The “xHyH” case and “xHyL” case showed a crack pattern that differed a lot from the reference case crack pattern. The “xLyL” case was more moderate with respect to the crack pattern, compared with the reference case.

For the “xHyH” case, where both DSSX and DSNY are prescribed high values, crack initiation starts already at load step 2. Already at this load step, the tensile strength is exceeded somewhere in the panel. This phenomenon occurs at the start and end nodes of the reinforcement, where the reinforcement stresses are largest. When DSSX is prescribed a such a high value as in this case, it results in an unrealistically high stiffness between the concrete and the reinforcement, which will result in local cracking early in the analysis in elements around the reinforcement start and end nodes. The interface tractions are much lower for the “xHyH” case. At load step 82, the maximum interface traction stresses for the reference case is approximately 5,319 MPa, while for the “xHyH” case, the maximum interface traction stresses are only 0,246 MPa. Also, the interface relative displacements are significantly small compared to the reference case. At load step 82, the maximum relative displacement is approximately 0,135 mm, compared with the xHyH case where the maximum relative displacement is approximately 0,0051 mm.

For the “xLyL” case, cracks start to propagate right after load step 28, which corresponds well to the reference case. At load step 82, an almost identical interface relative displacement when comparing with the reference case, is observed. This also applies for the reinforcement interface tractions, although slightly higher interface tractions are observed for the “xLyL” case. The crack patterns for the the “xLyL” case and the reference case are very similar.

The “xHyL” case is very similar to the “xHyH” case. Also here crack initiation starts at step 2 by the same mechanism, i.e. high stresses in the concrete elements close to the reinforcement start and end nodes. For this case also, very low values for the interface relative displacements and the interface tractions are seen.

TP2

For the model with cubic bond slip, cracking initiates slightly sooner than the reference model. Initiation starts at step 35 and happens at the same places but at a later stage for the reference, at step 42. At load step 75 the maximum interface traction is reached with cubic bond slip. Instead of developing new cracks, the areas with maximum interface traction is increasing along the bars as more load is applied. The number of places along the bars where the maximum interface traction is reached also increases. The increased DSSX is suspected to be the reason for earlier cracking, as the cubic has a value of 386 N/mm^3 compared to 47.1 N/mm^3 for the reference. Compared to the bond slip curve from MC2010, the maximum interface traction is much lower, 4,636 MPa compared to 11,83 MPa. At load step 198 for both models, the reference model has a much higher maximum interface traction meaning more of the stresses in the reinforcement is transferred to the concrete.

In the xHyH panel, cracks initiates at load step 31 at the concrete upper and lower edge as well as in the center of the panel. This initiation happens much sooner than for the reference panel. Relative displacement between the reinforcement and concrete in X-direction is much lower for this model. Maximum 0,094 mm resulting in an interface traction of 4,44 MPa compared to 0,14 mm and 5.31 MPa for the reference model. The crack pattern also shows more cracks following the reinforcement compared to the reference model. It should be noted that this model experienced load steps without convergence that can have taken effect on the crack pattern.

For the xLyL panel cracks initiate slightly later than for the reference panel. The panel also reaches much higher interface relative displacement than the reference at the same stress level. This leads to higher interface tractions. The effect of a low DSNY is best seen at the supports in the reinforcement. At these points the relative displacement of the interface elements in the Y-direction to the concrete is 0,172 mm, compared to $1,83 \cdot 10^{-5}$ mm for the reference case. When comparing the crack patterns with the reference, there are some differences. Reference case have 6 cracks while xLyL have 5 cracks. Common for the panels is that the cracks cross the whole panel and areas of increased strain is limited.

The model with xHyL got several small cracks spread across the panel. The first cracks initiate earlier than for the reference panel, at load step 35. Before these cracks initiates, there are large areas of increased strain making a checkered pattern in the strain plots. These areas develop from the left and right edge where the reinforcement reaches the panel edge. Biggest relative displacement of 0.010 mm in x-direction resulting in an interface traction of only 0,479 MPa in the reinforcement at

the left and right edge at load step 211. Crack pattern differs from the reference panel in the length of the individual cracks and the large areas with increased strain.

8.2 Material models

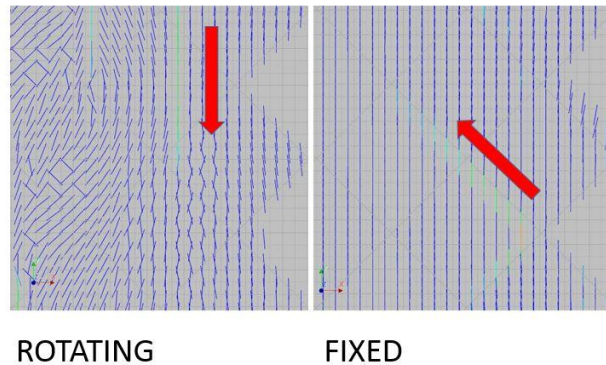
A total strain crack model has been applied in all analyses. An investigation regarding the fixed and rotating crack model was conducted in order to study the impact on the cracking behavior. In section 2.6, the difference between the rotating and the fixed crack model was presented. For the fixed crack model, the direction of the crack plane is fixed upon violation of the fracture criterion, and during subsequent loading, shear strains may arise along the crack plane which results in an increase in shear stress along the crack plane. For a rotating crack model, the normal to the crack and the direction of the major principal stress is aligned at all time.

TP1

By comparing the crack patterns for the reference case and the case where a fixed crack model is utilized, it is seen that the two patterns differ to some extent. Crack initiation for the case with a fixed crack model is load step 27, which corresponds well to the reference case. At this load step all stresses and strains are equal for both cases as expected. As the loading increases, the tensile principal stresses increase more rapidly for the fixed crack model case than for the reference case, resulting in a crack propagating in the middle of the panel for the fixed case. From the load-displacement curve presented in section 7.2. with a fixed crack model vs. the reference case, it is seen that the curve for the fixed crack model flattens out around load step 34, while for the reference case, the curve continues to increase. The flattening of the curve implies low increase in reinforcement force as the load increases. This might explain the more rapid increase in concrete stresses for the fixed crack model. The behavior of the panel seems to depend highly on the crack model that is being used. For the fixed crack model, small micro cracks seem to propagate along the reinforcement bars.

TP2

The crack pattern for the model with fixed crack model is quite different from the reference model. Cracks in this model are following the reinforcement bars, making a zigzag pattern.



The image above shows the crack propagation direction on top of a plot of the crack strain E_{knn} in load step 49. As the crack strains appeared in the elements around load step 40, the strains were aligned in the same direction. As more load is applied the crack strains for the reference model rotate as the direction of the principal strain changes. The crack strains for the fixed model remain in the same direction. Cracks then propagate along the reinforcement bars.

8.3 Mesh properties and sensitivity

In all analyses, a linear meshing order was used, and DIANA10 interpret this as 1.st order elements. 4-noded quadrilateral elements with incompatible modes were used in all analyses. The choice to add incompatible modes to the shape functions of the element would decrease the chance for the elements to exhibit locking behavior, and seemed reasonable. Given the loading situation of the panels, plane stress elements were thought to be well suited to reproduce results. It was assumed that a relatively fine mesh was needed in order to obtain crack contour plots. An element size equal to $H/60$ was used in the reference case, and was in correspondence with Hendriks et.al. [13]. It was of interest to investigate whether the numerical models were sensitive to mesh size change. Two additional meshes were evaluated. One with element size $H/20$, which will be denoted “coarse” and one mesh with element size $H/100$ which will be denoted “fine”. Although the modelling was performed in 2D, an increasing computational time occurred for mesh refinement.

TP1

A quite different global behavior was observed for the coarse and the fine mesh compared with the reference case. The coarse mesh shows a linear behavior upon crack initiation, then a sudden drop in reaction force in the load-displacement curve is observed. This sudden drop may be caused by a sudden force re-distribution along the reinforcing bars as a result of a sudden crack development in the middle of the panel. The reinforcement starts to yield already at load step 68. This is caused by the increasing crack in the middle of the panel, resulting in large reinforcement stresses in the cracked cross section. The coarse mesh shows a quite different crack pattern compared to the reference case. Also, this particular mesh seems a bit too coarse for the study of the development of crack patterns. For the fine mesh, crack initiation starts at load step 24, i.e. the crack initiation stage does not differ much from the reference case. A stabilized crack pattern develops around load step 88, which differs much from the course mesh, but correspond to some extent with the reference case.

Reinforcement yielding occurs around load step 101. For the reference case, reinforcement yielding takes place around load step 94. On the other hand, the fine mesh seems to correspond better with the reference case with respect to the crack pattern than compared to the course mesh.

TP2

The mesh size study showed that the TP2 model is mesh depended. The coarse mesh H/20 did not have any localization propagating into a proper crack. Instead, strain was distributed over a large area making a checkered pattern. This pattern started on the left and right side and spread inward towards the center. Some localization happened at the lower and upper edges but no propagation occurred.

The fine mesh H/100 got a crack pattern with five distinct cracks across the panel. Initiation started around load step 50. The end result shows clearly defined cracks with small areas of increased strain in the concrete. The interface traction and relative displacement are higher for this model then the reference with 5,874 MPa at 0,178 mm displacement.

8.4 Numerical iterative procedures

In DIANA10, one may choose between Newton-Raphson and Quasi-Newton iteration methods for the nonlinear analysis. All analyses performed in this thesis were first tried with the Newton Raphson methods. However, when using these types of iteration methods, divergence would occur. When divergence occurred, DIANA10 would automatically abort the entire analysis. It is uncertain why the Newton-Raphson methods were unable to obtain convergence, but it might have to do with the complexity of the numerical models. When implementing bond-slip reinforcement for instance, the reinforcement bars are also meshed and obtain degrees of freedom. This results in many more equilibrium equations that need to be solved. Because of the problem related to divergence, the Quasi-Newton methods were used. The Broyden version of the Quasi-Newton methods was used in the analyses, and this iteration gave quite stable results. For TP1 and TP2, the line search option was switched on in every analysis. As stated in section 3.1.8, this method is highly recommended, and may be used in combination with all iteration methods. It was seen that convergence was more easily obtained by using the line search method.

For the analyses of TP1, each step in every analysis converged, except for the (xHyH) case and the cubic bond-slip case, where no convergence occurred in load step 152 and load step 44, respectively. For most of the analyses, convergence in each step was obtained after 10-30 iterations. In critical steps, the number of iterations needed to obtain convergence would sometimes exceed 30 iterations.

For the TP2 panel only two models experienced steps with no convergence. The panel with cubic bond had no convergence in step 339, resulting in a sudden drop in reaction forces. Cracks for this panel were studied at load step 198 so this had no effect on the crack pattern. Panel with xHyH had a total of 7 steps without convergence. This might have had an effect on the crack pattern that was observed. In general convergence was often reached within 10 iterations, but some steps needed more time.

8.5 NLFEA versus Eurocode 2 and fib Model Code 2010

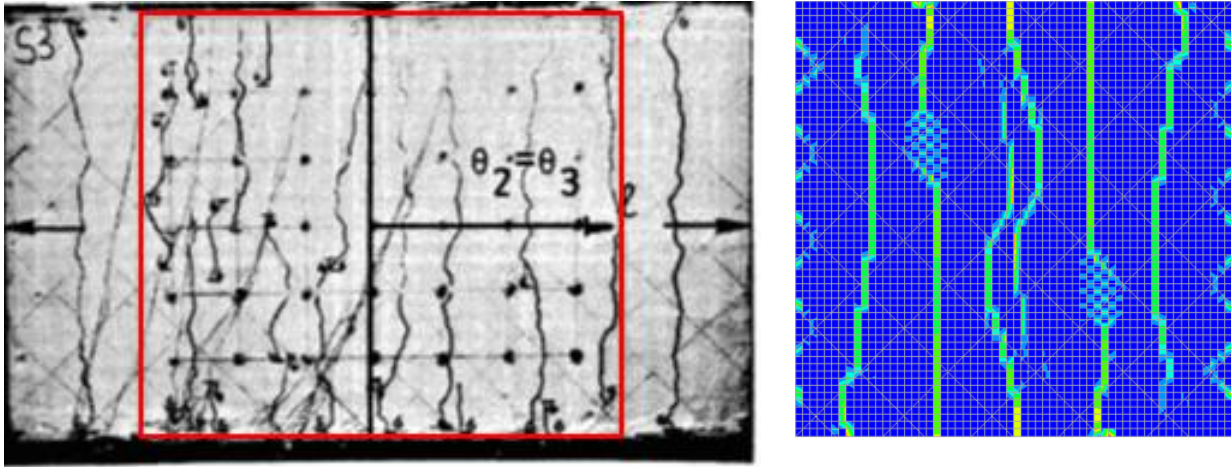
A great deal of time was spent on calculating mean crack widths and crack spacing for the two concrete panels. The aim was to compare calculations that were based on results from the nonlinear finite element analyses with calculations based on the Eurocode 2 and fib Model Code 2010, as well as the experimental results from Dyngeland 1989 [8]. DIANA10 calculates the crack width in an element by multiplying the over strain over the element by a crack bandwidth, while the crack widths from the codes are based on a length (maximum spacing or de-bonding length), multiplied with the difference in average strain between the reinforcement and the concrete.

In Table 8, the calculated crack widths based on the results from the nonlinear analyses are shown. It is seen that method 1, which is based on the difference in displacement between the left and the right edge, divided by number of cracks, in most cases estimates a larger crack width than method 2, which is based on the average principal strain of an element multiplied with the crack bandwidth of the element. This is valid both for TP1 and TP2. The problem with this approach is that it is based on the number of cracks that develops in the panels. This number is not always easily defined, especially for TP2. Nonetheless, some tendencies may be observed. For TP1, the lowest crack width is calculated for the “xHyL” case. The largest crack width is derived from the reference case. For TP2 the smallest crack width is also derived from the “xHyL” case when method 1 is being used. The largest crack width for TP2 with method 1 is derived from the “xLyL” case. It would have been convenient if the calculated crack widths for the two methods corresponded. Sadly, this is not the case. For TP1, and with the largest crack width calculated by method 2 is derived from the cubic bond-slip case and the lowest crack width is derived from the case with mesh H/100. For TP2, the “xLyL” case gives the highest crack width, while the “xHyL” case gives the lowest crack width. It seems that DSSX have a large influence on the crack widths. It was found very difficult to establish a general way of calculating the crack widths from the nonlinear analyses results, and the two methods, displacement based and average strain based, are at best a pointer for the crack widths given the assumptions that the methods are based on.

In Table 9 calculated crack widths and associated crack spacing according to Eurocode 2 and fib Model Code 2010 are shown. It is observed that the crack widths according to Eurocode 2 in general are larger than those calculated by fib Model Code 2010. This is valid, especially for TP1, where the maximum crack spacing $s_{r,max}$ is quite large. This large maximum crack spacing derives from a large effective tension area of the cross section, resulting in a small reinforcement ratio which evidently impacts the maximum spacing of the cracks. It is also noted that for TP1 the crack widths calculated from nonlinear analyses results, both method 1 and method 2, all over are smaller than those calculated from Eurocode 2 and fib Model Code 2010. For TP2, the crack widths calculated from the codes are all over smaller than those calculated from nonlinear analysis results in Table 8. The contribution from the concrete, i.e. the average concrete strain between cracks, was neglected, and may cause some over estimation of the crack widths calculated from the codes. The average concrete strain between cracks was neglected because of difficulties with respect to the sampling.

When assessing at the calculated crack widths and spacing for TP2, a much better correspondence between the two codes are observed. However, because of the small maximum crack spacing and de-bonding length, the code crack widths correspond rather poorly with respect to the nonlinear analysis crack widths. For TP2, an under estimation are seen from the codes.

8.6 Comparison of numerical and experimental crack patterns



The two figures above shows the experimental crack pattern for panel S3 and the numerical crack pattern for TP2 reference sampled at load step 214. By comparing the dark lines within the red square with the principal strain plot some similarities are seen.

8.7 Sources to error

The numerical models were established with the aim of reflecting the experimental panels as good as possible. However, it was quickly discovered that it was a challenging task to re-create the experimental panels exact. There exist many sources of error with respect to the numerical models and the obtained results of this thesis.

In reality, the concrete panels have different dimensions than the numerical models. Only a part of the experimental panels were modelled, illustrated by the red square in Figure 40. In the experiments, the strains were sampled within this area, and this area is also where the experimental crack widths and spacing were sampled. When modelling only the area marked in red, it is possible that the numerical results suffer from edge disturbances.

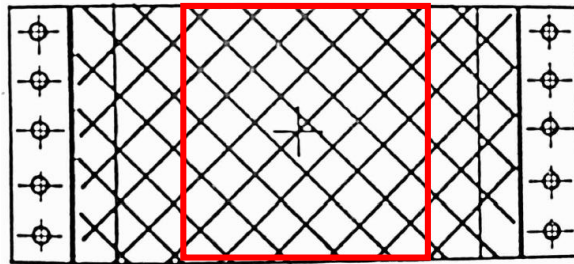


Figure 40: Panel S3/S4, experimental

Also, a source of error is related to the load application. In the numerical models, the reinforcement end nodes were subjected to point loads. In the experiment, the reinforcing bars were welded to steel plates on each edge of the panel. To these steel plates five loading arms were connected. The loading arms were attached to a loading jack that pulled in the horizontal direction. This may have caused some loading in the concrete as well. In the numerical models it seemed reasonable to apply point loads in the reinforcement bars only, and no loading was applied to the concrete.

Another source of error related to the boundary conditions. For the case with horizontal reinforcement, all the reinforcing bars are welded to the steel loading plates. In the numerical model, this is re-created with translational constraints in x- and y-direction. For the case with orthogonal reinforcement, the reinforcing bars are welded to the steel loading plates along the vertical edges, and along the horizontal edges, welded to small, separate steel plates. The latter weld situation was re-created with tyings in the numerical model. The tying function may not represent the displacement of the reinforcement bars in a realistic manner compared with the experiment.

Lastly, exact measurements were not available regarding the position of the reinforcing bars for the case with orthogonal reinforcement, which results in small differences in the reinforcement position of the numerical model compared to the experimental panel.

9. Conclusion

In this thesis, nonlinear analyses of two reinforced concrete panels have been performed. The aim has been to study the cracking behavior of the concrete when the reinforcement bars are given bond-slip reinforcement properties.

The bond-slip model from MC10 resulted in the highest interface reinforcement tractions. This is due to the fact that the MC10 bond-slip curve is defined with a higher bond stress plateau compared with the cubic bond-slip model.

The cubic bond-slip model lead to an earlier crack initiation stage for both panels due to the initial stiffness which is higher for the cubic bond-slip model than the MC10 bond-slip model.

A high value for DSSX and DSNY resulted in a significant decrease in both interface tractions and interface relative displacement for both panels. Furthermore, the high prescribed values for the stiffness moduli resulted in a much earlier crack initiation for TP1 compared to the reference case. The same applies for panel TP2. Five cracks developed in panel TP1 as a result of the large stiffness moduli. Only two cracks propagated for the reference model. For TP2, fewer clear cracks developed as a result of high stiffness moduli. However, the crack pattern was quite different.

A high value for DSSX and a low value for DSNY differed insignificantly with respect to the case with a high DSSX and a high DSNY for panel TP1. A high shear stiffness modulus and a low normal stiffness modulus resulted in crack initiation a few load steps later for panel TP2 compared with the reference case. It also resulted in a spread of small cracks all over the panel.

A low DSSX and a low DSNY had no significant impact on the panel TP1 with respect to the reference case. For the panel TP2, a low value for both of the stiffness moduli resulted in much higher interface tractions and interface relative displacements. Also, for panel TP2, fewer cracks developed in as a result of low stiffness moduli.

The value of the shear stiffness moduli, DSSX has a large influence on the cracking behavior of the two panels. With horizontal reinforcement only, the effect of a high DSSX is best seen with respect to the crack pattern. With orthogonal reinforcement, the crack pattern did not change drastically, but a difference is present. However, the interface tractions and relative displacements decreases drastically when the stiffness modulus is prescribed a high value, compared to the reference case.

For the case with horizontal reinforcement only, changing the parameter DSNY has small and almost negligible effect. Furthermore, with orthogonal reinforcement, the normal stiffness plays a more important role, since the reinforcement to some extent will try to penetrate the concrete.

It was attempted to analyze the two panels with Regular Newton Raphson and Modified Newton Rapson, but all analyses ended in divergence after a varying number of steps. The bond slip formulations seem to require numerical iterative methods that are more sophisticated, and it is concluded that a Quasi-Newton method is best suited for the task. The Broyden type Quasi-Newton method worked well for both panels.

For the reference case with a rotating crack model, two straight cracks develop in a certain distance from the center of the panel for TP1. For TP2, six relatively straight cracks develop in the panel. For the fixed crack model, three cracks propagate for TP1. For TP2, the estimated number of cracks remained unchanged. However, both for TP1 and TP2, very different crack patterns were observed as cracks would develop along the reinforcement bars. For the fixed crack model, the normal to the crack remain unchanged during cracking while the principal direction of the stress changes. This causes an increase in shear stresses at the crack surface and may explain cracking along the reinforcement bars.

For TP2 the optimal crack pattern with respect to the experimental crack patterns was obtained with the reference case. With orthogonal reinforcement and reference loading situation, the rotating crack model simulates the experimental cracking behavior more accurate than the fixed crack model.

10. Suggestions to further work

The analyses performed in this thesis have been useful with respect to obtaining crack patterns for the different bond-slip model implemented in the numerical models. However, uncertainties have arisen underway that may be of interest to investigate more in depth.

To get a deeper insight regarding bond-slip and how it affects the behavior of the model, the two other bond-slip models available in DIANA10, *Power law* and *Shima et.al.* may be assessed. A straightforward answer to what values DSSX and DSNY should be assigned for different bond-slip models was not managed to be established in this thesis, and might be an interesting field to look further into.

All of the analyses were carried out with first order quadrilateral plane stress elements with a bubble-function. The influence of performing the analyses with second order quadrilateral plane stress elements can be interesting to investigate. In addition, it could be of interest to model in 3-D and use volume elements. Also, a deeper investigation of the “tying” function may be of interest. For TP2 the start/end node of a reinforcing bar was applied the same displacements as the closest concrete node. When the reinforcement start/end node is located between two concrete nodes, a linear interpolation could for instance be assessed.

Obtaining convergence with the Newton Raphson methods was not managed in this thesis. Only the Broyden version of the Quasi-Newton methods was utilized in the analyses. It may be of interest to assess the Chrisfield version and the BFGS version of the Quasi-Newton methods.

11. References

- [1] Allam, S.M, Shoukry, M.S, Rashad, G.E. and Hassan, A.S. (2013). *Evaluation of tension stiffening effect on the crack width calculation of flexural RC members*. Available from: <http://www.sciencedirect.com/science/article/pii/S1110016813000045>. [Read 10.05.2016]
- [2] Besson J., Cailletaud G., Chaboche J.L., Forest S. and Blétry M. (2010). *Non-Linear Mechanics of Materials – Solid Mechanics and its application*. Volume 167. Springer Publisher.
- [3] Brisotto, D.D.S., Bittencourt, E., Bessa, V.M.R.d’A.(2012). *Simulating bond failure in reinforced concrete by a plasticity model*. Available from: <http://www.sciencedirect.com/science/article/pii/S0045794912001046>. [Read 05.04.2016]
- [4] Chen, W.F. (2007). *Plasticity in Reinforced Concrete*. J. Ross Publishing.
- [5] Chrisfield, M.A. (1991). *Non-Linear Finite Element Analysis of Solids and Structures*. Volume 1: Essentials. John Wiley and Sons.
- [6] Cook, R.D., Malkus, D.S., Plesha, M.E. and Witt, R.J (2001) *Concepts and applications of finite element analysis*. 4th ed.
- [7] De Borst, R., Chrisfield, M.A., Remmers, J.J.C. and Verhoosel, C.V. (2012). *Nonlinear Finite Element Analysis of Solids and Structures*. 2nd edition. John Wiley & Sons Ltd.
- [8] Dyngeland, T. (1989). *Behavior of Reinforced Concrete Panels*. Doktor ingeniøravhandling 1989:19, Institutt for betongkonstruksjoner, NTH, Trondheim.
- [9] E.A, de Souza Neto, D. Peric, DRJ. Oven(2008). *Computational Methods for Plasticity – Theory and applications*. 1.st edition. John Wiley and Sons.
- [10] Feenstra, P.H. and de Borst. R. *A Comparison of different crack models applies to plain and reinforced concrete*. Available from: https://scholar.google.no/scholar?rlz=1C1AVNE_enNO681NO681&ion=1&espv=2&bav=on.2.or.&bvm=bv.121421273,d.bGs&biw=1280&bih=884&dpr=1&um=1&ie=UTF-8&lr&q=related:hf8pH2vvQAGGDM:scholar.google.com/. [Read 09.05.2016]
- [11] *fib Model Code for Concrete Structures 2010*. International Federation for Structural Concrete (fib).
- [12] Hendriks, M.A.N., den Uijl, J.A., de Boer, A., Feenstra, P.H., Belletti, B. and Damoni C. (2012) *Guidelines for nonlinear finite element analysis of concrete structures*
- [13] Hendriks, M.A.N and Rots, JG (2002). *Finite Elements in Civil Engineering Applications – Proceedings of the Third DIANA World Conference*. Tokyo, Japan, 9-11 October 2002.
- [14] Mathisen, K.M. (2012). *Solution Methods for Nonlinear Finite Element Analysis (NFEA)*. Lecture 11: Geilo Winter School.
- [15] Svenska Cementföreningen (1970). *Armering – Handbok i armeringsteknik för betongkonstruktions*.
- [16] Standard Norge. NS-EN 1992-1-1:2004 + NA: 2008. Eurocode 2: *Design of concrete structures – Part 1-1: General rules and rules for buildings*.
- [17] Tejchman, J. and Bobinski, J. (2013). *Continuous and Discontinuous Modelling of Fracture in Concrete Using FEM*. Springer-Verlag Berlin Heidelberg.
- [18] TNO DIANA (2015) *User’s Manual*. Release 10.

Part V: Appendices

Appendix A – Python Scripts TP1

Modelling Script TP1

```
"""
Python Script created by Magnus Eriksen and Magnus Kolstad for their Master's
thesis 2016
Concrete panel TP1
"""

closeProject()
newProject( "TP1", 100 )
setModelAnalysisAspects( ["STRUCT"] )
setModelDimension( "2D" )
setDefaultMeshOrder( "LINEAR" )
setDefaultMesherType( "HEXQUAD" )
setUnit( "LENGTH", "MM" )
setUnit( "FORCE", "N" )

#GEOMETRY
SHAPELIST = []
SHAPENUMBER = 1
SELTOL = 0.01
HEIGHT = 630
WIDTH = 630
THICKNESS =100
"""Geometry is created, and panel name stored in SHAPELIST. """
createSheet("Tension panel", [[0,0,0],[WIDTH,0,0],[WIDTH,HEIGHT,0],[0,HEIGHT,0]])
SHAPELIST=["Tension panel"]
fitAll()

#REINFORCEMENT
"""Importing function for pi. Reinforcement diameter set to 8 mm. Reinforcement
area and
perimeter calculated for two bars in depth."""
import os
from math import pi
DIAMX = 8
ASX = pi/4*DIAMX**2*2
PERIM = pi*DIAMX*2
COVER = 45

#CONCRETE PROPERTIES
YOUNGSMOD = 21900 #Modulus of elasticity concrete
POISSONRATIO = 0.2
ECT = 2.51 #Tensile strength
FC = 23.05 #Compressive strength
GF = 73*FC**0.18*0.001 #Fracture energy (MC10)
GC = 250*GF #Compressive fracture energy

#REINFORCEMENT PROPERTIES
ES = 210000 #Modulus of elasticity reinforcement
FY = 403 #Yield stress reinforcement
FU =555 #Ultimate stress reinforcement
EPSMAX = 0.1 #Ultimate strain

#CREATE REINFORCEMENT
"""SPACING is the distance between the bars in the y-direction"""
SPACING = 90
"""NUMBEROFBARS and SNUM are counters to be used in "for" loops. REINFBARS is a
list of
```

```

reinforcement names.""
NUMBEROFBARS=7
SNUM=1
REINFBARS=[]
"""Y-coordinates are generated for the reinforcement startin from the bottom of
the panel
and all the way to the top of the panel."""
YBAR=[COVER]
for i in range (1,NUMBEROFBARS):
    YBAR.append(YBAR[i-1]+SPACING)
"""Coordinates P1 and P2 are created. A reinforcement name is made. Reinforment
bars are
created from point P1 to P2 and reinforcement name is stores in REINFBARS."""
for i in range(0,len(YBAR)):
    P1=[0,YBAR[i],0]
    P2=[WIDTH,YBAR[i],0]
    LINENAMEY='BARY{}'.format(SNUM)
    createLine( LINENAMEY, P1,P2)
    REINFBARS.append(LINENAMEY)
    SNUM=SNUM+1

#CONCRETE PROPERTIES
"""Material properties for the concrete are applied to a material named
"Concrete".
Exponential and parabolic curve for concrete in tension and compression."""
addMaterial("Concrete", "CONCR", "TSCR", []) #
setParameter( MATERIAL, "Concrete", "LINEAR/ELASTI/YOUNG", YOUNGSMOD )
setParameter( MATERIAL, "Concrete", "LINEAR/ELASTI/POISON", POISSONRATIO )
setParameter( MATERIAL, "Concrete", "MODTYP/TOTCRK", "ROTATE" )
setParameter( MATERIAL, "Concrete", "TENSIL/TENSTR", FCT )
setParameter( MATERIAL, "Concrete", "TENSIL/TENCRV", "EXPONE" )
setParameter( MATERIAL, "Concrete", "TENSIL/GF1", GF )
setParameter( MATERIAL, "Concrete", "COMPRS/COMCRV", "PARABO" )
setParameter( MATERIAL, "Concrete", "COMPRS/COMSTR", FC )
setParameter( MATERIAL, "Concrete", "COMPRS/GC", GC )
"""Reduction due to lateral cracking by Vecchio and Collins, damage based
poisson's ratio
reduction and confinement model by Selby and Vecchio."""
setParameter( MATERIAL, "Concrete", "TENSIL/REDUCT/REDCRV", "VC1993" )
setParameter( MATERIAL, "Concrete", "TENSIL/POISRE/POIRED", "DAMAGE" )
setParameter( MATERIAL, "Concrete", "COMPRS/CONFIN/CNFCRV", "VECCHI" )
"""Geometry property is crated to assign the thickness of the the panel."""
addGeometry("Concrete", "SHEET", "MEMBRA", [])
setParameter( GEOMET, "Concrete", "THICK", THICKNESS )
"""Material properties and geometry properties are assigned to the geometry."""
assignMaterial("Concrete", "SHAPE", SHAPELIST)
assignGeometry("Concrete", "SHAPE", SHAPELIST)

#REINFORCEMENT PROPERTIES
"""The reinforcement geometry is assigned as reinforcement in DIANA10"""
setReinforcementAspects( REINFBARS )
RMATNAME = "Steel Reinforcement"
"""The reinforcement is given material properties. REBOND sets bond-slip
reinforcement. The
material is given hardeneing parameters and bond-slip parameters."""
addMaterial( RMATNAME, "REINFO", "REBOND", [] )
setParameter( MATERIAL, RMATNAME, "REBARS/ELASTI/YOUNG", ES )
setParameter( MATERIAL, RMATNAME, "REBARS/PLATYP", "VMISES" )
setParameter( MATERIAL, RMATNAME, "REBARS/PLASTI/TRESSH", "KAPSIG" )
setParameter( MATERIAL, RMATNAME, "REBARS/PLASTI/KAPSIG", [] )
setParameter( MATERIAL, RMATNAME, "REBARS/PLASTI/KAPSIG", [ 0, FY, EPSMAX, FU ] )

```

```

setParameter( MATERIAL, RMATNAME, "RESLIP/DSNY", 48 ) #Normal stiffness
setParameter( MATERIAL, RMATNAME, "RESLIP/DSSX", 48 ) #Shear stiffness DSSX

# Model Code bond-slip curve Bond-slip Curve
# Good bond conditions
"""Bond-slip model from Model Code 2010. DUSTSX is a list that defines a curve
with bond
stress and slip."""
setParameter( MATERIAL, RMATNAME, "RESLIP/SHFTYP", "DUSTSX" )
setParameter( MATERIAL, RMATNAME, "RESLIP/SLIP1/DUSTSX", [ -100, -4.80, -6.0, -
4.80, -2.0, -
12.00, -1, -12.00, -0.9, -11.50, -0.8, -10.98, -0.7, -10.40, -0.6, -9.78, -0.5, -
9.09, -0.4,
-8.32, -0.3, -7.41, -0.2, -6.30, -0.1, -4.78, 0,0, 0.1, 4.78, 0.2, 6.30, 0.3,
7.41, 0.4, 8.32
, 0.5, 9.09, 0.6, 9.78, 0.7, 10.40, 0.8, 10.98, 0.9, 11.50, 1.0, 12.00, 2.0,
12.00, 6.0, 4.80
, 100, 4.80 ] )
"""Reinforcement geomtry is added. The reinforcement area and perimeter is
assigned to the
geometry. REITRU denotes TRUSS."""
addGeometry( RMATNAME, "RELIN", "REBAR", [ ] )
setParameter( GEOMET, "Steel Reinforcement", "REITYP", "REITRU" )
setParameter( GEOMET, "Steel Reinforcement", "REITRU/CROSSE", ASX )
setParameter( GEOMET, "Steel Reinforcement", "REITRU/PERIME", PERIM )
"""Material properties and geometry are assigned to the reinforcement bars."""
assignMaterial( RMATNAME, "SHAPE", REINFBARS )
assignGeometry( RMATNAME, "SHAPE", REINFBARS )

#ELEMENT DATA
"""Element data for the concrete is added and assigned. Integration scheme is set
to
regular."""
addElementData( "Element data 1" )
setParameter( DATA, "Element data 1", "INTEGR", "REGULA" )
"""Bubble function added. This adds incompatible modes to the shape functions."""
setParameter( DATA, "Element data 1", "./BUBBLE", [ ] )
assignElementData( "Element data 1", SHAPE, SHAPELIST )

#START AND END NODES REINFORCEMENT BARS
"""The loop creates start and end nodes for the reinforcement bars as well as
assigning
element data to all reinforcement bars. ELEMENTDATANAME is a list of element
datas.
Interface elements are created, and teinforcement bars are set to TRUSS."""
REINFNODESTART=((HEIGHT/ELEMENTSIZE)+1)**2
ELEMENTDATANAME=[]
ELEMENTDATANUM=2
ENDNODE_GROUP=[]
STARTNODE_GROUP=[]
for i in range (1,NUMBEROFBARS+1):
    ZZZZ='Element data {}'.format(ELEMENTDATANUM)
    ELEMENTDATANAME.append(ZZZZ)
    addElementData( ELEMENTDATANAME[i-1] )
    setParameter( DATA, ELEMENTDATANAME[i-1], "INTERF", "TRUSS")
    STARTNODE=REINFNODESTART+(HEIGHT/ELEMENTSIZE)*(i-1)+i
    ENDNODE=REINFNODESTART+(HEIGHT/ELEMENTSIZE)*(i)+1 +i-1

```

```

ENDNODE_GROUP.append(ENDNODE)
STARTNODE_GROUP.append(STARTNODE)
setParameter( DATA, ELEMENTDATANAME[i-1], "BEGINN", STARTNODE )
setParameter( DATA, ELEMENTDATANAME[i-1], "ENDNOD", ENDNODE )
assignElementData( ELEMENTDATANAME[i-1], SHAPE, REINFBARS[i-1] )
ELEMENTDATANUM=ELEMENTDATANUM+1

# Parameter Study
"""Input for the parameter study is presented. For instance, if cubic bond-slip
is to be
investigated, simply remove the "#" in front the command below."""

"""Cubic bond-slip"""
#setParameter( MATERIAL, RMATNAME, "RESLIP/SHFTYP", "BONDS1" )
#setParameter( MATERIAL, RMATNAME, "RESLIP/BONDS1/SLPVAL", [ FCT, 0.06 ] )

"""Fixed Cracking"""
#setParameter( MATERIAL, "Concrete", "MODTYP/TOTCRK", "FIXED" )
#BETA = 0.01
#setParameter( MATERIAL, "Concrete", "SHEAR/SHRCRV", "CONSTA" )
#setParameter( MATERIAL, "Concrete", "SHEAR/BETA", BETA )

"""xHyH"""
#setParameter( MATERIAL, RMATNAME, "RESLIP/DSNY", 5475000 )
#setParameter( MATERIAL, RMATNAME, "RESLIP/DSSX", 5475000 )

"""xLyL"""
#setParameter( MATERIAL, RMATNAME, "RESLIP/DSNY", 48 )
#setParameter( MATERIAL, RMATNAME, "RESLIP/DSSX", 48 )

"""xHyL"""
#setParameter( MATERIAL, RMATNAME, "RESLIP/DSNY", 48 )
#setParameter( MATERIAL, RMATNAME, "RESLIP/DSSX", 5475000)

"""Mesh size"""
#ELEMENTSIZE = HEIGHT/20
ELEMENTSIZE = HEIGHT/60
#ELEMENTSIZE = HEIGHT/100

#MESHING
"""Element size set to all shapes in SHAPELIST, i.e. 1 sheet. Element class type
MEMBRA:
Plane stress elements. """
setElementSize( SHAPELIST, ELEMENTSIZE )
setElementClassType( SHAPELIST, "MEMBRA" )
"""Mesh generator. All shapes are meshed; concrete and reinforcement bars."""
generateMesh( shapes() )
"""Adds load case DEFROMLOAD: Prescribed displacements. Adds SUPPORTSET: Supports
for start
and end nodes of reinforcement bars."""
addLoadCase( "DEFORMLoad" )
addSet( SUPPORTSET, "SUPPORT_REBAR" )
"""Loop attaches supports and load to start and end nodes of the reinforcement.
Load= 0.01
mm per load step i x-direction on each reinforcement end node. Support:
Restrained against
translation in x- and y-direction for reinforcement start and end nodes."""

```

```
for i in range(len(ENDNODE_GROUP)):
    addDeformationLoad( "DEFORMLOAD", 0.01, 1, TR, str(int(ENDNODE_GROUP[i])) )
    addSupport( "SUPPORT_REBAR", TR, [ 1, 2 ], str(int(ENDNODE_GROUP[i])) )
    addSupport( "SUPPORT_REBAR", TR, [ 1, 2 ], str(int(STARTNODE_GROUP[i])) )
```

Analysis Script TP1

```
"""
Python Script created by Magnus Eriksen and Magnus Kolstad for their Master's
thesis 2016
Analysis Script Concrete panel TP1
"""

"""Adding an analysis named Nonlinear Analysis. Command: Structural Nonlinear."""
analysis = "Nonlinear analysis"
command = "Structural nonlinear"
addAnalysis( analysis )
addAnalysisCommand( analysis, "NONLIN", command )
"""Number of load steps and maximum number of iterations are set as analysis
details. 1 and
3 denotes 1*0.01mm displacement per load step for 100 load steps and 3*0.01mm per
load steps
for 100 load steps, respectively."""
setAnalysisCommandDetail( analysis, command, "EXECUT(1)/LOAD/STEPS/EXPLIC/SIZES",
"1(100)
3(100)" )
setAnalysisCommandDetail( analysis, command, "EXECUT(1)/ITERAT/MAXITE", 100 )
"""Different convergence criterion and tolerances. CONTIN: no convergence in step
"i", move
on to step "i+1"."""
"""
setAnalysisCommandDetail( analysis, command, "EXECUT(1)/ITERAT/CONVER/ENERGY",
True )
#Energy based convergence criteria
setAnalysisCommandDetail( analysis, command,
"EXECUT(1)/ITERAT/CONVER/ENERGY/TOLCON", 0.001 )
setAnalysisCommandDetail( analysis, command,
"EXECUT(1)/ITERAT/CONVER/ENERGY/NOCONV",
"CONTIN" )
"""
setAnalysisCommandDetail( analysis, command, "EXECUT(1)/ITERAT/CONVER/FORCE",
True )

#Force based convergence criteria
setAnalysisCommandDetail( analysis, command,
"EXECUT(1)/ITERAT/CONVER/FORCE/TOLCON", 0.01 )
setAnalysisCommandDetail( analysis, command,
"EXECUT(1)/ITERAT/CONVER/FORCE/NOCONV", "CONTIN"
)
setAnalysisCommandDetail( analysis, command, "EXECUT(1)/ITERAT/CONVER/RESIDU",
True )

#Residual based convergence criteria
setAnalysisCommandDetail( analysis, command,
"EXECUT(1)/ITERAT/CONVER/RESIDU/TOLCON", 0.01 )
setAnalysisCommandDetail( analysis, command,
"EXECUT(1)/ITERAT/CONVER/RESIDU/NOCONV",
"CONTIN" )
#Total strain based cracking: Tangent: Secant
#Solver for system of equations: Sparse Cholesky
#No substructuring
"""Nonlinear effects: Total strain cracking, Tangent: CONSISTENT. Solver for
system of
equations: Sparse Cholesky. No substructuring."""
setAnalysisCommandDetail( analysis, command, "TYPE/PHYSIC/TOTCRK/TANGEN",
"CONSIS" )
```

```

setAnalysisCommandDetail( analysis, command, "SOLVE/TYPE", "CHOLES" )
setAnalysisCommandDetail( analysis, command, "SOLVE/CHOLES/SUBSTR", False )

#LINESEARCH
setAnalysisCommandDetail( "Nonlinear analysis", "Structural nonlinear",
"EXECUT(1)/ITERAT/LINESE", True )

#Arc Length
#setAnalysisCommandDetail( "Nonlinear analysis", "Structural nonlinear",
"EXECUT(1)/LOAD/STEPS/EXPLIC/ARCLEN", True )

#LOGGING
""Full report written to the .out-file.""
setAnalysisCommandDetail( analysis, command, "EXECUT(1)/LOGGIN/REPORT/AMOUNT",
"FULL" )
setAnalysisCommandDetail( analysis, command, "EXECUT(1)/LOGGIN/REPORT/TERMIN",
"STEP" )

#Crack strain, Green, sampled at integration points (LOCATI: INTPNT)
#Crack width local coordinates, Green, sampled at integration points
#Crack width, Green principal, sampled at integration points
#Total principal strains , sampled at integration points
#Total principal stresses

#OUTPUT
""Setting the output of the analysis. Crack Strain, Crack width, total principal
strains
and total principal stresses.LOCATI: Sampling points: Integration Points.""
setAnalysisCommandDetail( analysis, command, "OUTPUT(2)/SELTYP", "USER" )
addAnalysisCommandDetail( analysis, command, "OUTPUT(2)/USER" )
addAnalysisCommandDetail( analysis, command,
"OUTPUT(2)/USER/STRAIN(1)/CRACK/GREEN")
setAnalysisCommandDetail( analysis, command,
"OUTPUT(2)/USER/STRAIN(1)/CRACK/GREEN/LOCATI",
"INTPNT" )
addAnalysisCommandDetail( analysis, command,
"OUTPUT(2)/USER/STRAIN(2)/CRKWDT/GREEN/GLOBAL")
setAnalysisCommandDetail( analysis, command,
"OUTPUT(2)/USER/STRAIN(2)/CRKWDT/GREEN/GLOBAL/LOCATI", "INTPNT" )
addAnalysisCommandDetail( analysis, command,
"OUTPUT(2)/USER/STRAIN(3)/CRKWDT/GREEN/LOCAL" )
setAnalysisCommandDetail( analysis, command,
"OUTPUT(2)/USER/STRAIN(3)/CRKWDT/GREEN/LOCAL/LOCATI", "INTPNT" )
addAnalysisCommandDetail( analysis, command,
"OUTPUT(2)/USER/STRAIN(4)/CRKWDT/GREEN/PRINCI" )
setAnalysisCommandDetail( analysis, command,
"OUTPUT(2)/USER/STRAIN(4)/CRKWDT/GREEN/PRINCI/LOCATI", "INTPNT" )
addAnalysisCommandDetail( analysis, command,
"OUTPUT(2)/USER/STRAIN(5)/TOTAL/GREEN/PRINCI" )
setAnalysisCommandDetail( analysis, command,
"OUTPUT(2)/USER/STRAIN(5)/TOTAL/GREEN/PRINCI/LOCATI", "INTPNT" )
addAnalysisCommandDetail( analysis, command,
"OUTPUT(2)/USER/STRESS(1)/TOTAL/CAUCHY/PRINCI" )
addAnalysisCommandDetail( analysis, command,
"OUTPUT(2)/USER/STRESS(2)/TOTAL/CAUCHY/LOCAL" )
addAnalysisCommandDetail( analysis, command,
"OUTPUT(2)/USER/STRAIN(6)/TOTAL/GREEN/LOCAL" )
""Different iteration methods. Regular and modified Newton Raphson and Quasi
Newton,
Broyden.""

```

```

#REGULAR NEWTON RAPSON
"""
setAnalysisCommandDetail( "Nonlinear analysis", "Structural nonlinear",
"EXECUT(1)/ITERAT/METHOD/METNAM", "NEWTON" )
setAnalysisCommandDetail( "Nonlinear analysis", "Structural nonlinear",
"EXECUT(1)/ITERAT/METHOD/NEWTON/TYPNAM", "REGULA" )
setAnalysisCommandDetail( "Nonlinear analysis", "Structural nonlinear",
"EXECUT(1)/ITERAT/METHOD/NEWTON/START", "PREVIO" )
"""

#MODIFYED NEWTON RAPSON
"""
setAnalysisCommandDetail( analysis, command, "EXECUT(1)/ITERAT/METHOD/METNAM",
"NEWTON" )
setAnalysisCommandDetail( analysis, command,
"EXECUT(1)/ITERAT/METHOD/NEWTON/TYPNAM",
"MODIFI" )
setAnalysisCommandDetail( analysis, command,
"EXECUT(1)/ITERAT/METHOD/NEWTON/START",
"PREVIO" )
#setAnalysisCommandDetail( analysis, command,
"EXECUT(1)/ITERAT/METHOD/NEWTON/START",
"LINEAR" )
"""

#SECANT BROYDEN PREVIOUS
setAnalysisCommandDetail( analysis, command, "EXECUT(1)/ITERAT/METHOD/METNAM",
"SECANT" )
setAnalysisCommandDetail( analysis, command,
"EXECUT(1)/ITERAT/METHOD/SECANT/TYPNAM",
"BROYDE" )
setAnalysisCommandDetail( analysis, command,
"EXECUT(1)/ITERAT/METHOD/SECANT/START", "PREVIO"
)
"""All analysis details are set. runSolver starts the analysis "Nonlinear
Analysis"."""
runSolver( analysis )
showView( "RESULT" )
setViewPoint( "TOP" )
setViewSettingValue( "result view setting", "DEFORM/MODE", "ABSOLU")

# FIND LOAD DISPLACEMENT CURVE
#DISPLACEMENT
"""DISPNODE = Random Reinforcement end node. The reinforcement node numbers vary
with the
mesh size. First, run Tension Panel script with desired mesh. Activate mesh nodes
and mark a
random reinforcement end node. Switch on "Show id", and type in the respective
node number
in DISPNODE"""

#Mesh h/60
DISPNODE = [4026]
"""
#Mesh h/20
DISPNODE = [525]
"""
"""
#mesh h/100
DISPNODE= [10302]
"""

```



```

#MAKE A LIST WITH NODES WITH REACTIONFORCES (FORCENODES)
"""FORCENODES: List with reinforcement start nodes"""
FORCENODES = []
VVVV=[HEIGHT/ELEMENTSIZE]
#First reinforcement node number
UUUU=[ (HEIGHT/ELEMENTSIZE+1)**2+1]

"""The loop dumps all reinforcement start nodes into FORCENODES."""
for i in range (0,7):
    #FORCENODES.append(int (UUUU[0])+1+(i-1)*(int (VVVV[0])))
    FORCENODES.append(int (UUUU[0])+(i*(1+int (VVVV[0]))))

#highlight(NODE, 170)
highlight(NODE, FORCENODES)
showIds( NODE, FORCENODES )

#DISPLACEMENT
DISPLACEMENTS = []
LASTCASE = len(resultCases(analysis, ''))
for i in range(0, LASTCASE):
    DISPLACEMENTS.append(resultData([analysis, "Output", resultCases(analysis, "Output") [i],
    "Total Displacements", "TDtX"], DISPNODE) [0] [1])

#REACTIONFORCES
REACTIONS = []
FORCE = 0
for i in range(0, LASTCASE):
    for j in FORCENODES:
        FORCE = FORCE +
            resultData([analysis, "Output", resultCases(analysis, "Output") [i],
            "Reaction Forces", "FBX"], (j,)) [0] [1]
    REACTIONS.append(FORCE)
    FORCE = 0

#WRITE TO FILE
"""f: writes a text file with displacements."""
f = open('ResultDisplacementS1.TXT', 'w')
"""g: writes a text file with reaction forces."""
g = open('ResultReactionforceS1.TXT', 'w')
"""Sets the accuracy (Number of digits) in the text files"""
for i in range(0, len(REACTIONS)):
    f.write('{0:20.5f}\n'.format(DISPLACEMENTS[i]))
    g.write('{0:20.6f}\n'.format(REACTIONS[i]))
f.close()
g.close()

"""In order to write the load-displacement curve, all of the user output
(OUTPUT(2)) must be
commented out. DIANA10 provides a default output."""

```

Appendix B – Python Scripts TP2

Modelling Script TP2

```
"""
Python script created by Magnus Eriksen and Magnus Kolstad for their master
thesis at NTNU
2016
Concrete panel TP2
Explanation: If this script is run in DIANA the reference panel is created. To
change
properties to perform our parameter study the "#" in different places needs to be
removed.
"""

#PROJECT SETTINGS
closeProject()
newProject( "TP2", 10 )
setModelAnalysisAspects( [ "STRUCT" ] )
setModelDimension( "2D" )
setDefaultMeshOrder( "LINEAR" )
setDefaultMesherType( "HEXQUAD" )
setUnit( "LENGTH", "MM" )
setUnit( "FORCE", "N" )

#GEOMETRY
HEIGHT=630
WIDTH=630
THICKNESS=100
"""Geometry are created, and panel name stored in SHAPELIST. """
createSheet("Tension panel", [[0,0,0],[WIDTH,0,0],[WIDTH,HEIGHT,0],[0,HEIGHT,0]])
SHAPELIST=["Tension panel"]
fitAll()

#REINFORCEMENT PROPERTIES
"""Importing function for pi. Reinforcement diameter set to 8mm. Reinforcement
area and
perimeter calculated for two bars in depth."""
import os
from math import pi
DIAMLONG=8
ASL=pi/2*DIAMLONG**2
PERIM=DIAMLONG*pi*2
FY = 403 #yield stress
FU = 555 #ultimate stress
EPSMAX = 0.1 #strain at ultimate stress
DSNY = 5906250 #normal stiffness of interface
DSSX = 47.1 #shear stiffness of interface

#CONCRETE PROPERTIES
EC = 23625 #Youngs modulus
POISSONRATIO = 0.15 #Poissons ratio
FC = 22.4 #Compressive strength
FCT = 2.44 #Tensile strength
GF = 73*FC**0.18*0.001 #Fracture energy tension, formula from MC10
GC = 250*GF #Fracture energy compression

#CREATE REINFORCEMENT
"""SPACING is the distance between bars in the X-direction. INIBARDISPX and
INIBARDISPY are
initial "displacement" to place reinforcement in the right place in relation to
the
```

```

concrete. """
SPACING=127
INIBARDISPX=122
INIBARDISPY=58.5
""" NUMBEROFBARS and SNUM are counters to be used in "for" loops. Asbars is a
list of the
reinforcement-names. """
NUMBEROFBARS=10
SNUM=1
ASBARS=[]
"""X-coordinates are generated for the reinforcement starting in bottom left
going up to the
right(XBAR). """
XBAR=[-WIDTH+INIBARDISPX]
for i in range (1,NUMBEROFBARS-1):
    XBAR.append(XBAR[i-1]+SPACING)
"""Coordinates P1 and P2 are created. Reinforcement bars are created from point
P1 to P2. A
reinforcement name is made and stored in ASBARS"""
for i in range(0,len(XBAR)):
    P1=[XBAR[i],0,0]
    P2=[XBAR[i]+WIDTH,HEIGHT,0]
    LINENAMEX='BARX{}'.format(SNUM)
    createLine( LINENAMEX, P1,P2)
    ASBARS.append(LINENAMEX)
    SNUM=SNUM+1
"""X-coordinates are generated for the reinforcement starting in top left going
down to the
right(YBAR). """
YBAR=[-WIDTH+INIBARDISPY]
for i in range (1,NUMBEROFBARS):
    YBAR.append(YBAR[i-1]+SPACING)
"""Coordinates P3 and P4 are created. Reinforcement bars are created from point
P1 to P2. A
reinforcement name is made and stored in ASBARS"""
for i in range(0,len(YBAR)):
    P3=[YBAR[i],HEIGHT,0]
    P4=[YBAR[i]+WIDTH,0,0]
    LINENAMEY='BARY{}'.format(SNUM)
    createLine( LINENAMEY, P3,P4)
    ASBARS.append(LINENAMEY)
    SNUM=SNUM+1

#CONCRETE PROPERTIES
"""Material properties for the concrete are applied to a material named
"Concrete".
Exponential and parabolic curve for concrete in tension and compression. """
addMaterial( "Concrete", "CONCR", "TSCR", [] )
setParameter( MATERIAL, "Concrete", "LINEAR/ELASTI/YOUNG", EC )
setParameter( MATERIAL, "Concrete", "LINEAR/ELASTI/POISON", POISSONRATIO )
setParameter( MATERIAL, "Concrete", "MODTYP/TOTCRK", "ROTATE" )
setParameter( MATERIAL, "Concrete", "TENSIL/TENSTR", FCT )
setParameter( MATERIAL, "Concrete", "TENSIL/TENCRV", "EXPONE" )
setParameter( MATERIAL, "Concrete", "TENSIL/GF1", GF )
setParameter( MATERIAL, "Concrete", "COMPRS/COMCRV", "PARABO" )
setParameter( MATERIAL, "Concrete", "COMPRS/COMSTR", FC )
setParameter( MATERIAL, "Concrete", "COMPRS/GC", GC )
"""Reduction due to lateral cracking by Vecchio and Collins, damage based
poissons ratio
reduction and confinement model by Selby and Vecchio."""
setParameter( MATERIAL, "Concrete", "TENSIL/REDUCT/REDCRV", "VC1993" )

```

```

setParameter( MATERIAL, "Concrete", "TENSIL/POISRE/POIRED", "DAMAGE" )
setParameter( MATERIAL, "Concrete", "COMPRS/CONFIN/CNFCRV", "VECCHI" )
"""Geometry property is created to assign the thicknes of the panel"""
addGeometry( "Concrete", "SHEET", "MEMBRA", [ ] )
setParameter( GEOMET, "Concrete", "THICK", THICKNESS )
"""Material properties and geometry properties are assigned to the geometry"""
assignMaterial( "Concrete", "SHAPE", SHAPELIST )
assignGeometry( "Concrete", "SHAPE", SHAPELIST )

#RIENFORCEMENT PROPERTIES
"""The reinforcement geometry is defined as reinforcement in DIANA"""
setReinforcementAspects( ASBARS )
"""Renamed the reinforcement to RMATNAME for easier use"""
RMATNAME = "Steel Reinforcement"
"""Reinforcement is defined as bond slipp reinforcement and properties applied to
RMATNAME"""
addMaterial( RMATNAME, "REINFO", "REBOND", [ ] )
setParameter( MATERIAL, RMATNAME, "REBARS/ELASTI/YOUNG", 210000 )
setParameter( MATERIAL, RMATNAME, "REBARS/PLATYP", "VMISES" )
setParameter( MATERIAL, RMATNAME, "REBARS/PLASTI/TRESSH", "KAPSIG" )
setParameter( MATERIAL, RMATNAME, "REBARS/PLASTI/KAPSIG", [ 0, FY, EPSMAX, FU ] )
setParameter( MATERIAL, RMATNAME, "RESLIP/DSNY", DSNY )
setParameter( MATERIAL, RMATNAME, "RESLIP/DSSX", DSSX )
"""Bond slip cureve is defined"""
setParameter( MATERIAL, RMATNAME, "RESLIP/SHFTYP", "DUSTSX" )
setParameter( MATERIAL, RMATNAME, "RESLIP/SLIP1/DUSTSX", [ -100, -4.73, -6, -
4.73, -2, -11.83
, -1, -11.83, -0.9, -11.34, -0.8, -10.82, -0.7, -10.25, -0.6, -9.64, -0.5, -8.97,
-0.4, -8.20
, -0.3, -7.31, -0.2, -6.21, -0.1, -4.71, 0, 0, 0.1, 4.71, 0.2, 6.21, 0.3, 7.31,
0.4, 8.20,
0.5, 8.97, 0.6, 9.64, 0.7, 10.25, 0.8, 10.82, 0.9, 11.34, 1.0, 11.83, 2, 11.83,
6, 4.73, 100,
4.73 ] )
"""Geometry properties are defined for the reinforcement"""
addGeometry( RMATNAME, "RELINE", "REBAR", [ ] )
setParameter( GEOMET, RMATNAME, "REITYP", "REITRU" )
setParameter( GEOMET, RMATNAME, "REITRU/CROSSE", ASL )
setParameter( GEOMET, RMATNAME, "REITRU/PERIME", PERIM )
"""Material properties and geometry properties are applied to reinforcement """
assignMaterial( RMATNAME, "SHAPE", ASBARS )
assignGeometry( RMATNAME, "SHAPE", ASBARS )

#ELEMENT DATA
"""Integration scheme and bubble function to add incompatible strain modes to the
concrete
elements. """
addElementData( "Element data 1" )
setParameter( DATA, "Element data 1", "INTEGR", "REGULA" )
setParameter( DATA, "Element data 1", "./BUBBLE", [ ] )
assignElementData( "Element data 1", SHAPE, SHAPELIST )

#START AND END NODES
"""To apply element data to the reinforcement, the start and end nodes must be
defined.
There where no easy way to find these by python script so they have been found
manually and
put in a list. The node numbers dependent on the mesh size."""
#mesh is H/20
#STARTNODEREINF=[442,450,466,490,522,543,575,599,615,623,627,639,659,687,723,759,
787,807,819]

```

```

#ENDNODEREINF=
[449,465,489,521,542,574,598,614,622,626,638,658,686,722,758,786,806,818,822]
#mesh H/60
STARTNODEREINF=[3722,3746,3794,3866,3962,4023,4119,4191,4239,4263,4275,4311,4371,
4455,4563,
4671,4755,4815,4851]
ENDNODEREINF=
[3745,3793,3865,3961,4022,4118,4190,4238,4262,4274,4310,4370,4454,4562,4670,
4754,4814,4850,4862]
#mesh H/100
#STARTNODEREINF=[10202,10242,10322,10442,10602,10703,10863,10983,11063,
11103,11123,11183,11283,11423,11603,11783,11923,12023,12083]
#ENDNODEREINF= [10241,10321,10441,10601,10702,10862,10982,11062,11102,
11122,11182,11282,11422,11602,11782,11922,12022,12082,12102]

"""A for loop is used to generate a spesific element data for each reinforcemnet
bar and
applies it. The element date defines the reinforcement as truss-bond-slip-
reinforcement and
applies the start and end node to the first and last node in each bar"""

ELEMENTDATANAME=[]
ELEMENTDATANUM=2
for i in range (1,len(STARTNODEREINF)+1):
    ZZZZ='Element data {}'.format(ELEMENTDATANUM)
    ELEMENTDATANAME.append(ZZZZ)
    addElementData( ELEMENTDATANAME[i-1] )
    setParameter( DATA, ELEMENTDATANAME[i-1], "INTERF", "TRUSS" )
    setParameter( DATA, ELEMENTDATANAME[i-1], "BEGINN", STARTNODEREINF[i-1] )
    setParameter( DATA, ELEMENTDATANAME[i-1], "ENDNOD", ENDNODEREINF[i-1] )
    assignElementData( ELEMENTDATANAME[i-1], SHAPE, ASBARS[i-1] )
    ELEMENTDATANUM=ELEMENTDATANUM+1

#PARAMETE STUDY
"""CUBIC BOND SLIP"""
#setParameter( MATERIAL, RMATNAME, "RESLIP/SHFTYP", "BONDS1" )
#setParameter( MATERIAL, RMATNAME, "RESLIP/BONDS1/SLPVAL", [ FCT, 0.06 ] )

"""FIXED CRACKING"""
#setParameter( MATERIAL, "Concrete", "MODTYP/TOTCRK", "FIXED" )
#BETA = 0.01
#setParameter( MATERIAL, "Concrete", "SHEAR/SHRCRV", "CONSTA" )
#setParameter( MATERIAL, "Concrete", "SHEAR/BETA", BETA )

"""xHyH"""
#DSSX = 5906250
#DSNY = 5906250

"""xHyL"""
#DSSX = 5906250
#DSNY = 47.1

"""xLyL"""
#DSSX = 47.1
#DSNY = 47.1

"""MESH SIZE"""
#ELEMENTSIZE=HEIGHT/20
ELEMENTSIZE=HEIGHT/60
#ELEMENTSIZE=HEIGHT/100

```

```

#MESHING
"""Mesh size is applied and mesh is generated. Membran type is selected"""
setElementSize( SHAPELIST, ELEMENTSIZE )
setElementClassType( SHAPELIST, "MEMBRA" )
generateMesh(shapes())

#LOADS AND SUPPORTS
"""Load case and support set are created"""
addLoadCase( "DEFORMLOAD" )
addSet( SUPPORTSET, "SUPPORT_REBAR" )
"""Loads and supports are applied to the reinforcement crossing the left and
right side of
the panel."""
for i in range(4):
    addSupport( "SUPPORT_REBAR", TR, [ 1 ], str(int(STARTNODEREINF[i])) )
    addSupport( "SUPPORT_REBAR", TR, [ 2 ], str(int(STARTNODEREINF[i])) )
    addSupport( "SUPPORT_REBAR", TR, [ 1 ], str(int(ENDNODEREINF[i+5])) )
    addSupport( "SUPPORT_REBAR", TR, [ 2 ], str(int(ENDNODEREINF[i+5])) )
    addDeformationLoad( "DEFORMLOAD", 0.01, 1, TR, str(int(ENDNODEREINF[i+5])) )
for i in range(5):
    addSupport( "SUPPORT_REBAR", TR, [ 1 ], str(int(STARTNODEREINF[i+9])) )
    addSupport( "SUPPORT_REBAR", TR, [ 2 ], str(int(STARTNODEREINF[i+9])) )
    addSupport( "SUPPORT_REBAR", TR, [ 1 ], str(int(ENDNODEREINF[i+14])) )
    addSupport( "SUPPORT_REBAR", TR, [ 2 ], str(int(ENDNODEREINF[i+14])) )
    addDeformationLoad( "DEFORMLOAD", 0.01, 1, TR, str(int(ENDNODEREINF[i+14])) )

#highlight(NODE, STARTNODEREINF)
#showIds( NODE, ENDNODEREINF )

# APPLICATION OF TYINGS
"""To apply the styings, the python script must be run in DIANA and then exported
to a .DAT
- file. Then one of the tying-sets below must be pasted into the .DAT file. This
must be
pasted in between the 'LOADS'-section and the 'SUPPOR'-section in the .DAT-file.
The tyings
are dependent on the mesh size, so the right tying-set must be copied from
below."""
"""The tying applies a master slave relation between one reinforcement node and
one concrete
node. In this case an equal displacement relation in X and Y direction is
applied.

"""
#H/60:
"""
'TYINGS'
NAME SET_1
EQUAL TR_1 2
4274 69
4023 75
4310 81
4119 87
4370 93
4191 99
4454 105
4239 111
4562 117
4563 235

```

3745 229
4671 223
3793 217
4755 211
3865 205
4815 199
3961 193
4851 187
4022 1
3962 3
""

#H/20:
""

'TYINGS'
NAME SET_1
EQUAL TR 1 2
626 25
543 27
638 29
575 31
658 33
599 35
686 37
615 39
722 41
723 79
449 77
759 75
465 73
787 71
489 69
807 67
521 65
819 63
522 3
542 1
""

#H/100:
""

'TYINGS'
NAME SET_1
EQUAL TR 1 2
10703 123
10863 143
10983 163
11063 184
11122 112
11182 132
11282 153
11422 173
11602 193
11923 351
11603 391
10241 382
11783 371
10321 362
10441 341
12023 330
10601 321

12083 310
11923 351
10602 3
10702 1
""

Analysis Script TP2

```
"""
Python script created by Magnus Eriksen and Magnus Kolstad for their master
thesis at NTNU
2016
Concrete panel TP2
"""

#mesh is H/20
#STARTNODEREINF=[442,450,466,490,522,543,575,599,615,623,627,639,659,687,723,759,
787,807,819]
#ENDNODEREINF=
[449,465,489,521,542,574,598,614,622,626,638,658,686,722,758,786,806,818,822]

#mesh H/60
STARTNODEREINF=[3722,3746,3794,3866,3962,4023,4119,4191,4239,4263,4275,4311,4371,
4455,4563,
4671,4755,4815,4851]
ENDNODEREINF=
[3745,3793,3865,3961,4022,4118,4190,4238,4262,4274,4310,4370,4454,4562,4670,
4754,4814,4850,4862]

#mesh H/100
#STARTNODEREINF=[10202,10242,10322,10442,10602,10703,10863,10983,11063,
11103,11123,11183,11283,11423,11603,11783,11923,12023,12083]
#ENDNODEREINF= [10241,10321,10441,10601,10702,10862,10982,11062,11102,
11122,11182,11282,11422,11602,11782,11922,12022,12082,12102]

# SET UP ANALYSIS
analysis = "Nonlinear analysis"
command = "Structural nonlinear"
addAnalysis( analysis )
addAnalysisCommand( analysis, "NONLIN", command )
setAnalysisCommandDetail( analysis, command, "EXECUT(1)/LOAD/STEPS/EXPLIC/SIZES",
"1(10)" )
setAnalysisCommandDetail( analysis, command, "EXECUT(1)/ITERAT/MAXITE", 100 )
setAnalysisCommandDetail( analysis, command, "EXECUT(1)/ITERAT/CONVER/DISPLA",
False )
"""
setAnalysisCommandDetail( analysis, command, "EXECUT(1)/ITERAT/CONVER/ENERGY",
True )
setAnalysisCommandDetail( analysis, command,
"EXECUT(1)/ITERAT/CONVER/ENERGY/TOLCON", 0.001 )
setAnalysisCommandDetail( analysis, command,
"EXECUT(1)/ITERAT/CONVER/ENERGY/NOCONV",
"CONTIN" )
"""
setAnalysisCommandDetail( analysis, command, "EXECUT(1)/ITERAT/CONVER/FORCE",
True )
setAnalysisCommandDetail( analysis, command,
"EXECUT(1)/ITERAT/CONVER/FORCE/TOLCON", 0.01 )
setAnalysisCommandDetail( analysis, command,
"EXECUT(1)/ITERAT/CONVER/FORCE/NOCONV", "CONTIN"
)
setAnalysisCommandDetail( analysis, command, "EXECUT(1)/ITERAT/CONVER/RESIDU",
True )
setAnalysisCommandDetail( analysis, command,
"EXECUT(1)/ITERAT/CONVER/RESIDU/TOLCON", 0.01 )
setAnalysisCommandDetail( analysis, command,
"EXECUT(1)/ITERAT/CONVER/RESIDU/NOCONV",
```

```

"CONTIN" )
setAnalysisCommandDetail( analysis, command, "EXECUT(1)/ITERAT/CONVER/SIMULT",
False )
addAnalysisCommandDetail( analysis, command, "EXECUT(1)/SOLVE/CHOL" )
#LINESEARCH
setAnalysisCommandDetail( "Nonlinear analysis", "Structural nonlinear",
"EXECUT(1)/ITERAT/LINESE", True )
#Arc Length
#setAnalysisCommandDetail( "Nonlinear analysis", "Structural nonlinear",
"EXECUT(1)/LOAD/STEPS/EXPLIC/ARCL" , True )
#LOGGING
setAnalysisCommandDetail( analysis, command, "EXECUT(1)/LOGGIN/REPORT/AMOUNT",
"FULL" )
setAnalysisCommandDetail( analysis, command, "EXECUT(1)/LOGGIN/REPORT/TERMIN",
"STEP" )

#ITERATION METHOD
#MODIFIED NEWTON RAPSON
""
setAnalysisCommandDetail( analysis, command, "EXECUT(1)/ITERAT/METHOD/METNAM",
"NEWTON" )
setAnalysisCommandDetail( analysis, command,
"EXECUT(1)/ITERAT/METHOD/NEWTON/TYPNAM",
"MODIFI" )
#setAnalysisCommandDetail( analysis, command,
"EXECUT(1)/ITERAT/METHOD/NEWTON/START",
"PREVIO" )
setAnalysisCommandDetail( analysis, command,
"EXECUT(1)/ITERAT/METHOD/NEWTON/START",
"LINEAR" )
""

#REGULAR NEWTON RAPSON
""
setAnalysisCommandDetail( "Nonlinear analysis", "Structural nonlinear",
"EXECUT(1)/ITERAT/METHOD/METNAM", "NEWTON" )
setAnalysisCommandDetail( "Nonlinear analysis", "Structural nonlinear",
"EXECUT(1)/ITERAT/METHOD/NEWTON/TYPNAM", "REGULA" )
setAnalysisCommandDetail( "Nonlinear analysis", "Structural nonlinear",
"EXECUT(1)/ITERAT/METHOD/NEWTON/START", "PREVIO" )
""

#SECANT BROYDEN PREVIOUS
setAnalysisCommandDetail( analysis, command, "EXECUT(1)/ITERAT/METHOD/METNAM",
"SECANT" )
setAnalysisCommandDetail( analysis, command,
"EXECUT(1)/ITERAT/METHOD/SECANT/TYPNAM",
"BROYDE" )
setAnalysisCommandDetail( analysis, command,
"EXECUT(1)/ITERAT/METHOD/SECANT/START", "PREVIO"
)
setViewSettingValue( "result view setting", "DEFORM/MODE", "ABSOLU" )

#Physical nonlinear - Total Strain based cracking, TANGENT CONSISTENT
setAnalysisCommandDetail( "Nonlinear analysis", "Structural nonlinear",
"TYPE/PHYSIC/TOTCRK/TANGEN", "CONISIS" )

#substructure off
setAnalysisCommandDetail( "Nonlinear analysis", "Structural nonlinear",
"EXECUT(1)/SOLVE/CHOL/SUBSTR", False )

```

```

#SPARSE CHOLESKY solution method
setAnalysisCommandDetail( "Nonlinear analysis", "Structural nonlinear",
"SOLVE/TYPE",
"CHOLES" )

#OUTPUT USER
"""The selected output"""
setAnalysisCommandDetail( analysis, command, "OUTPUT(2)/SELTYP", "USER" )
addAnalysisCommandDetail( analysis, command, "OUTPUT(2)/USER" )
addAnalysisCommandDetail( analysis, command,
"OUTPUT(2)/USER/STRAIN(1)/CRACK/GREEN")
setAnalysisCommandDetail( analysis, command,
"OUTPUT(2)/USER/STRAIN(1)/CRACK/GREEN/LOCATI",
"INTPNT" )
addAnalysisCommandDetail( analysis, command,
"OUTPUT(2)/USER/STRAIN(2)/CRKWDT/GREEN/GLOBAL")
setAnalysisCommandDetail( analysis, command,
"OUTPUT(2)/USER/STRAIN(2)/CRKWDT/GREEN/GLOBAL/LOCATI", "INTPNT" )
addAnalysisCommandDetail( analysis, command,
"OUTPUT(2)/USER/STRAIN(3)/CRKWDT/GREEN/LOCAL" )
setAnalysisCommandDetail( analysis, command,
"OUTPUT(2)/USER/STRAIN(3)/CRKWDT/GREEN/LOCAL/LOCATI", "INTPNT" )
addAnalysisCommandDetail( analysis, command,
"OUTPUT(2)/USER/STRAIN(4)/CRKWDT/GREEN/PRINCI" )
setAnalysisCommandDetail( analysis, command,
"OUTPUT(2)/USER/STRAIN(4)/CRKWDT/GREEN/PRINCI/LOCATI", "INTPNT" )
addAnalysisCommandDetail( analysis, command,
"OUTPUT(2)/USER/STRAIN(5)/TOTAL/GREEN/PRINCI" )
setAnalysisCommandDetail( analysis, command,
"OUTPUT(2)/USER/STRAIN(5)/TOTAL/GREEN/PRINCI/LOCATI", "INTPNT" )
addAnalysisCommandDetail( analysis, command,
"OUTPUT(2)/USER/STRESS(1)/TOTAL/CAUCHY/PRINCI" )
addAnalysisCommandDetail( analysis, command,
"OUTPUT(2)/USER/STRESS(2)/TOTAL/CAUCHY/LOCAL" )
addAnalysisCommandDetail( analysis, command,
"OUTPUT(2)/USER/STRAIN(6)/TOTAL/GREEN/LOCAL" )

#STARTING THE ANALYSIS
runSolver( analysis )
showView( "RESULT" )
setViewPoint( "TOP" )
setResultPlot( "contours", "Cauchy Total Stresses/mappedintegrationpoint", "S2" )
setViewSettingValue( "result view setting", "DEFORM/MODE", "ABSOLU")

# FIND LOAD DISPLACEMENT CURVE
"""To make the load displacement date the outputblock above must be commented
out."""

#DISPLACEMENT
"""The end of one of the reinforcement bars are selected to sample displacements
from"""
DISPNODE = [int(ENDNODEREINF[7])]

#highlight(NODE,DISPNODE)

#MAKE A LIST WITH NODES WITH REACTIONFORCES (FORCENODES)
FORCENODES=[]
for i in range(4):
FORCENODES.append(int(STARTNODEREINF[i]))
for i in range(5):
FORCENODES.append(int(STARTNODEREINF[i+9]))

```

```

highlight(NODE, DISPNODE)
showIds( NODE, FORCENODES )

#SAMPELING OF DISPLACEMENTS
DISPLACEMENTS = []
LASTCASE = len(resultCases(analysis, ''))
for i in range(0, LASTCASE):
DISPLACEMENTS.append(resultData([analysis, "Output", resultCases(analysis, "Output")
[i],
"Total Displacements", "TDtX"], DISPNODE) [0] [1])

#SAMPELING OF REACTION FORCES
REACTIONS = []
FORCE = 0
for i in range(0, LASTCASE):
for j in FORCENODES:
FORCE = FORCE + resultData([analysis, "Output", resultCases(analysis, "Output") [i],
"Reaction Forces", "FBX"], (j,)) [0] [1]
REACTIONS.append(FORCE)
FORCE = 0

#WRITE TO FILE TEXT FILES
f = open('Result45DisplacementS2.TXT', 'w')
g = open('Result45ReactionforceS2.TXT', 'w')
for i in range(0, len(REACTIONS)):
f.write('{0:20.5f}\n'.format(DISPLACEMENTS[i]))
g.write('{0:20.6f}\n'.format(REACTIONS[i]))
f.close()
g.close()
"""Warnings are ignored. One unwanted load is removed by diana when analysis
starts, wich is
OK. Error in the end is ignored. """

```

Appendix C – Calculations according to Eurocode 2 and Model Code

In this appendix follows simplified calculations of crack widths and maximum crack spacing for panel TP1 and panel TP2.

Material Properties

$f_{ct,TP1} = 2,51 \text{ MPa}$, tensile strength TP1

$f_{ct,TP2} = 2,44 \text{ MPa}$, tensile strength TP2

$E_s = 210000 \text{ MPa}$, Elastic modulus reinforcing steel

$E_{c,TP1} = 21900 \text{ MPa}$, Elastic modulus of concrete TP1

$E_{c,TP2} = 23625 \text{ MPa}$, Elastic modulus of concrete TP2

Reinforcement

$f_y = 403 \text{ MPa}$, yield limit reinforcement

$\phi = 8 \text{ mm}$, diameter of reinforcing bar

$A_{s1} = 14 \cdot \pi \cdot (8 \text{ mm})^2 \cdot 0,25 = 703,716 \text{ mm}^2$ Total amount of reinforcement in TP1

$A_{s2} = 38 \cdot \pi \cdot (8 \text{ mm})^2 \cdot 0,25 = 1910,088 \text{ mm}^2$ Total amount of reinforcement in TP2

Cover

$c_{TP1} = c_{TP2} = \min(45,10) \text{ mm} = 10 \text{ mm}$, cover taken in the thickness direction of the panel.

Eurocode 2

$k_1 = 0,8$

$k_2 = 1,0$

$k_3 = 3,4$

$k_4 = 0,425$

$h_{c,eff,TP1} = (10 + 8 + 20) \text{ mm} = 38 \text{ mm}$

$h_{c,eff,TP2} = h_{c,eff,TP1} = 38 \text{ mm}$

$A_{c,eff,TP1} = A_{c,eff,TP2} = h_{c,eff} \cdot b = 23940$

$\rho_{p,eff,TP1} = \frac{7 \cdot \pi \cdot (4 \text{ mm})^2}{A_{c,eff}} = 0,01469$

$\rho_{p,eff,TP2} = \frac{10 \cdot \pi \cdot (4 \text{ mm})^2}{A_{c,eff}} = 0,020996$

$$s_{r,max,TP1} = k_3 \cdot c + k_1 \cdot k_2 \cdot k_4 \cdot \frac{\phi}{\rho_{p,eff,TP1}} = 219,160 \text{ mm}$$

$$s_{r,max,y,TP2} = s_{r,max,z,TP2} = k_3 \cdot c + k_1 \cdot k_2 \cdot k_4 \cdot \frac{\phi}{\rho_{p,eff,TP2}} = 163,548 \text{ mm}$$

$$s_{r,max,TP2} = \frac{1}{\frac{\cos(\varphi)}{s_{r,max,y,TP2}} + \frac{\sin(\varphi)}{s_{r,max,z,TP2}}} = 115,646 \text{ mm}$$

Model code 2010

$$k = 1,0$$

$$\tau_{bm,TP1} = 1,8 \cdot f_{ct,TP1} = 4,518 \text{ MPa}$$

$$\tau_{bm,TP2} = 1,8 \cdot f_{ct,TP2} = 4,392 \text{ MPa}$$

$$h_{c,eff} = \min\left(2,5 \cdot \left(c + \frac{\phi}{2}\right), \frac{t}{2}\right) = 35 \quad t=100 \text{ mm}$$

$$A_{c,eff} = h_{c,eff} \cdot b = 22050 \text{ mm}^2$$

$$\rho_{s,eff,TP1} = \frac{7 \cdot \pi \cdot (4 \text{ mm})^2}{A_{c,eff}} = 0,01596$$

$$\rho_{s,eff,TP2} = \frac{10 \cdot \pi \cdot (4 \text{ mm})^2}{A_{c,eff}} = 0,02278$$

$$l_{s,max,TP1} = k \cdot c + \frac{1}{4} \cdot \frac{f_{ct,TP1}}{\tau_{bm,TP1}} \cdot \frac{\phi}{\rho_{s,eff,TP1}} = 79,618 \text{ mm}$$

$$l_{s,max,x,TP2} = l_{s,max,y,TP2} = k \cdot c + \frac{1}{4} \cdot \frac{f_{ct,TP2}}{\tau_{bm,TP1}} \cdot \frac{\phi}{\rho_{s,eff,TP2}} = 58,776 \text{ mm}$$

$$l_{s,max,TP2} = \frac{1}{\frac{\cos(\varphi)}{l_{s,max,x,TP2}} + \frac{\sin(\varphi)}{l_{s,max,y,TP2}}} = 44,490 \text{ mm}$$

Calculation of crack widths

- Eurocode 2:
 - $w_d = s_{r,max} \cdot (\varepsilon_s - \varepsilon_c)$
- Model Code 2010
 - $w_d = 2 \cdot l_{s,max} \cdot (\varepsilon_s - \varepsilon_c)$